Global patterns of commodity-driven deforestation and associated carbon emissions

Chandrakant Singh[1,2] and U. Martin Persson[1]

[1]Department of Space, Earth and Environment, Chalmers University of Technology, Gothenburg, Sweden
[2]Stockholm Resilience Centre, Stockholm University, Stockholm, Sweden

Corresponding authors: Chandrakant Singh (chandrakant.singh@chalmers.se) and
U. Martin Persson (martin.persson@chalmers.se)

Abstract

Rapid agriculture-driven deforestation raises significant concerns about achieving climate and biodiversity targets. Linking deforestation to food production is crucial for guiding the development, implementation, and evaluation of forest conservation and climate change mitigation efforts. However, the limited scope and comprehensiveness of available datasets restrict the effectiveness of these efforts. Recognising this, we present the Deforestation Driver and Carbon Emission (DeDuCE) model, merging the best available spatial and statistical datasets to enhance the quantification of deforestation due to the production of agriculture and forestry commodities. DeDuCE reports 9,332 unique country-commodity deforestation-carbon footprints across 179 countries and 184 commodities from 2001-2022, surpassing existing databases in scope and detail. The model provides critical data for public and private sector actors assessing deforestation risks, evaluating the sustainability of investments, and reporting food sector carbon emissions. Notably, our deforestation emissions constitute nearly half of previously reported emissions from land-use activities within global food systems. Moreover, global efforts to curb deforestation are inadequately focused on staple crops, which are also significant drivers of deforestation.

1. Introduction

Food is a necessity for human survival. However, meeting the demand of an ever-growing global population has led to extensive deforestation, with over 90% of global deforestation linked to agriculture[1,2]. When natural forests are cleared for agricultural production, they are replaced by land systems that often lack the biodiversity and carbon storage capacity of the natural forests. A recent Food and Agriculture Organization (FAO) report[1] suggests that over the past three decades, the world has lost forests more than the size of India[3,4]. Consequently, deforestation is estimated to be the largest driver of biodiversity loss on land[5], contributing nearly one-tenth of total anthropogenic greenhouse gas (GHG) emissions[6,7], with agricultural deforestation and other land-use activities accounting for one-third of total food system emissions[8]. These impacts from global food production raise alarming concerns about future food security, as well as the suitability and sustainability of our living environments[9–11].

Recognising these impacts, local governments, companies and civil societies have pushed for forest conservation and climate change mitigation initiatives such as the Reducing Emissions from Deforestation and forest Degradation[12] (REDD+), the New York Declaration on Forests[13], and corporate Zero Deforestation Commitments[14]. These initiatives aim to engage public and private sectors in combating deforestation, incentivising conservation and promoting deforestation-free supply chains. Notably, the recently adopted European Union Deforestation Regulation (EUDR)[15] mandates companies to conduct due diligence reporting to ensure the EU's supply chains are free from imported deforestation.

A key to the successful implementation and evaluation of these policy initiatives is the ability to comprehensively monitor agricultural deforestation and its climate impact[2]. However, while spatial datasets linking food production to deforestation exist for some commodities, they are often geographically limited and do not provide a comprehensive view of global food system impacts[16–18]. Conversely, national and sub-national agricultural statistics offer extensive coverage of commodity production but lack the spatial precision required for linking food systems to deforestation[19]. As a result, traditional deforestation attribution models have primarily been bookkeeping models[8,19,20], with limited integration of remote sensing datasets[18,21,22]. This limited use of remotely sensed data can primarily be attributed to computational challenges in handling and processing large data volumes[23]. Consequently, datasets that do integrate remote sensing often lack ongoing updates or refinements post-publication and tend to aggregate data over lengthy periods[18,21,22,24], diminishing their relevance over time.

With the growing trend among organisations to adopt more advanced and innovative methods for forest resource assessments[25,26], shifting the paradigm from traditional statistical methods requires the integration of remote sensing datasets and the utilisation of powerful cloud-computing resources[27]. Such integration is imperative for stakeholders to adapt to the rapidly evolving food systems landscape and make informed decisions that balance growing food demand with forest conservation. To assist with this, we introduce the Deforestation Driver and Carbon Emission (DeDuCE) model, which, leveraging the computational power of Google Earth Engine (GEE), melds the spatio-temporal precision of best available remote sensing data and comprehensiveness of agricultural statistics. The model tracks deforestation and associated carbon emissions, and links them with the production of agriculture and forestry commodities globally.

2. State-of-the-art of the model

The DeDuCE model provides annual estimates of deforestation and associated carbon emissions due to the production of agriculture and forestry commodities. Covering 179 countries and 184 commodities between 2001 and 2022, the model delivers 9,332 unique deforestation-carbon footprint estimations (Supplementary Tables 1 and 2). The model achieves this comprehensive deforestation attribution by overlaying global spatio-temporal data of tree cover loss[28] with best-available datasets on crops, land uses, dominant deforestation drivers[24], and state of forest management (Extended Data Fig. 1 and Supplementary Table 3). Each tree cover loss pixel is linked to the most detailed information available about the direct land-use change (dLUC)[29,30] (i.e., a specific commodity or land use).

In cases where deforestation is not spatially attributed to a specific commodity, the model uses agricultural statistics (at the national and sub-national level[3,31]) to identify the likely or potential driver of deforestation (reflecting statistical land-use change (sLUC), which is a measure of deforestation risk) through a two-step statistical land-balance approach[19] (Supplementary Fig. 1). Through this, the model accounts for key land-use change dynamics, such as competition between cropland, pasture, and other land uses, as well as cropland and pasture abandonment. These factors are crucial for attributing deforestation to agricultural commodity production but are poorly captured in existing life-cycle inventory databases[32]. Additionally, carbon emissions associated with deforestation are estimated by overlaying identified deforestation drivers with data on forest[33] and soil[34] carbon stocks, including emissions from peatland[35] drainage (Extended Data Fig. 1).

By combining GEE's computational capabilities to process terabytes of high-resolution spatio-temporal data with Python's open-source programming for deforestation-emission accounting, we align with FAIR data principles[36], striving to promote accessibility, integrity and transparency. This integration also ensures replicability of model results, while fostering community engagement, inviting researchers and stakeholders to contribute and refine the model. Such engagements are especially crucial as growing food demand greatly influences regional and remote landscapes owing to different environmental, technological, regulatory and socio-economic factors[37–40].

Presently, the lack of clear, mandatory guidelines on data and methodologies for deforestation-emission accounting[41,42] leads to inconsistent practices across organisations. The DeDuCE model addresses this by providing a homogeneous framework for attributing commodity-driven deforestation and estimating carbon emissions globally. Compared to other models or datasets (Supplementary Table 4), DeDuCE offers better spatio-temporal resolution and representation across biomes, land uses, and commodities, while accounting for all possible sources of carbon emissions. This uniformity allows for consistent comparison of deforestation-carbon footprints between countries, reducing discrepancies arising from differences in the inputs and methodological assumptions across regional or national-scale assessments.

Furthermore, the model's versatility allows for the inclusion of diverse datasets (Supplementary Table 3) and is designed to integrate emerging datasets, ensuring its relevance and adaptability over time. It allows for adjusting parameters such as tree cover density for forest classification, lag periods between forest clearing and agricultural land establishment, control over attribution methodology, and amortisation periods, as per the required use case (Table 1). Through quality assessment (Extended Data Fig. 1), the model quantifies the reliability of deforestation estimates, highlighting countries and commodities that require better data representation. This enhances the model's utility as a tool for supporting global sustainability and conservation efforts.

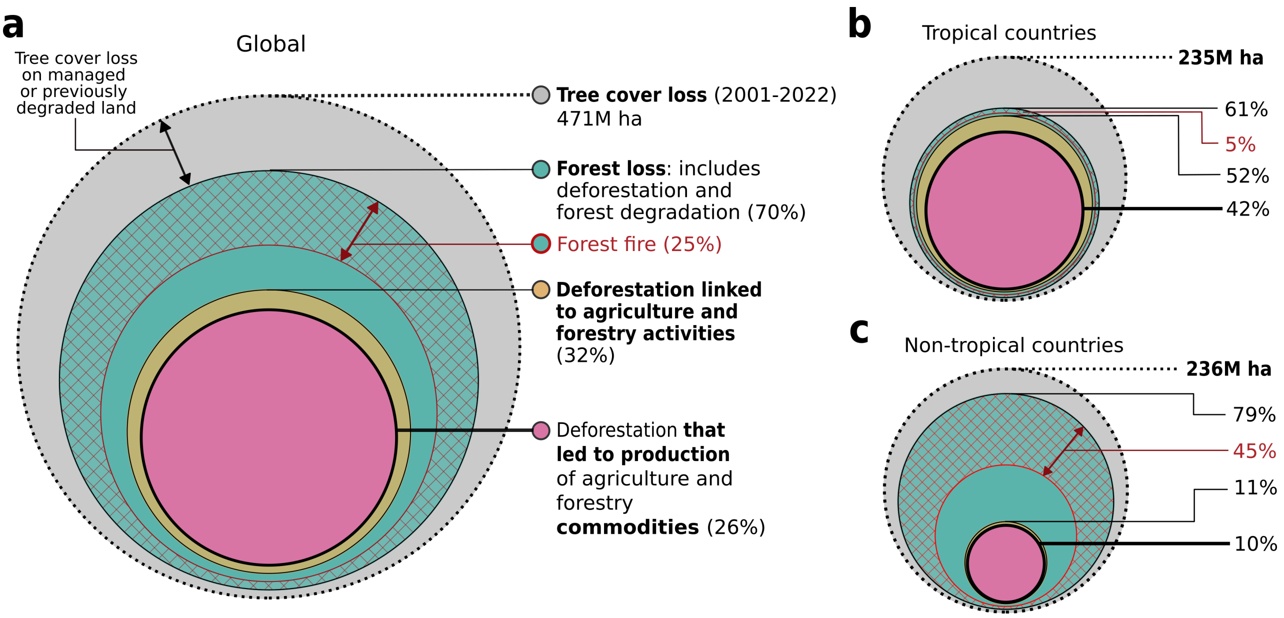

Fig. 1 | Assessing deforestation from global tree cover loss estimates (2001-2022). (a) The nested circles provide an insight into deforestation driven by agriculture and forestry activities derived from global tree cover loss estimates (refers to loss of tree canopy within a 30-m pixel globally between 2001-2022[28]; tree cover density ≥ 25%). Forest loss, which includes deforestation and forest degradation, captures the loss of natural forests by excluding loss on managed or degraded lands established before the year 2000 (e.g., rotational clearing on forest plantations or loss of sparse growth on degraded land systems). Within this, losses due to forest fires are indicated with hatch patterns. Additionally, the scope of deforestation driven by agriculture and forestry activities extends to include the instances where deforestation is directly linked to the production of commodities, and where it occurs independently of such production. The latter scenario is examined by evaluating the extent of this deforestation that cannot be linked to any specific commodity in the DeDuCE's land balance approach (Extended Data Fig. 1). Possible mechanisms where deforestation does not lead to the production of commodities are explored in ref.[2]. The size of the circles in the diagram is proportional to their respective shares in the total area of tree cover loss. To offer a comparative insight into deforestation dynamics across different biomes, we have also separated our analysis for (b) tropical and (c) non-tropical countries. The design of the figure is inspired by ref.[2].

3. Global overview of deforestation and carbon emissions

The DeDuCE model suggests that of the 471 million hectares (Mha) of global tree cover loss observed from 2001 to 2022, only 26% is driven by expanding croplands, pastures, and forest plantations for commodity production (5.5±0.8 Mha yr^{-1}; Fig. 1a). This estimate is considerably smaller than FAO's[3] reported range of 7-13 Mha yr^{-1} (Fig. 2a). In comparison, Curtis et al.[24,43] estimate that 44-76% of global tree cover loss is attributed to agriculture and forestry activities. This discrepancy occurs because Curtis et al.[24] overlook spatio-temporal heterogeneity – by attributing only the dominant forest loss driver over the whole timeframe – and finer land-use change dynamics (e.g., rotational clearing) (Fig. 1). Furthermore, the share of commodity-driven deforestation from DeDuCE exhibits stark contrasts between tropical and non-tropical regions: 42% of the tree cover loss in tropical countries is attributed to expanding agricultural land and forest plantations, compared to just 10% in non-tropical countries (Fig. 1b,c).

Compared to prior assessments[2], DeDuCE presents a lower overall estimate of deforestation due to agriculture and forestry activities, yet it shows marginally higher figures for deforestation leading to production (Fig. 1b). Notably, Pendrill et al.[2] estimated that as much as a third to half of agriculture-driven deforestation did not result in any identifiable agricultural production. In contrast, our analysis puts this number much lower, at just over a fifth (25 Mha from a total of 118 Mha agricultural-driven deforestation; Fig. 1b). This improved understanding about the role of food production in driving deforestation is due to our use of high-resolution agricultural land-use maps, reducing reliance on coarse dominant forest-loss driver data and poor-quality agricultural statistics. Additionally, our integration of forest fire data[44] and the sequential attribution framework of DeDuCE model (i.e., attributing forest loss pixels to agricultural land use before attributing forest loss to fire; see Methods) enables us to distinguish wildfires, often propagating in grass-dominated natural and semi-natural landscapes[45], from fires used to clear land for agricultural expansion. The remaining discrepancies between agriculture-driven deforestation and productive use of the cleared land in the tropics—which still are substantial—likely reflect challenges in land tenure clarity and disputes[2]. For instance, speculative clearing anticipating future agricultural returns, planned infrastructural developments, uncertain future forest conservation legislations and availability of large expanses of undesignated public lands may fail to evolve into productive agricultural or forestry ventures[46,47].

We estimate nearly 41.2 $GtCO_2$ emissions from commodity-driven deforestation globally from 2001-2022 (1.9±0.3 $GtCO_2$ yr^{-1}). Additionally, emissions from peatland drainage on deforested lands contribute to approximately 2.9 $GtCO_2$ (0.13±0.08 $GtCO_2$ yr^{-1}; Fig. 2b and 3), accounting for about 7% of global annual peatland drainage emissions[48]. Our carbon emission estimates are substantially lower than previously reported (Fig. 2b), except for Pendrill et al.[49], who only cover the tropics. Crippa et al.[8], using FAOSTAT data[31], estimate agricultural land-use emissions (including those from deforestation) at 4.3±0.3 $GtCO_2$ yr^{-1}, which is twice our estimate (excluding deforestation emissions from forestry activities from Fig. 2b; Supplementary Table 2). Since forests hold the majority of carbon stocks, other agricultural land-use changes, excluding deforestation, are unlikely to account for the remaining land-use change emissions. The likely reason for this discrepancy is that Crippa et al.[8] estimates do not utilise spatial information on deforestation, agricultural land use or carbon stocks, but simply assume that 80% of all deforestation is due to agricultural land-use change. This underscores the value of utilising remote sensing-based data for assessing agriculture-driven deforestation.

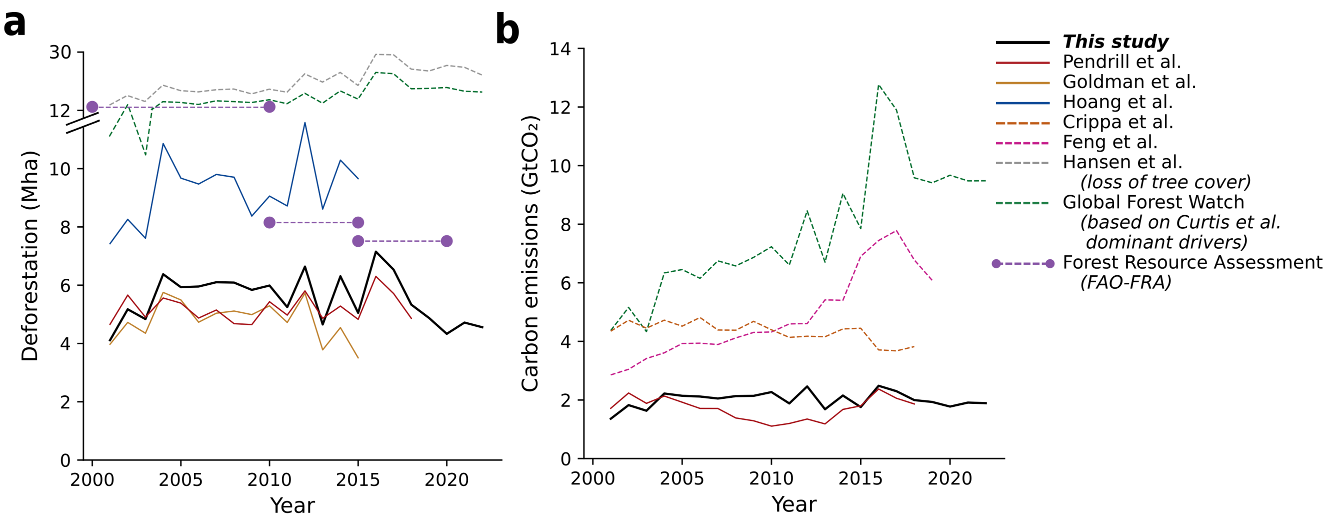

Fig. 2 | Comparing different commodity-driven deforestation and carbon emission estimates. A comparison between our (a) deforestation and (b) associated carbon emission estimates with those from established literature sources. The comparison includes estimates from Pendrill et al.[49] (covering only tropical counties), Goldman et al.[18] (covering only EUDR commodities), Hoang et al.[21], Crippa et al.[8] (including all food production-driven land use activities), Feng et al.[22] (accounting for tree cover loss due to agriculture- and forestry-activities across the tropics), Hansen et al.[28] (tree cover ≥ 25%), Global Forest Watch[50] (tree cover ≥ 25%; including tree cover loss due to commodity-driven deforestation, shifting agriculture and forestry from Curtis et al.[24]), and FAO's global forest resource assessment report (FAO-FRA)[3]. A brief summary of the studies and datasets used for this comparison can be found in Supplementary Table 4.

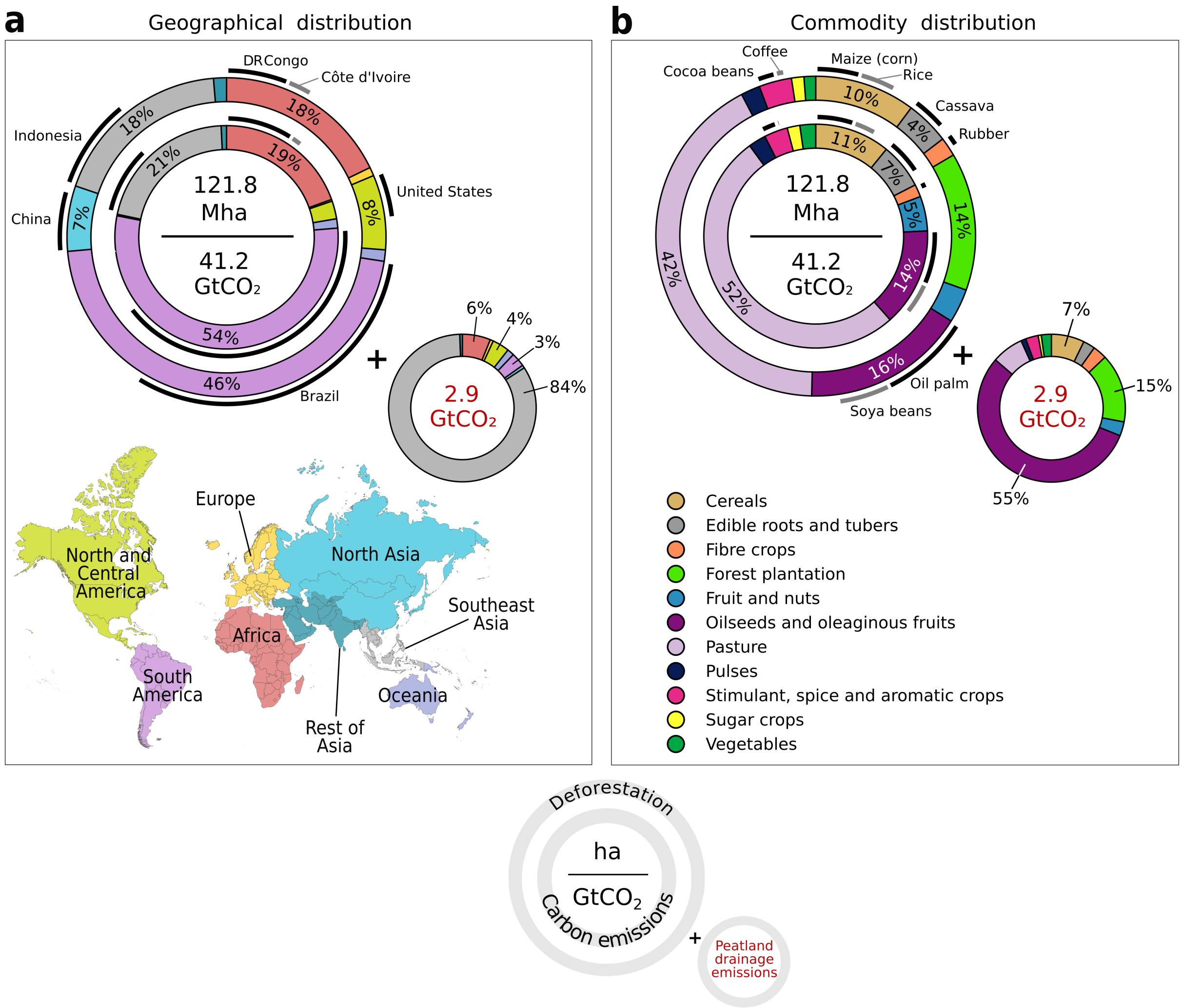

Fig. 3 | Global overview of deforestation and carbon emissions (2001-2022). Deforestation is attributed to agriculture and forestry commodities and corresponding carbon emissions globally, categorised by (a) geographical regions and (b) commodity groups. In the concentric rings, the outer ring depicts the proportional deforestation by area, while the inner ring shows carbon emissions. Emissions from peatland drainage are presented separately. Central insets mention total deforestation (in million ha) and carbon emissions (in $GtCO_2$), with selected major deforestation contributors and commodities accentuated along the periphery of the concentric circles. All values represent the total sum of deforestation and carbon emission estimates from 2001 to 2022. The contribution of commodities, broken down by geographical regions, is illustrated in Supplementary Fig. 2.

Our analysis also reveals an uneven distribution of both deforestation and the resulting carbon emissions across regions and commodities (Fig. 3): South America leads in both, with

Southeast Asia and Africa also showing major contributions. Together, these three regions account for roughly 82% of global deforestation and 94% of carbon emissions due to expanding agriculture and forest plantations. Additionally, deforestation in Southeast Asia alone is responsible for nearly 84% of global peatland drainage emissions (Fig. 3a). Still, two countries outside the tropics – China and the United States – closely trail the top three countries globally – Brazil, Indonesia, and the Democratic Republic of Congo (DR Congo) – in terms of deforestation area, though not in carbon emissions (Fig. 3a). We suspect that the lower deforestation estimates associated with forest plantations in boreal regions (Fig. 4) may be due to datasets inadequately capturing the conversion of natural forests and the absence of a primary forest mask[51], likely leading to their underestimation in our estimates.

In terms of specific commodity groups, deforestation driven by pasture expansion (primarily for cattle meat production) represents about 42% of total deforestation and 52% of the carbon emissions (Fig. 3b and 4). This is followed by the cultivation of oilseeds and oleaginous fruits, especially oil palm and soybeans, which account for 16% of total deforestation and 14% of carbon emissions. Notably, oil palm-induced deforestation, primarily in Southeast Asia, alone accounts for nearly 55% of peatland emissions (Fig. 3b and 4). Other significant contributors to deforestation include forest plantations (14%), stimulant and aromatic crops (3%, largely driven by cocoa beans and coffee cultivation), and fibre crops (2%, mostly rubber) (Fig. 3b).

While these commodities are included in the EUDR[15] due to their high deforestation and trade shares, our analysis also reveals that staple crops—specifically maize, rice and cassava—cumulatively account for about 11% of total deforestation (Fig. 3b), exceeding that of cocoa, coffee, and rubber. Unlike other commodities, whose production and deforestation are concentrated in specific regions (e.g., oil palm in Southeast Asia, soybeans in South America), the deforestation hotspots for staple crops are globally distributed (Fig. 4). Moreover, given that nearly half of the global average human diet consists of staple commodities[52], and their cultivation is expected to increase to feed the growing population[53], incorporating staple crops into deforestation monitoring and regulatory frameworks will be vital for curbing global deforestation, promoting sustainable agricultural supply chain and ensuring future food security.

When comparing our estimates for major deforestation-risk agricultural commodities with other datasets (Supplementary Fig. 3), we find that while trends for certain commodities, such as cocoa beans in Côte d'Ivoire and Ghana, oil palm in Indonesia, and pasture in Brazil, are consistent across different datasets, significant differences arise for other major forest-risk commodities. While these discrepancies are less pronounced at the global or pan-tropical level, they become quite stark at the individual country-commodity level (Supplementary Fig. 3). Depending on the use case—such as assessing the deforestation footprint of production or imports—the choice of dataset can substantially impact a country's forest conservation and carbon emission reduction targets.

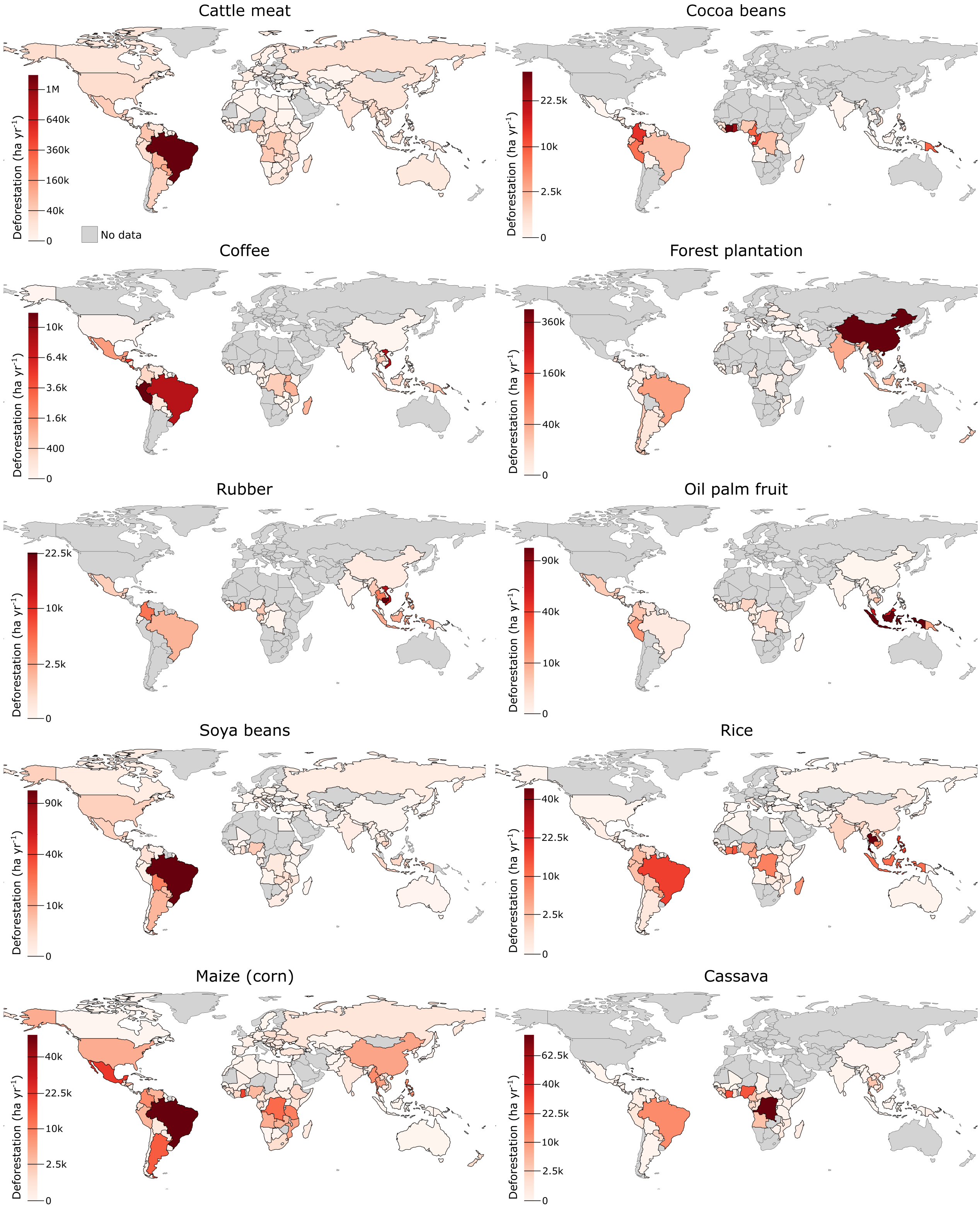

Fig. 4 | Hotspots of major deforestation-risk commodities (aggregated for 2018-2022). This figure illustrates the spatial distribution of deforestation-risk commodities regulated under the European Union Deforestation Regulation (EUDR), along with major staple crops. In this figure, the deforestation estimates are averaged over the recent five years (2018-2022) and represented in ha yr^{-1}. The quality index for these commodities is detailed in Supplementary Fig. 4. Deforestation-risk hotspots for the commodities (shown above) in Brazil at the municipality-level are illustrated in Supplementary Fig. 5.

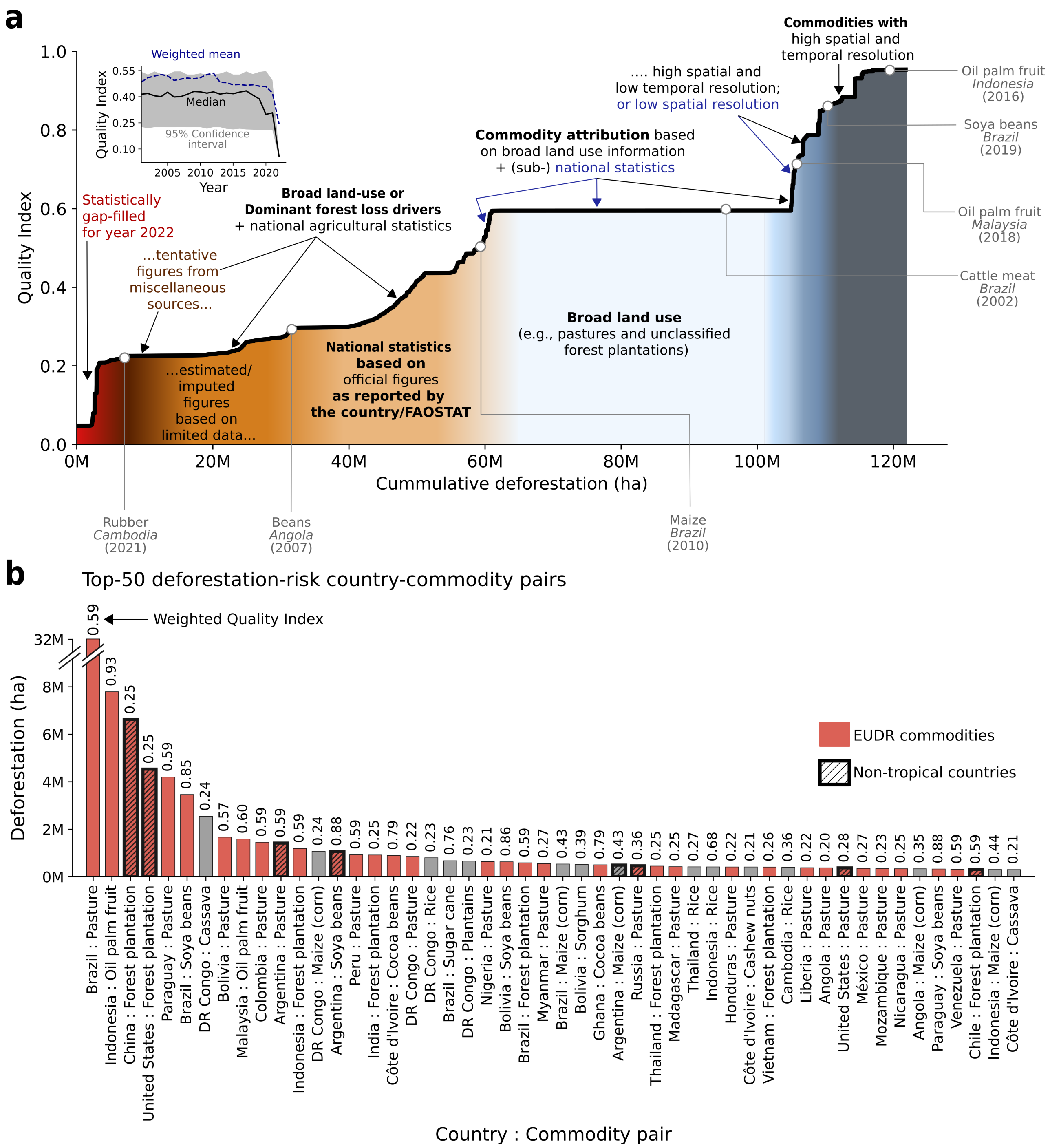

Fig. 5 | Evaluating the quality of commodity-driven deforestation estimates (2001-2022). (a) The ranked line plot visualises the quality index score of all deforestation estimates for different country-commodity pairs, arranged from the lowest quality index score (on the left) to the highest (on the right) between 2001-2022. The insets (in a) provide insights into the dominant data types and their level of explicitness, which contribute to the respective quality index rankings. The 95% confidence interval in the temporal quality index subplot (in a) represents the 2.5th and 97.5th percentiles of the quality index values. (b) To highlight the quality of data currently used for deforestation attribution (2001-2022), we present the top 50 deforestation-risk country-commodity pairs along with their respective weighted average quality index. These top 50 country-commodity pairs account for approximately 70% of global deforestation.

4. Quality assessment and potential for model improvement

The Quality Index, which is based on the spatio-temporal granularity and the explicitness of the spatial and statistical datasets used as model inputs, indicates the quality or reliability of the resulting deforestation estimates (see 'Quality assessment' in Methods). Only 12-15% of attributed deforestation in DeDuCE is derived from spatial commodity-specific datasets, representing dLUC (Quality Index ≥ 0.6; Fig. 5a). In contrast, 30-35% of the attribution uses broad spatial land-use information (e.g., the extent of pastures), mainly attributing deforestation to cattle meat and forest plantations (dLUC; 0.6 > Quality Index ≥ 0.55). The remaining 50-58% blends spatial and statistical datasets, where the resulting estimates should be interpreted as a measure of deforestation risk (sLUC; Quality Index < 0.55) (Fig. 5a). In this case, deforestation estimates derived from officially reported agricultural statistics (including sub-national statistics) receive a higher score, whereas those imputed or estimated by FAOSTAT are assigned a lower score, as illustrated by the progression of FAO quality flags in Fig. 5a.

Despite using the best available datasets, pixel- or municipality-level deforestation attribution is limited to certain commodities and countries (Supplementary Tables 1-3). Thus, we must target areas where enhancements will significantly boost the quality of deforestation estimates. Examining the quality index of the top-50 deforestation-risk country-commodity pairs (accounting for 70% of global deforestation; Fig. 5b), we find that forest plantations (in China, the United States, and India) and pastures (outside South America) often receive lower quality index scores. This is likely due to the challenge of mapping pastures and forest plantations, as their spectral signatures are similar to natural grasslands and forests. Additionally, staple commodities are not well represented in terms of data quality, even though several countries have significant deforestation associated with these commodities (Fig. 5b). Furthermore, due to poor-quality spatial data and agricultural statistics, African countries show consistently lower-quality deforestation estimates, which include commodities such as cassava, maize, rice, beans, and cocoa (Fig. 5b).

Consequently, global deforestation attribution could be significantly improved by incorporating global maps of (i) pastures, (ii) forest plantations, and (iii) cereals (primarily for maize and rice), as well as (iv) improving spatial representation of agricultural commodities contributing to deforestation in Africa (particularly in DR Congo and Nigeria). Existing initiatives like Global Pasture Watch[54], the Spatial Database of Planted Trees[55] (SDPT), the WorldCereal database[56], and the Global Subnational Agricultural Production[57] (GSAP) database could provide critical data to help close these gaps in the near future.

5. Influence of modelling assumptions on deforestation and carbon emission estimates

To assess the robustness of the DeDuCE model, we examined the sensitivity of deforestation and carbon emission estimates to various modelling assumptions (Table 1). The most notable changes were observed when we ran the model solely or primarily as a statistical deforestation attribution model, using the global forest change[28] (GFC) data only (similar to ref.[49]) or together with data on dominant forest loss drivers[24] (similar to refs.[21,22]). In these cases, deforestation and carbon emission estimates were inflated by 40-85% compared to our current estimates (Table 1), explaining the discrepancy with Crippa et al.[8]. This inflation occurs because these attribution methodologies use poor-quality data that overlook spatio-temporal heterogeneities.

Another significant source of uncertainty regards forest and deforestation definitions: changing tree cover thresholds or baseline forest maps changed deforestation estimates by as much as -30% to +7% (Table 1). Notably, using the EU Joint Research Centre's (JRC's) recent forest cover map[58] resulted in a 12% reduction in deforestation estimates. Although this map closely aligns with

FAO's forest definition[3] and excludes agriculture and forest plantations – despite its flaws[59] – its 2020 base year makes it unsuitable for our 2001-2022 deforestation attribution. Comparing our results with JRC's tropical moist forest (TMF) deforestation data[60,61] led to a nearly 30% reduction in estimates. The core reason lies in methodological differences: GFC detects the first tree cover loss event annually, whereas JRC TMF only identifies deforestation when disturbances in a tree cover pixel persist for more than 2.5 years[62]. Additionally, JRC TMF deforestation does not account for the loss of dry forests, making its deforestation estimates more conservative.

Another parameter significantly influencing model estimates is the period between forest loss detection and agricultural land establishment used for attributing deforestation. We find that a longer lag period captures more delayed land-use changes (often in the case of tree crops and forest plantations), while a shorter lag period does the opposite (Table 1). Interestingly, another major source of model uncertainty that is difficult to account for globally is multiple cropping (i.e., multiple harvesting cycles on the same land). Analysing results for Brazil, we found that not accounting for multi-cropping increased deforestation estimates by about 20-50% for commodities with larger harvested areas (e.g., maize, beans; potentially due to proportional commodity attribution in Supplementary equations (9)-(12)) while reducing estimates for those with lower harvested areas (e.g., groundnuts) (Table 1). Despite 12-20% of global croplands being multi-cropped[63], assessing their dynamics on a global scale remains challenging due to the lack of appropriate data that captures the multiple harvest cycles of globally diverse crop combinations.

Table 1 | Sensitivity of deforestation and carbon emission estimates to modelling parameters. The absolute reference and sensitivity analysis values are provided in Supplementary Table 5. The deforestation attribution and carbon emission estimates from all sensitivity analyses are made available on Zenodo (see Data availability).

Broad category	Sensitivity control		% Change from reference: Deforestation	% Change from reference: Carbon Emissions
Forest and deforestation	Tree cover density[28]	≥ 10%	6.59	1.42
		≥ 75%	-29.98	-10.97
	JRC Global forest cover 2020[58] *(only compared with estimates from 2020-2022)*		-11.15	-39.72
	JRC TMF Deforestation[60,61] *(only compared for TMF countries)*		-28.17	-18.84
Forest plantation	All plantations from SDPT[55] established before the year 2000	All commodities	-0.03	<0.01
		Only forest plantations	-0.17	-0.41
Lag period	Spatial lag period *(only compared for MapBiomas countries)*	1 year	-9.95	-8.97
		5 years	4.25	3.82
	Statistical lag period	1 year	-0.72	-0.84
		5 years	0.09	0.54
Inclusion of spatial datasets	Partial statistical attribution (only using Global forest change[28], dominant driver of forest loss[24] dataset and agricultural statistics[31])	All commodities-Global	40.53	39.48
		Oil palm-Indonesia	19.72	38.82
		Cocoa-Côte d'Ivoire	-29.21	-42.56
		Soya beans-Brazil	234.81	373.56
	Full statistical attribution (only using Global forest change[28] dataset and agricultural statistics[31])	All commodities-Global	86.00	73.12
		Oil palm-Indonesia	20.27	36.19
		Cocoa-Côte d'Ivoire	-28.87	-42.16

		Soya beans-Brazil	151.83	246.03
Land-use expansion	Croplands do not expand over pastures first, directly forests		0.22	0.31
	Net agricultural expansion		-7.63	-9.20
	All statistical land-use attribution restricted by FAOSTAT		-1.23	-1.65
	All statistical land-use attribution not restricted by FAOSTAT		20.78	28.08
Agriculture statistics *(only for Brazil)*	National-level agricultural statistics		0.12	0.10
Multiple cropping *(only for Brazil)*	Not accounting for the harvested area from multiple cropping	Maize	35.38	35.83
		Beans	19.56	29.11
		Potatoes	47.63	39.65
		Groundnuts	-7.13	-9.16
Amortisation period *(compared with amortised estimates of year 2020)*	10 years		-0.58	-1.13
	15 years		1.68	2.24
	20 years		-0.33	1.01

6. Discussion

The DeDuCE model reinforces that food systems are the primary driver of deforestation (Fig. 1 and 3) and a major source of global carbon emissions[8]. The data produced by the model can serve as a strong evidence base for developing national GHG inventories[64], reporting standards[30], targeted policies[12], and regulatory frameworks[29]. Such guidance is crucial for private and public sector organisations to manage and adapt their operations and value chains in line with global sustainability targets[65].

The importance of developing food system emission inventories was highlighted at COP 28, where nations were urged to integrate agriculture and food systems into their national climate and biodiversity plans[66]. To meet this commitment, governments must comprehensively assess their food system impacts – by estimating agricultural land-use changes and associated carbon emissions – and set targets to reduce emissions in their Nationally Determined Contributions (NDCs) by 2025. Shifting from broad-stroke assessments[8] to detailed, commodity-specific deforestation and carbon emission estimates will help identify priority areas for targeted actions. Furthermore, globally consistent food system emission estimates are crucial for coordinating global action and aligning conservation and mitigation strategies[67].

The private sector also stands to gain from globally comprehensive deforestation and carbon emission accounting. A prime example is the Science-Based Targets initiative for Forest, Land, and Agriculture (SBTi FLAG)[29], which guides companies in setting emission reduction targets and provides independent validation of these targets against current sustainability goals. With a specific focus on deforestation due to EUDR commodities, rice, maize, and wheat, among other products, companies should use the best and most complete data available per commodity and region, trailing back 20 years, to comprehensively assess their present emissions[29]—a requirement for which the DeDuCE data is highly suited. This also applies to financial institutions, which are increasingly called upon to evaluate the sustainability of their investments[68].

The estimates from the DeDuCE model can also support assessments of the environmental footprint of food consumption and the deforestation exposure of global supply chains. Combining our deforestation estimates with a physical trade model[69] (see Data availability), we find that in 2022, about 30% of global agricultural deforestation was embodied in traded goods. South America and Southeast Asia are major exporting hubs for these deforestation-risk commodities, while China, the EU, the United States, India, and Japan are major importers (Extended Data Fig. 2a).

Furthermore, the EU, being the second largest trader of deforestation-risk agricultural commodities, accounts for about 14% of all globally traded deforestation-risk agricultural commodities. Major EU economies, such as Germany, Spain, Italy, France and the Netherlands, are primary importers of cocoa, coffee, oil palm, soybeans, cattle meat, and maize (Extended Data Fig. 2b).

The EUDR—set to launch by the end of 2024[15]—requires food system actors to establish due diligence systems that mitigate deforestation risks within supply chains[70]. These systems must reflect the deforestation-risk of exporter countries, based on a benchmarking system designed to account for rates of deforestation, agricultural expansion, and commodity production[15]. However, unclear thresholds for classifying deforestation-risk benchmarks[15] due to the lack of global-scale spatio-temporal deforestation data have posed significant challenges for implementing the EUDR[59]. We believe that the commodity-driven deforestation estimates provided by the DeDuCE model can offer essential input for EUDR risk benchmarking.

While the EUDR aims to promote sustainable land-use practices, many exporter countries have expressed concerns about its implications on trade due to their economic priorities, legal frameworks, and the additional costs required to develop enforcement capabilities[71,72]. These factors can, in turn, increase the potential for leakages to non-EU markets[73] (Extended Data Fig. 2a). The estimates from the DeDuCE model can be used to assess such leakages for countries committed to achieving their climate goals.

In conclusion, we believe that the versatility of the DeDuCE model, combined with the comprehensiveness of its results, which integrate the best available spatial and statistical data to provide up-to-date estimates of commodity-driven deforestation and carbon emissions, makes it ideal for a broad range of global forest conservation and climate change mitigation efforts.

7. Methods

The DeDuCE model leverages a comprehensive array of spatial datasets and agricultural statistics to quantify deforestation and the associated carbon emissions from agricultural and forestry activities. The modelling framework involves three primary steps (Extended Data Fig. 1): (i) *Deforestation attribution*, categorised into spatial and statistical attribution, pinpoints the locations (wherever possible) and extent of forest loss attributable to the production of agriculture and forestry commodities. By superimposing multiple datasets on tree cover loss pixels, each with varying degrees of scope and detail, we aim to capture the most comprehensive information possible regarding the drivers of forest loss. (ii) *Carbon emissions calculation* assesses the carbon emissions generated from deforestation linked to production of agriculture and forestry commodities, including emissions from deforestation over peatlands (through peatland drainage). (iii) *Quality assessment or flagging* scrutinises the reliability of our deforestation estimates by examining the quality of the input data and its contribution to model's estimates (Extended Data Fig. 1).

The model generates annual deforestation and carbon emission estimates, along with a quality index for each country-commodity pairing at the national level (and sub-national level for Brazil), adhering to the administrative boundaries defined by the Database of Global Administrative Areas (GADM) version 4.1[74]. Detailed information on the datasets used in this model is presented in Supplementary Table 3.

7.1 Deforestation attribution

Spatial attribution directly utilises a wealth of remote sensing data to allocate tree cover loss to either specific commodities (e.g., soybeans or oil palms), specific land uses (e.g., croplands, pastures, forest plantations, or mixed land-use mosaics), or broad deforestation drivers (e.g., commodity-driven deforestation or forestry activities) (Extended Data Fig. 1). When the proximate cause of deforestation is not attributable to a single commodity via spatial attribution, we employ statistical attribution using agricultural and forestry statistics to attribute deforestation to specific commodities (Supplementary Fig. 1). Presently, the model cannot attribute deforestation to commodities for which we don't have any spatial and statistical data available. However, building on existing datasets help provide an internally consistent picture of deforestation drivers globally[18,49].

7.1.1 Spatial attribution

We begin by defining forest and deforestation. Forests are composed of trees established through natural regeneration[3]. The conversion of these natural forests to other land uses is referred to as deforestation[3]. This definition excludes forest plantations, which are intensively managed for wood, fiber, and energy[3]. To delineate these categories, we use the global forest change dataset[28] as a foundational layer (Extended Data Fig. 1). This dataset defines tree cover based on the presence of woody vegetation exceeding 5m in height, with tree cover loss representing the replacement of woody vegetation within each 30m pixel. Recognising that not all woody vegetation constitutes natural forest, we adopt a tree cover density threshold of ≥25% per pixel[75] and apply a global forest plantation mask (Supplementary Fig. 6; see 'Forest plantation mask' discussion in Supplementary Methods) to distinguish natural forests from managed forests (i.e., natural forest loss from rotational clearing of forest plantations). Pixels not meeting this natural forest criterion are excluded from further assessments. While we apply this ≥25% tree cover density threshold, our DeDuCE model is designed with the flexibility to adjust this threshold to suit varying definitions of forest and deforestation (Table 1).

To assess the contribution of agricultural and forestry activities to annual deforestation, we overlay different land-use products that demarcate cropland[76], forest plantation[77] and pasture extents[78], crop commodities such as soybeans[16] and cocoa[79] on an annual tree cover loss layer[28] spanning from 2001 to 2022 (Extended Data Fig. 1 and Supplementary Table 3; see 'Processing temporally explicit and temporally aggregated datasets' discussion in Supplementary Methods). Through this, we gain insights into (i) whether a given pixel of forest loss constitutes deforestation and (ii) what was the proximate cause of that deforestation (Extended Data Fig. 1).

To ensure a coherent integration of this data, we employ a hierarchical attribution based on a scoring system that evaluates each dataset's relevance based on spatial coverage, temporal frequency, and the specificity of deforestation driver and causation (i.e., explicitness) (Supplementary Table 6). Further particulars of this scoring system are delineated in the 'Quality assessment' subsection below, but for each forest loss pixel, we prioritise the most detailed information on the direct cause of forest loss. This means that we prioritise spatial data on specific agricultural commodities, then broader land use categories, and finally general or dominant forest loss drivers. Whenever datasets overlap in content (similar land use or commodity), those with higher spatio-temporal resolution take precedence. Furthermore, our model refrains from attributing forest loss to spatial data beyond the most recent year of available information, ensuring that our analysis reflects the latest land use status. This approach ensures that once a pixel's forest loss driver is accounted for, it is no longer considered in the further attribution process.

In the final step of the spatial attribution, we address forest loss resulting from fires, a natural process crucial for ecological equilibrium, particularly in boreal regions. We systematically remove fire-related forest loss from our deforestation attribution, using spatio-temporal data[44] that identifies such events. Additionally, for regions not captured by the commodity and land-use datasets listed in Supplementary Table 3, we employ a global dataset by Curtis et al.[24] that identifies the dominant drivers of forest loss (supplemented with the global forest plantation mask to segregate natural forest loss from the rotational clearing over managed plantations post the year

2000; Supplementary Fig. 6). All preprocessing methodologies applied to these spatial datasets are detailed in Supplementary Table 7.

The result of the spatial attribution is a dataset that summarises, at the (sub-)national level, the amount of deforestation attributed to specific commodities and land uses (croplands, pastures, or forest plantations), as well as mosaics of multiple land-use and deforestation drivers (Extended Data Fig. 1). The entire process of spatial deforestation attribution, involving the analysis of terabytes of spatial data, is conducted utilising GEE.

7.1.2 Statistical attribution

Despite spatial attribution, considerable deforestation remains unclassified to specific commodities. This occurs for three main reasons: (i) when we have specific land-use information indicating the cause of deforestation is either a cropland, pasture or forest plantation; (ii) the presence of land-use mosaics, specifically the MapBiomas[78] dataset, which identifies pixels as a cropland and pasture mosaic when the algorithm cannot distinctly separate the two, or the Curtis et al.[24] dataset, which determines the primary driver of forest loss aggregated over a 22-year period; or (iii) instances where forest loss is not linked to any specific commodity or land-use by the existing spatial datasets (Supplementary Table 3). To address the ambiguity in the latter two cases and attribute forest loss to a specific commodity, we follow a two-step statistical land-balance approach (Supplementary Fig. 1).

In this two-step statistical attribution (Supplementary Fig. 1), we first attribute deforestation (from the latter two cases) to either cropland, pasture, or forest plantations. This method utilises annual land use data from FAOSTAT[31] and FRA[3] to inform on the extent of land-use expansion in these indeterminate areas of deforestation (referred to as 'statistical land-use attribution' in Extended Data Fig. 1; see 'Statistical land-use attribution' discussion in Supplementary Methods). Building on these land-use expansions, we further attribute cropland-driven deforestation to various crop commodities according to their respective increases in harvested area (again using FAOSTAT[31]; referred to as 'statistical commodity attribution' in Extended Data Fig. 1 and Supplementary Fig. 1). Similarly, deforestation from pasture expansion is allocated between cattle meat and leather. Deforestation attributed to forest plantations is allocated broadly to forestry products, due to the absence of detailed forestry-commodity information. A detailed description about the 'Statistical commodity attribution' is presented in Supplementary Methods.

7.2 Carbon emissions calculation

To calculate carbon emissions, excluding those from peatland drainage, we assess changes in carbon stocks due to forest loss. Our analysis concentrates on five key stocks: aboveground biomass (AGB), belowground biomass (BGB), dead wood, litter and soil organic carbon (SOC) (Extended Data Fig. 1). Notably, belowground biomass and soil organic carbon losses are typically delayed responses to aboveground disturbances[22]. However, for the purpose of our analysis, these losses are treated as if they are an inevitable consequence of the deforestation, often referred to as 'one-off' or 'committed' losses. Essentially, it implies that once a region is deforested, the belowground carbon and associated SOC is also considered lost, even though it might happen slowly over time.

AGB per pixel (in Mg px^{-1}) is derived from the aboveground live biomass density data for year 2000 at 30-m resolution[33]. Based on this spatial AGB map and a 1-km resolution map of root-to-shoot biomass ratio[80], we estimate BGB. Deadwood and litter biomass densities are also spatially calculated as proportions of AGB, informed by biome-specific lookup tables that factor in elevation and precipitation (lookup table in ref.[33]) (Supplementary Table 3). These biomass densities are converted to carbon densities (i.e., MgC px^{-1}) using a standard biomass-to-carbon conversion ratio of 0.47 for forest ecosystems, as recommended by the IPCC[81].

We commence by calculating the committed carbon emissions from AGB, BGB, dead wood, and litter. For spatially attributed commodities, carbon emissions are calculated by overlaying forest loss pixels onto the corresponding total carbon stock maps. For statistically attributed commodities, emissions are apportioned based on their proportion to the total forest loss associated with that commodity's land-use (carbon emissions are also partitioned and aggregated using the same logic as commodity attribution; see Supplementary Methods). Hence, if maize's statistically attributed forest loss accounts for 50% of all forest loss from croplands, maize would also bear 50% of the total (statistical) carbon emissions attributed to (statistical) cropland expansions.

Soil organic carbon (SOC) stock data is obtained from the SoilGrids2.0 dataset[34], which provides SOC stocks at varying depths at 250-m resolution (in MgC ha^{-1}). For our purposes, we consider SOC within the top 100cm of soil, the layer most affected by land-use changes, and upscale this data to a 30-m resolution (estimates expressed in MgC px^{-1}). In light of limited data on SOC losses over deforested regions, we adopt an alternative approach informed by meta-analyses – which indicates that converting natural forests to either a cropland, pasture or forest plantation will typically result in decreased SOC stocks. Consequently, we represent the emission from SOC loss as a fraction of the existing SOC stocks for different replacing land use and biome of deforestation (Supplementary Table 8). These emissions from SOC losses are then added to the carbon emissions calculated from AGB, BGB, deadwood and litter, culminating in a comprehensive gross carbon emission estimate (equation (1)).

From the emissions outlined above, we deduct the committed carbon sequestration potential of the replacing commodity (e.g., carbon stored as vegetation biomass if the replacing land use is maize or forest plantation) (equation (1)). This deduction is informed by a meta-analysis of mature plant carbon stocks across commodities (in MgC ha^{-1}), and categorised into 40 commodities across 11 commodity groups (Supplementary Table 9). If a specific commodity data is absent, we associate it with plant carbon stocks of its respective commodity group (see Lookup table in Data availability). The resulting net carbon emissions are then expressed in megatonnes of CO_2 ($MtCO_2$).

$$\begin{matrix}\text{Net carbon}\\\text{emissions}\end{matrix} = \text{AGB} + \text{BGB} + \text{Deadwood} + \text{Litter} + \text{SOC loss} - \begin{matrix}\text{Plant carbon stocks of}\\\text{replacing commodity}\end{matrix} \quad (1)$$

7.2.1 Peatland drainage emissions

To align with the deforestation attribution analysis, our model concentrates on carbon emissions from deforestation occurring on peatlands post-2000, deliberately excluding continuous emissions from established agricultural peatlands or those deforested earlier. By superimposing a high-resolution global peatland map (a composite map prepared from multiple sources at 30-m resolution; see ref.[35]) onto identified forest loss, we isolate peatland deforestation linked to specific commodities and land-uses post-2000 (Extended Data Fig. 1). In the presence of spatial commodity data, overlapping peatland deforestation is directly attributed to the corresponding commodity. In their absence, however, we evenly allocate deforested peatland areas among all identified commodities expansions within a country (similar to statistical attribution).

To estimate the emissions from peatland drainage, we use emission factors reported by published literature (often represented in $MgCO_2$ ha^{-1} yr^{-1}). These factors are informed by subsidence observations and standardised rates of peat oxidation, providing a scientifically grounded approach to these emission factor calculations[81,82]. Based on previous meta-analyses of peatland emission factors[81–84] (Supplementary Table 10), we have stratified emission factors by land-use expansions (such as peatland drainage due to cropland, pasture or forest plantation expansions; or oil palm expansions specifically) and deforestation biome (i.e., tropical, temperate and boreal), which allows us to apply these factors to specific drainage conditions for different biomes. We multiply these emission factors with peatland drainage area (result expressed in $MgCO_2$ yr^{-1}). Unlike committed emissions, these peatland drainage emissions continue to accumulate, year on year, from the initial deforestation event until the conclusion of our study period (see 'Peatland drainage emissions' discussion in Supplementary Methods). For instance, if a hectare of peatland is cleared and drained for oil palm in 2010 incurs annual emissions of 54.41 $MgCO_2$ every year, this yearly emission persists through to the year 2022, irrespective of subsequent deforestation activities in the interim period.

In addition to providing annual (i.e., unamortised) deforestation and carbon emission estimates for country-commodity pairings, we also present amortised estimates (excluding peatland drainage emissions). For amortisation, we distribute these estimates evenly over a 5-year period. This amortisation aligns the temporal scale of deforestation's impact with the timeframe of agricultural production, offering a more nuanced understanding of the long-term environmental footprint of crop cultivation and forestry activities[85,86] (see 'Intention of amortised and unamortised estimates' discussion in Supplementary Methods).

7.3 Quality assessment

Our methodology integrates multiple spatial and statistical datasets, making it necessary to assess the quality or reliability of our deforestation estimates aggregated for each country-commodity pairing (Extended Data Fig. 1 and Fig. 5). This assessment should not be confused with just the accuracy of underlying datasets or the model's deforestation estimates, as the latter is particularly challenging to assess for a dataset of this scale and comprehensiveness. To quantify the quality of our deforestation estimates, we take into account three factors (equation (2)):

i. Forest loss or deforestation ($FL_{i,t}$) attributed to a specific commodity (i) in a specific region and year (t).
ii. Overall Accuracy (OA_j) of the input dataset (j), which contributed to the aggregation of final deforestation estimates. This value is provided by the respective studies and datasets (Supplementary Table 3) and is assumed to encompass all aspects of input data's accuracy. Thus, $FL_{i,j}$ represents the contributions from each input data source (j) to the deforestation estimates attributed to a specific commodity (i).
iii. $Score_j$, a metric developed by us to normalise OA_j and make it comparable between all the input datasets of different types (i.e., remote sensing-based and statistical) (see 'Scoring metric justification' in Supplementary Methods and Supplementary Table 6). This normalisation hinges on three pivotal (and equally weighted) criteria assessing each input dataset's spatial and temporal granularity, as well as explicitness or specificity of deforestation driver (Supplementary Table 11).

Spatially, a maximum score (of '1') is assigned to datasets with a resolution finer than or equal to 10-m, tailored to individual countries. Temporally, annual datasets from 2001-2022 for herbaceous crops, and comprehensive data from 2000 or earlier for tree crops and forest plantations, receive the top score. For tree crops and forest plantations, data from the year 2000 or earlier allows us to distinguish post-2000 deforestation from rotational clearing, thus removing the need for plantation mask. For explicitness, datasets mapping a singular agricultural or forestry commodity, validated by field data, are scored highest. Fluctuating from these conditions, the score of the dataset is penalised. The detailed scoring criteria are mentioned in Supplementary Table 11.

This approach above works well when only spatial commodity datasets contribute to deforestation estimates (dLUC) (equation (2) and see 'Calculation of Quality Index' discussion in Supplementary Methods). However, the datasets we use also include broad spatial land-use information, which, when combined with agricultural land-use and commodity production statistics, provide estimates of commodity-driven deforestation (sLUC). In such cases, it is crucial to reflect the reliability of these agricultural statistics in the quality of our deforestation estimates. Since FAOSTAT do not provide overall accuracy, but report *Flags*—a qualitative assessment of the reported value (see the description of FAOSTAT flags in Supplementary Table 12)—we incorporate them into our quality assessment framework. We achieve this by multiplying the overall accuracy of the spatial land-use dataset (OA_j ; Supplementary Table 6) with the agricultural statistics quality flags (equation (2) and see 'Calculation of Quality Index' discussion in Supplementary Methods). Within these quality flags, data reported by official sources to FAOSTAT receive the highest score, while those that are estimated, imputed, or extracted from unofficial sources are assigned progressively lower scores (see Supplementary Table 12).

$$Quality\ Index_{i,t} = \frac{\sum_{j=1}^{n}\left(FL_{i,j} \times OA_{\mathrm{j}} \times Score_{j}\right)_{t}}{FL_{i,t}}, \quad OA_j = \begin{cases} OA_j & \text{if only spatial commodity datasets contribute to deforestation attribution} \\ OA_j \times \left(\dfrac{Flag_{land\ use} + Flag_{production}}{2}\right) & \text{otherwise} \end{cases} \tag{2}$$

In the DeDuCE model's two-step land-balance approach, we use two agricultural statistics. Here, $Flag_{land\ use}$ and $Flag_{production}$ represent the quality of land-use and commodity production data, respectively. It is important to note that the IBGE dataset for Brazil does not provide flags for commodity production ($Flag_{production}$). Thus, we assign a value of '1', reflecting the official figure flag as IBGE directly reports the data. Examples of Quality Index calculations under various scenarios are provided in the Supplementary Methods.

Data availability: The unamortised and amortised deforestation and carbon emission estimates generated by the DeDuCE model, including those from sensitivity analyses are available on Zenodo: https://doi.org/10.5281/zenodo.13624636. All the datasets used in this study are documented in Supplementary Table 3. The insights from the DeDuCE model can be viewed at: https://www.deforestationfootprint.earth.

Code availability: The Google Earth Engine and Python code for running the DeDuCE model, and those needed to replicate the analysis presented in this study are available at GitHub: https://github.com/chandrakant6492/DeDuCE.

Acknowledgements: This research contributes to the Global Land Programme (https://www.glp.earth). C.S. and U.M.P acknowledge the funding support from ÅForsk Foundation (Project name: ReDUCE and grant no.: 22-64) and the Belmont Forum, through FORMAS (Project name: BEDROCK and grant no.: 2022-02563). We also acknowledge the constructive feedback provided by Chris West, Simon Croft and Vivian Ribeiro from the Stockholm Environment Institute, Nancy Harris and Elizabeth Goldman from the World Resources Institute, during various stages of this manuscript's development. We would also like to thank Thomas Kastner from the Senckenberg Biodiversity and Climate Research Centre for his assistance in running the trade model.

Author contributions: C.S. and U.M.P conceived the study. C.S. led the data analysis, visualisations and writing of the original draft, with substantial feedback from U.M.P. Both authors contributed to interpreting the results and subsequent revisions to the paper.

References

1. FAO. The State of the World's Forests 2022 – Forest Pathways for Green Recovery and Building Inclusive, Resilient and Sustainable Economies. (FAO, Rome, 2022). doi:10.4060/cb9360en.
2. Pendrill, F. et al. Disentangling the numbers behind agriculture-driven tropical deforestation. Science **377**, eabm9267 (2022).
3. FAO-FRA. Global Forest Resource Assessment 2020. https://fra-data.fao.org/assessments/fra/2020 (2023).
4. Ritchie, H. & Roser, M. Deforestation and Forest Loss. Our World in Data (2023).
5. IPBES. Global Assessment Report on Biodiversity and Ecosystem Services of the Intergovernmental Science-Policy Platform on Biodiversity and Ecosystem Services. https://zenodo.org/record/3831673 (2019) doi:10.5281/ZENODO.3831673.
6. Friedlingstein, P. et al. Global Carbon Budget 2023. Earth System Science Data **15**, 5301–5369 (2023).
7. Intergovernmental Panel on Climate Change (IPCC). Summary for Policymakers. Climate Change 2021: The Physical Science Basis. Contribution of Working Group I to the Sixth Assessment Report of the Intergovernmental Panel on Climate Change 3−32 (2021) doi:10.1017/9781009157896.001.
8. Crippa, M. et al. Food systems are responsible for a third of global anthropogenic GHG emissions. Nat Food **2**, 198–209 (2021).
9. Poore, J. & Nemecek, T. Reducing food's environmental impacts through producers and consumers. Science **360**, 987–992 (2018).
10. Li, Y. et al. Changes in global food consumption increase GHG emissions despite efficiency gains along global supply chains. Nat Food **4**, 483–495 (2023).
11. Xu, C., Kohler, T. A., Lenton, T. M., Svenning, J.-C. & Scheffer, M. Future of the human climate niche. Proceedings of the National Academy of Sciences **117**, 11350–11355 (2020).
12. Goetz, S. J. et al. Measurement and monitoring needs, capabilities and potential for addressing reduced emissions from deforestation and forest degradation under REDD+. Environ. Res. Lett. **10**, 123001 (2015).
13. New York Declaration on Forests - Action Statements and Action Plans. https://unfccc.int/media/514893/new-york-declaration-on-forests_26-nov-2015.pdf (2014).
14. Food and Agriculture Organization of the United Nations. Zero-Deforestation Commitments: A New Avenue towards Enhanced Forest Governance? (2018).
15. European Union. REGULATION (EU) 2023/1115 OF THE EUROPEAN PARLIAMENT AND OF THE COUNCIL of 31 May 2023 on the making available on the Union market and the export from the Union of certain commodities and products associated with deforestation and forest degradation and repealing Regulation (EU) No 995/2010. https://eur-lex.europa.eu/legal-content/EN/TXT/HTML/?uri=CELEX%3A32023R1115 (2023).
16. Song, X.-P. et al. Massive soybean expansion in South America since 2000 and implications for conservation. Nat Sustain 1–9 (2021) doi:10.1038/s41893-021-00729-z.

17. Gaveau, D. L. A. et al. Slowing deforestation in Indonesia follows declining oil palm expansion and lower oil prices. PLOS ONE **17**, e0266178 (2022).
18. Goldman, E., Weisse, M., Harris, N. & Schneider, M. Estimating the Role of Seven Commodities in Agriculture-Linked Deforestation: Oil Palm, Soy, Cattle, Wood Fiber, Cocoa, Coffee, and Rubber. WRIPUB (2020) doi:10.46830/writn.na.00001.
19. Pendrill, F., Persson, U. M., Godar, J. & Kastner, T. Deforestation displaced: trade in forest-risk commodities and the prospects for a global forest transition. Environ. Res. Lett. **14**, 055003 (2019).
20. Hong, C. et al. Global and regional drivers of land-use emissions in 1961–2017. Nature **589**, 554–561 (2021).
21. Hoang, N. T. & Kanemoto, K. Mapping the deforestation footprint of nations reveals growing threat to tropical forests. Nat Ecol Evol **5**, 845–853 (2021).
22. Feng, Y. et al. Doubling of annual forest carbon loss over the tropics during the early twenty-first century. Nat Sustain **5**, 444–451 (2022).
23. Li, S. et al. Geospatial big data handling theory and methods: A review and research challenges. ISPRS Journal of Photogrammetry and Remote Sensing **115**, 119–133 (2016).
24. Curtis, P. G., Slay, C. M., Harris, N. L., Tyukavina, A. & Hansen, M. C. Classifying drivers of global forest loss. Science **361**, 1108–1111 (2018).
25. Wassénius, E. & Crona, B. I. Adapting risk assessments for a complex future. One Earth **5**, 35–43 (2022).
26. Wells, G., Pascual, U., Stephenson, C. & Ryan, C. M. Confronting deep uncertainty in the forest carbon industry. Science **382**, 41–43 (2023).
27. FAO. The State of the World's Forests 2024 – Forest-Sector Innovations towards a More Sustainable Future. (FAO, Rome, 2024). doi:10.4060/cd1211en.
28. Hansen, M. C. et al. High-Resolution Global Maps of 21st-Century Forest Cover Change. Science **342**, 850–853 (2013).
29. Anderson, C. M., Bicalho, T., Wallace, E., Letts, T. & Stevenson, M. Forest, Land and Agriculture Science-Based Target-Setting Guidance. (2022).
30. WRI & WBCSD. Greenhouse Gas Protocol Land Sector and Removals Guidance.
31. FAOSTAT. https://www.fao.org/faostat/en/#data.
32. Wernet, G. et al. The ecoinvent database version 3 (part I): overview and methodology. Int J Life Cycle Assess **21**, 1218–1230 (2016).
33. Harris, N. L. et al. Global maps of twenty-first century forest carbon fluxes. Nat. Clim. Chang. **11**, 234–240 (2021).
34. Poggio, L. et al. SoilGrids 2.0: producing soil information for the globe with quantified spatial uncertainty. SOIL **7**, 217–240 (2021).
35. Global Forest Watch (GFW). Global Peatlands. https://data.globalforestwatch.org/datasets/gfw::global-peatlands/about.
36. Wilkinson, M. D. et al. The FAIR Guiding Principles for scientific data management and stewardship. Sci Data **3**, 160018 (2016).
37. Lambin, E. F. & Meyfroidt, P. Global land use change, economic globalization, and the looming land scarcity. Proc Natl Acad Sci USA **108**, 3465–3472 (2011).
38. Hazell, P. & Wood, S. Drivers of change in global agriculture. Philosophical Transactions of the Royal Society B: Biological Sciences **363**, 495–515 (2007).
39. Meyfroidt, P., Lambin, E. F., Erb, K.-H. & Hertel, T. W. Globalization of land use: distant drivers of land change and geographic displacement of land use. Current Opinion in Environmental Sustainability **5**, 438–444 (2013).
40. Archer, D. W., Dawson, J., Kreuter, U. P., Hendrickson, M. & Halloran, J. M. Social and political influences on agricultural systems. Renewable Agriculture and Food Systems **23**, 272–284 (2008).
41. Teo, H. C. et al. Uncertainties in deforestation emission baseline methodologies and implications for carbon markets. Nat Commun **14**, 8277 (2023).
42. Huettner, M., Leemans, R., Kok, K. & Ebeling, J. A comparison of baseline methodologies for 'Reducing Emissions from Deforestation and Degradation'. Carbon Balance Manage **4**, 4 (2009).
43. Forest Loss | Global Forest Review. https://research.wri.org/gfr/forest-extent-indicators/forest-loss.
44. Tyukavina, A. et al. Global Trends of Forest Loss Due to Fire From 2001 to 2019. Frontiers in Remote Sensing **3**, (2022).
45. Staver, A. C., Archibald, S. & Levin, S. A. The Global Extent and Determinants of Savanna and Forest as Alternative Biome States. Science **334**, 230–232 (2011).

46. Roebeling, P. C. & Hendrix, E. M. T. Land speculation and interest rate subsidies as a cause of deforestation: The role of cattle ranching in Costa Rica. Land Use Policy **27**, 489–496 (2010).
47. Junquera, V. & Grêt-Regamey, A. Crop booms at the forest frontier: Triggers, reinforcing dynamics, and the diffusion of knowledge and norms. Global Environmental Change **57**, 101929 (2019).
48. Mattila, T. J. The role of peatlands in carbon footprints of countries and products. Science of The Total Environment **947**, 174552 (2024).
49. Pendrill, F. et al. Agricultural and forestry trade drives large share of tropical deforestation emissions. Global Environmental Change **56**, 1–10 (2019).
50. Global Forest Watch (GFW). Global Deforestation Rates & Statistics by Country. https://www.globalforestwatch.org/dashboards/global/.
51. Ahlström, A., Canadell, J. G. & Metcalfe, D. B. Widespread Unquantified Conversion of Old Boreal Forests to Plantations. Earth's Future **10**, e2022EF003221 (2022).
52. Xia, L. et al. Global food insecurity and famine from reduced crop, marine fishery and livestock production due to climate disruption from nuclear war soot injection. Nat Food **3**, 586–596 (2022).
53. Stewart, B. A. & Lal, R. Chapter One - Increasing World Average Yields of Cereal Crops: It's All About Water. in Advances in Agronomy (ed. Sparks, D. L.) vol. 151 1–44 (Academic Press, 2018).
54. Parente, L. et al. Mapping global grassland dynamics 2000—2022 at 30m spatial resolution using spatiotemporal Machine Learning. Preprint at https://doi.org/10.21203/rs.3.rs-4514820/v2 (2024).
55. Harris, N., Goldman, E. D. & Gibbes, S. Spatial Database of Planted Trees (SDPT Version 1.0). https://www.wri.org/research/spatial-database-planted-trees-sdpt-version-10 (2019).
56. Van Tricht, K. et al. WorldCereal: a dynamic open-source system for global-scale, seasonal, and reproducible crop and irrigation mapping. Earth System Science Data **15**, 5491–5515 (2023).
57. Flach, R. The Global Subnational Agricultural Production (GSAP) database. (2024).
58. Bourgoin, C. et al. Global map of forest cover 2020 - version 1. (2023).
59. Rochmyaningsih, D. New European rules to curb deforestation have worrying flaws, scientists say. Science **385**, 485–485 (2024).
60. Vancutsem, C. et al. Long-term (1990–2019) monitoring of forest cover changes in the humid tropics. Science Advances **7**, eabe1603 (2021).
61. Tropical Moist Forests product - Data Access. https://forobs.jrc.ec.europa.eu/TMF/data.php.
62. Sims, M. et al. Differences Between Global Forest Watch's Tree Cover Loss Data and JRC's Tropical Moist Forest Data Explained. Global Forest Watch Content https://www.globalforestwatch.org/blog/data-and-tools/tree-cover-loss-and-tropical-moist-forest-data-compared (2024).
63. Zhang, M. et al. GCI30: a global dataset of 30-m cropping intensity using multisource remote sensing imagery. Earth System Science Data **13**, 4799–4817 (2021).
64. Crippa, M. et al. GHG Emissions of All World Countries: 2023. https://data.europa.eu/doi/10.2760/953322 (2023).
65. Global Sustainable Development Report 2023: Times of Crisis, Times of Change: Science for Accelerating Transformations to Sustainable Development. https://sdgs.un.org/sites/default/files/2023-09/FINAL%20GSDR%202023-Digital%20-110923_1.pdf (2023).
66. COP28 Declaration on Food and Agriculture. https://www.cop28.com/en/food-and-agriculture.
67. Crippa, M., Solazzo, E., Guizzardi, D., Tubiello, F. N. & Leip, A. Climate goals require food systems emission inventories. Nat Food **3**, 1–1 (2022).
68. Crona, B., Folke, C. & Galaz, V. The Anthropocene reality of financial risk. One Earth **4**, 618–628 (2021).
69. Kastner, T., Kastner, M. & Nonhebel, S. Tracing distant environmental impacts of agricultural products from a consumer perspective. Ecological Economics **70**, 1032–1040 (2011).
70. Helen Bellfield, Osvaldo Pereira, Toby Gardner, & Jane Siqueira Lino. Risk Benchmarking for the EU Deforestation Regulation: Key Principles and Recommendations. https://www.proforest.net/fileadmin/uploads/proforest/Documents/Publications/EU-deforestation-regulation-Key-principles-and-recommendations.pdf (2023).
71. Karkalakos, S. The Economic Consequences of Legal Framework. Statute Law Review **45**, hmae024 (2024).
72. Vasconcelos, A. A., Bastos Lima, M. G., Gardner, T. A. & McDermott, C. L. Prospects and challenges for policy convergence between the EU and China to address imported deforestation. Forest Policy and Economics **162**, 103183 (2024).
73. Köthke, M., Lippe, M. & Elsasser, P. Comparing the former EUTR and upcoming EUDR: Some implications for private sector and authorities. Forest Policy and Economics **157**, 103079 (2023).
74. GADM. Database of Global Administrative Areas (Version v4.1). https://gadm.org/.

75. Sexton, J. O. et al. Conservation policy and the measurement of forests. Nature Clim Change **6**, 192–196 (2016).
76. Potapov, P. et al. Global maps of cropland extent and change show accelerated cropland expansion in the twenty-first century. Nat Food **3**, 19–28 (2022).
77. Du, Z. et al. A global map of planting years of plantations. Sci Data **9**, 141 (2022).
78. MapBiomas. MapBiomas General “Handbook”: Algorithm Theoretical Basis Document (ATBD). https://mapbiomas-br-site.s3.amazonaws.com/ATBD_Collection_7_v2.pdf (2022).
79. Kalischek, N. et al. Cocoa plantations are associated with deforestation in Côte d’Ivoire and Ghana. Nat Food **4**, 384–393 (2023).
80. Huang, Y. et al. A global map of root biomass across the world’s forests. Earth System Science Data **13**, 4263–4274 (2021).
81. 2006 IPCC Guidelines for National Greenhouse Gas Inventories - Volume 4. https://www.ipcc.ch/report/2006-ipcc-guidelines-for-national-greenhouse-gas-inventories/ (2006).
82. John Couwenberg. Emission Factors for Managed Peat Soils - An Analysis of IPCC Default Values. https://www.wetlands.org/publications/emission-factors-for-managed-peat-soils-an-analysis-of-ipcc-default-values/ (2009).
83. Günther, A. et al. Prompt rewetting of drained peatlands reduces climate warming despite methane emissions. Nat Commun **11**, 1644 (2020).
84. Cooper, H. V. et al. Greenhouse gas emissions resulting from conversion of peat swamp forest to oil palm plantation. Nat Commun **11**, 407 (2020).
85. Persson, U. M., Henders, S. & Cederberg, C. A method for calculating a land-use change carbon footprint (LUC-CFP) for agricultural commodities – applications to Brazilian beef and soy, Indonesian palm oil. Global Change Biology **20**, 3482–3491 (2014).
86. Maciel, V. G. et al. Towards a non-ambiguous view of the amortization period for quantifying direct land-use change in LCA. Int J Life Cycle Assess **27**, 1299–1315 (2022).

Extended Figures

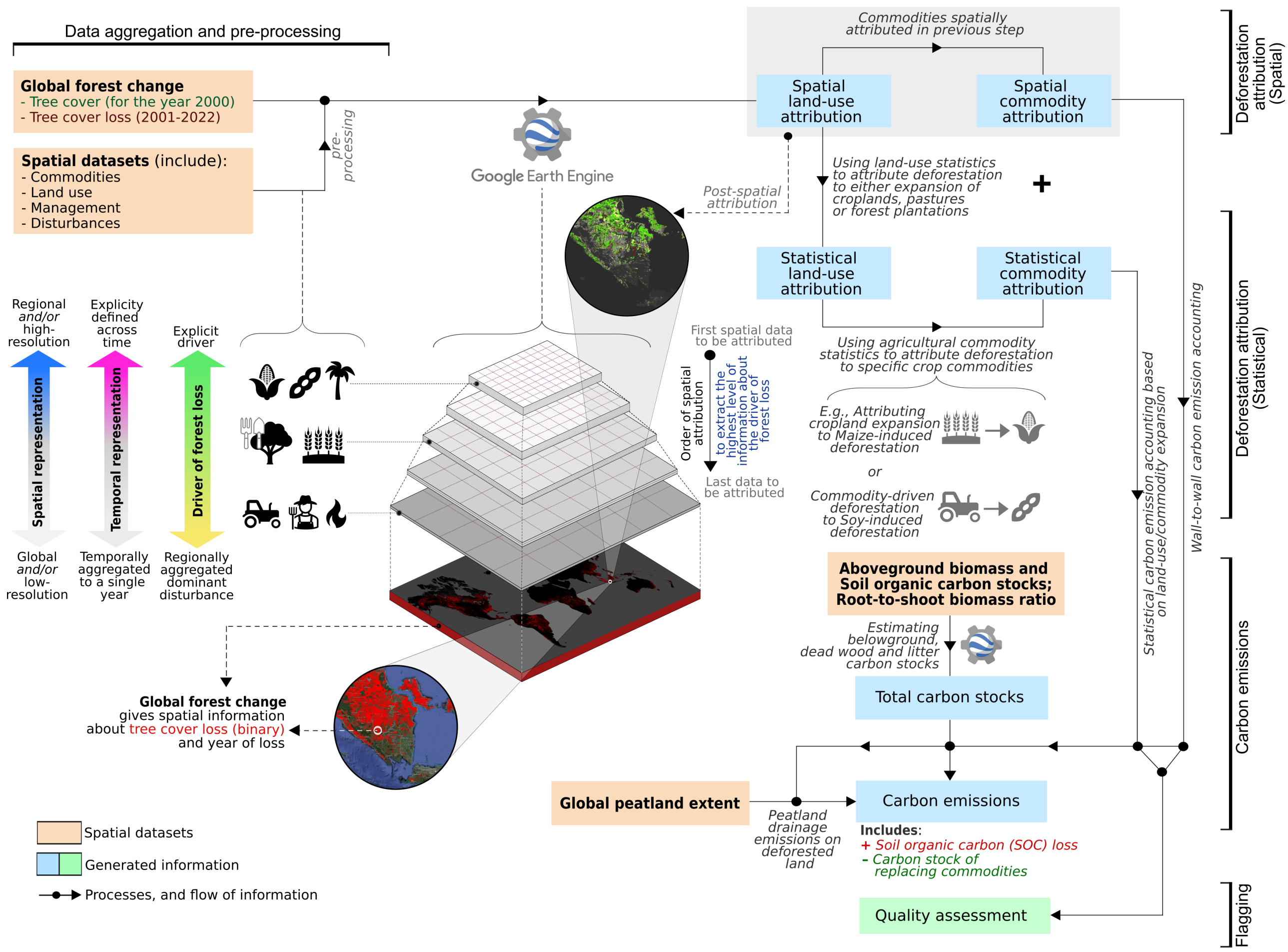

Extended Data Fig. 1 | Framework for the Deforestation Driver and Carbon Emission (DeDuCE) model. This framework consists of three key components: deforestation attribution (spatial and statistical), carbon emission calculation, and quality assessment. In the first step, we utilise remote sensing and (sub-) national agricultural statistics to determine what portion of the total annual tree cover loss is attributable to specific commodities. From this, we next calculate carbon emissions linked to commodity-driven deforestation, including emissions from peatland drainage on deforested lands. Finally, we evaluate the reliability of our deforestation estimates by assessing the quality of the input data used in our analysis. A detailed description of the datasets used in this model is provided in Supplementary Table 3.

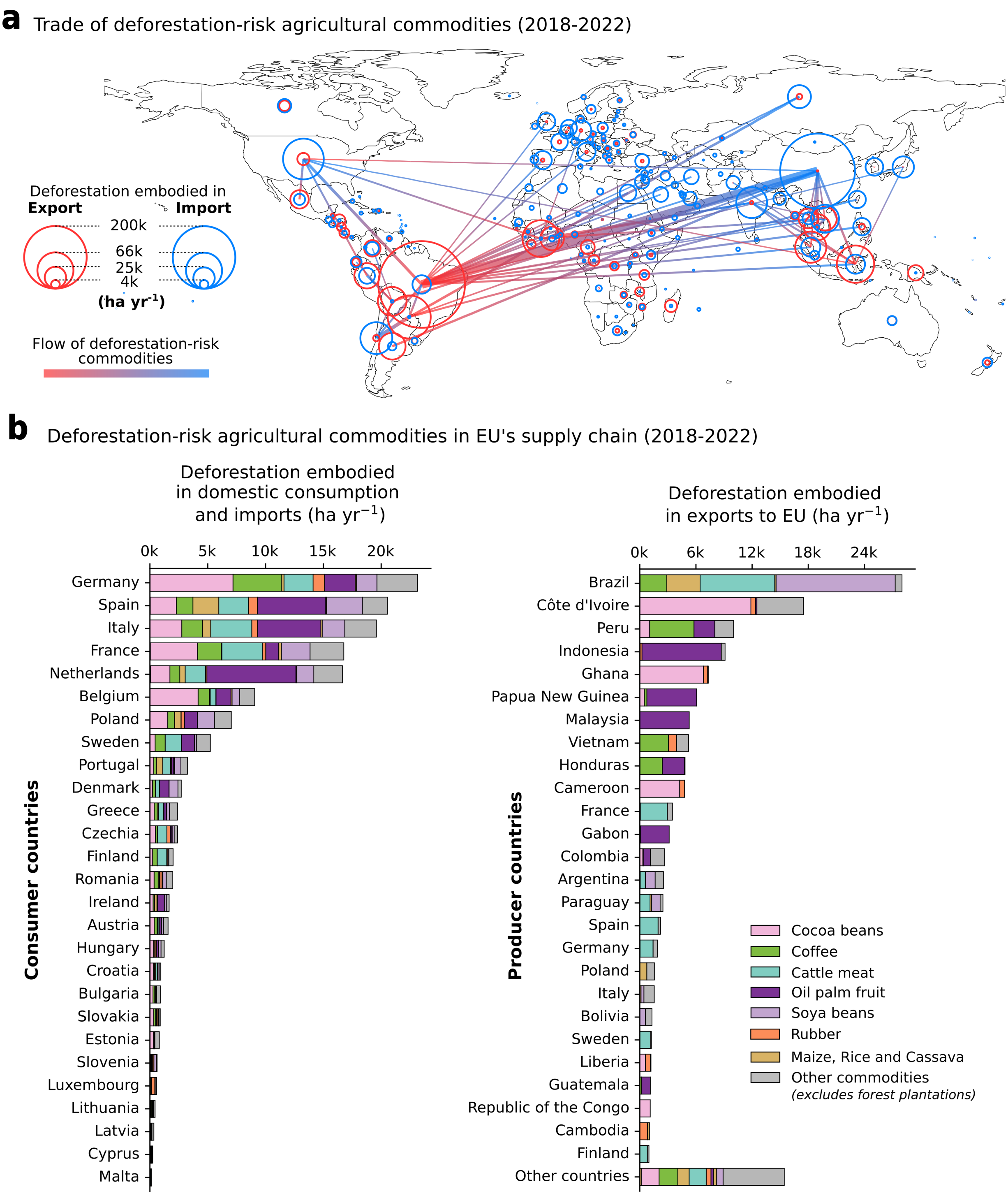

Extended Data Fig. 2 | Global supply chain's exposure to deforestation (aggregated for 2018-2022). (a) This figure illustrates the deforestation embodied in the trade of agricultural commodities worldwide, with exporter countries represented by red circles and importer countries by blue circles. The lines connecting these countries indicate the trade networks and the width of these lines highlights the extent of deforestation embodied in those trades. Minor trade flows, i.e., less than 2% of the maximum deforestation embodied in trade, are not shown for clarity. (b) The figure focuses on the EU's supply chain, showing deforestation embodied in both domestic consumption and trade. It quantifies the exposure of EU countries and their associated producer (or exporter) countries to agricultural commodities. To assess deforestation embodied in trade, we use DeDuCE's deforestation estimates averaged over 2018-2022 (or amortised year 2022 estimates) along with a physical trade model[69], following the methodology outlined in ref.[49].

Supplementary Information

Global patterns of commodity-driven deforestation and associated carbon emissions

Chandrakant Singh[1,2] and U. Martin Persson[1]
[1]Department of Space, Earth and Environment, Chalmers University of Technology, Gothenburg, Sweden
[2]Stockholm Resilience Centre, Stockholm University, Stockholm, Sweden

Corresponding authors: Chandrakant Singh (chandrakant.singh@chalmers.se) and
U. Martin Persson (martin.persson@chalmers.se)

Table of content

A. Supplementary Methods

1. Forest plantation mask

In our deforestation attribution, we filter out the tree cover loss over managed forests (i.e., both planted and plantation forests; see definition at ref.[1]), aiming to solely include the loss of natural forests. Since the global forest change dataset[2] does not differentiate between natural and managed forests, recognising any woody vegetation over 5m in height in a pixel as forested land, the signal from forest loss contains both removal of tree stands in natural forests (i.e., deforestation) and managed forests (due to logging/rotation harvesting in already established timber or oil palm plantation regions). To refine our analysis to only include deforestation, we exclude changes in tree cover associated with the management activities of planted and plantation forests established before 2001.

For datasets with annual updates, such as MapBiomas[3] and oil palm extent in Indonesia[4], which document land use since 2000 or earlier, we can readily discern whether tree cover losses occur in natural or managed forests. For those without such temporal land-use detail, we employ a forest plantation mask based on Du et al.[5] and Lesiv et al.[6] to identify and exclude managed forests (Supplementary Fig. 5). Du et al.[5] use the Spatial Database of Planted Trees (SDPT version 1.0[7]) – which is stated to cover nearly 82% of plantation forests globally – and time-series of Landsat satellite data (from 1982-2020) to detect when these plantations in a pixel were first established (referred to as 'start year'). For our deforestation attribution, we only included forest plantations established after the year 2000 (i.e., start year > 2000), while tree cover loss in plantations established before 2000 was classified as rotational clearing. However, this approach carries the risk of overestimating deforestation for plantations with rotation periods exceeding 20 years, as these plantations may have been established before the timeframe analysed in Du et al.[5]. Conversely, Lesiv et al.[6] offer a global perspective on managed forests using more recent satellite imagery (2014-2016) and expert classification.

When pixels corresponding to forest plantations or tree crops (e.g., oil palm, coconut, and cocoa), those lacking a land-use record for the year 2000, intersect with the forest plantation mask (Supplementary Fig. 5), we consider these pixels to have been established pre-2001 and exclude them from our deforestation attribution analysis. We give precedence to Du et al.[5] plantation mask due to its comprehensive temporal coverage, which allows us to distinguish between natural and manged forest cover changes before and after the year 2000. In regions without coverage from Du et al.[5], such as Canada and Russia, we defer to Lesiv et al.[6] plantation mask. The latter case, however, may lead to conservative estimates of deforestation where plantation expansion occurred between 2001-2016 (since Lesiv et al.[6] is defined using remote sensing data from 2014-16), but the impact on our overall results is deemed minimal given the breadth of the SDPT database[7]. This masking is selectively applied to forest plantation and tree crop commodities; temporary crop and pasture commodities, typically non-woody and less likely to replace forest plantations, are not subjected to this masking.

2. Processing temporally explicit and temporally aggregated spatial datasets

We process temporally explicit datasets, like MapBiomas and Soybeans, which offer yearly spatial extent from 2000 to 2022, differently from those that are temporally aggregated. Temporally explicit datasets facilitate direct attribution of deforestation to particular land-uses or commodities. We process them by applying a four-year moving window (i.e., a maximum three-year delay) from the year of detected forest loss. This window helps compensate for any delays between the observed forest loss and the actual conversion of that deforested land to agricultural land use. For instance, if a pixel shows forest loss in 2001 and is later identified as cropland in 2003 by MapBiomas, we attribute that forest loss to cropland. In cases where multiple land-use changes occur within the window, we prioritise the assignment in the order of forest plantations, woody perennial crops, pastures, herbaceous perennial and temporary crops (thus prioritising land-uses with higher rotation period over lower[8,9]).

Conversely, datasets that aggregate estimates over time pose challenges in pinpointing the immediate cause of deforestation, as they may not capture sequential land-use changes. Consider the cocoa plantations dataset as an example[10], which consolidates satellite data from 2018 to 2021 to create a cocoa plantation map for a single reference year. Suppose a forest loss occurred in a specific pixel in 2003, and that pixel overlaps with cocoa plantation extent. In the absence of intervening land use data from 2003 to 2017, there is a risk of identifying or misidentifying cocoa as the deforestation driver if land use has changed during those intervening years. Thus, here, we follow a simplistic approach by aligning these temporally aggregated datasets with the year of forest loss when spatial overlap occurs (i.e., simply assuming that the land use that is eventually identified represents the proximate cause of deforestation). However, the attribution of forest loss does not extend beyond the final year of the remote sensing dataset used for the development of the spatial dataset (e.g., spatial attribution for cocoa beans in Côte d’Ivoire and Ghana does not go beyond 2021, and for sugarcane in Brazil, it does not go beyond 2019; see Supplementary Table 3).

3. Statistical land-use attribution

3.1 Estimating gross land-use expansion

We start the first step of this statistical attribution by estimating the expansion of croplands (*CLE*), permanent pastures (*PPE*), and forest plantations (*FPE*) over a three-year time lag following the observed year of forest loss (t), such that lag = min {3, 2021 – t} (Supplementary equations (1)-(3); Supplementary Fig. 1; 2021 is the last year of FAOSTAT data). The duration of this lag period is set to three years, reflecting empirical data on the typical interval between the initial forest clearing and the subsequent establishment of agricultural land for production[11,12]. This time-lagged approach is integral to synchronising the observed changes in land cover with the likely temporal dynamics of land-use development.

$$CLE_t = \max\left\{\frac{\left(CL_{t+lag} - CL_t\right) + \sum_t^{t+lag} Crop\ loss_t}{lag} - GPL_t, 0\right\};\ GPL_t = \max\left\{\min\left\{\frac{\left(PP_{t+lag} - PP_t\right)}{lag}, \frac{\sum_t^{t+lag} Grass\ loss_t}{lag}\right\}, 0\right\} \tag{1}$$

$$PPE_t = \max\left\{\frac{\left(PP_{t+lag} - PP_t\right) + \sum_t^{t+lag} Grassloss_t}{lag}, 0\right\} \tag{2}$$

$$FPE_t = \max\left\{\frac{FP_{t+lag} - FP_t}{lag}, 0\right\} \tag{3}$$

Here CL_t, PP_t, FP_t quantify the extent of croplands, permanent pastures, and forest plantations for a given year t, respectively. The land-use extent data for croplands and permanent pastures are sourced from FAOSTAT[13] (Supplementary equation (1)-(2)), while information on forest plantations is obtained from the FRA[1] (Supplementary equation (3)). Our analysis is focused on gross land-use change; hence, we enhance the net expansion figures from FAOSTAT and FRA with estimates of crop and pasture loss. These losses are computed using methodologies from Li et al.[14], which utilise a time series of the ESA CCI land cover dataset[15] (2000-2022) to track changes in crop and grass areas (i.e., proxy for pasture loss area).

Acknowledging the frequent expansions of croplands over pastures, as evidenced by remote sensing studies[16], we adjust our cropland expansion (CLE_t) calculations by deducting the gross pasture loss (GPL_t) (Supplementary equation (1)). This reflects the tendency for croplands to expand initially into pasture areas before encroaching on forested lands. This displaces cattle ranching into forest frontiers due to cropland expansion[17,18], leading us to correlate pasture expansion directly with forest loss (Supplementary equation (2)). In contrast, for forest plantations, we account only for the net change, as data on gross plantation loss is not available. Consequently, the expansion of forest plantations is directly linked to forest loss (Supplementary equation (3)).

3.2 Handling land-use mosaics

When faced with multi-land-use mosaics (specifically for MapBiomas[3], Curtis et al.[19] dominant driver dataset, and unclassified forest loss) that blend croplands, pastures, or forest plantations without clear demarcation, we distribute the area of forest loss within these mosaics (FL_{mosaic}) in proportion to the extent of each land use relative to the total observed expansion of land use (Supplementary equation (4)-(6); Supplementary Fig. 1). This means that the mosaic of cropland, pasture, and forest plantation is divided among them based on their respective contributions to overall land use expansion (i.e., the sum of CLE_t, PPE_t and FPE_t) (Supplementary equation (4)-(6)). In scenarios where the mosaic is solely composed of cropland and pasture (presently only MapBiomas[3]), we allocate the area between these two categories proportionately, with the combined extent of CLE_t and PPE_t – informing the total area used for this allocation.

$$FL_{CL,statistical,t} = \underset{(certain)}{FL_{mosaic,t}} \times \frac{CLE_t}{CLE_t + PPE_t + FPE_t} \quad \text{or} \quad \min\left\{\max\left\{CLE_t - FL_{CL,spatial,t}, 0\right\}, \underset{(uncertain)}{FL_{mosaic,t}} \times \frac{CLE_t}{CLE_t + PPE_t + FPE_t}\right\} \tag{4}$$

$$FL_{PP,statistical,t} = FL_{\underset{(certain)}{mosaic,t}} \times \frac{PPE_t}{CLE_t + PPE_t + FPE_t} \quad \text{or} \quad \min\left\{ \max\left\{ PPE_t - FL_{PP,spatial,t}, 0 \right\}, FL_{\underset{(uncertain)}{mosaic,t}} \times \frac{PPE_t}{CLE_t + PPE_t + FPE_t} \right\} \tag{5}$$

$$FL'_{FP,statistical,t} = FL_{\underset{(certain)}{mosaic,t}} \times \frac{FPE_t}{CLE_t + PPE_t + FPE_t} \quad \text{or} \quad \min\left\{ \max\left\{ FPE_t - FL_{FP,spatial,t}, 0 \right\}, FL_{\underset{(uncertain)}{mosaic,t}} \times \frac{FPE_t}{CLE_t + PPE_t + FPE_t} \right\} \tag{6}$$

In this framework, mosaics are also divided into 'certain' and 'uncertain' categories. 'Certain' mosaics are those where the dataset confidently identifies the type of land use within the mosaics. For instance, MapBiomas[3] mosaics are certain that the mosaic land use is either a cropland or pasture. Conversely, 'uncertain' mosaics, specifically those from the Curtis et al.[20] dataset, suggest probable land uses solely based on the predominant cause of forest loss over space and time, which may not always accurately reflect direct drivers of forest loss (since aggregated in a 10-km pixel over the full time period). This also encompasses unclassified forest loss as well, given that the driver of such forest loss cannot be associated with a specific land use. We impose a limit for these ambiguous cases (i.e., uncertain mosaics) (Supplementary equation (4)-(6) on the right). This constrains the categorisation of forest loss to whichever is smaller: the expansion of land-use categories minus the spatially attributed forest loss or the forest loss proportionally assessed based on relative land-use expansions – to avoid overestimating forest loss due to agriculture.

3.3 Capping deforestation due to forestry activities

Additionally, despite using a forest plantation mask, certain areas might inaccurately identify themselves as forest loss within natural forest, when in reality, they represent rotational clearing. This misclassification is particularly prevalent when tree cover loss pixels coincide with areas identified by Curtis et al.[20] as dominated by forestry activities ($FL_{forestry,spatial,t}$), stemming from challenges in differentiating between natural and managed forest losses. This issue is especially notable in countries like Sweden, Canada, and Russia, where extensively managed forest areas are not categorised as plantation forests according to FAO's definitions[21]. To counter potential overestimation of deforestation driven by forestry activities, our methodology enforces a cap on the statistical accounting of forest loss attributed to forest plantations ($FL_{FP,statistical,t}$). This cap ensures that the reported forest loss does not surpass the forest plantation expansion estimates provided by the FRA (i.e., FPE_t; Supplementary equation (7)).

$$FL_{FP,statistical,t} = \begin{cases} FL'_{FP,statistical,t} & \text{if } FL_{forestry,spatial,t} > 0 \text{ and } FPE_t \le FL_{FP,spatial,t} + FL'_{FP,statistical,t} \\ \min\left\{ FPE_t - FL_{FP,spatial,t}, FL_{forestry,spatial,t} + FL'_{FP,statistical,t} \right\} & \text{if } FL_{forestry,spatial,t} > 0 \text{ and } FPE_t > FL_{FP,spatial,t} + FL'_{FP,statistical,t} \end{cases} \tag{7}$$

3.4 Gap filling

It should be noted that FAOSTAT provides land-use data up to the year 2021, which allows us to compute land-use expansion until 2020 (Supplementary equation (4)-(6)). To gap-fill for expansions in 2021 and 2022, we average the land use expansion from the preceding three years (i.e., 2018-2020) and then adjust it proportionally to the forest loss to estimates of 2021 and 2022 (Supplementary equation (8)).

$$CLE_t = \min\left\{ \overline{\sum_{i=t-3}^{t-1} CLE_i},\ \overline{\sum_{i=t-3}^{t-1} CLE_i} \times \frac{FL_t}{\sum_{i=t-3}^{t-1} FL_{CL,i}} \right\} \qquad PPE_t = \min\left\{ \overline{\sum_{i=t-3}^{t-1} PPE_i},\ \overline{\sum_{i=t-3}^{t-1} PPE_i} \times \frac{FL_t}{\sum_{i=t-3}^{t-1} FL_{PP,i}} \right\}$$

$$FPE_t = \min\left\{ \overline{\sum_{i=t-3}^{t-1} FPE_i},\ \overline{\sum_{i=t-3}^{t-1} FPE_i} \times \frac{FL_t}{\sum_{i=t-3}^{t-1} FL_{FP,i}} \right\} \qquad (8)$$

4. Statistical commodity attribution

4.1 Deforestation attributed to crop commodities

In the second-step of statistical attribution (Supplementary Fig. 1), we allocate total forest loss induced by cropland expansion ($FL_{CL,t}$, which is the sum of deforestation attributed to croplands spatially and statistically) to various crop commodities ($FL_{CL,statistical,i,t}$, where *i* refers to individual commodities). After excluding forest loss due to commodities already accounted for spatially ($\sum_i FL_{CL,spatial,i,t}$),the statistical land-use attribution step (Supplementary equation (9)) allocates cropland-driven deforestation proportionally to the expansion of each crop commodity ($CLE_{i,t}$) relative to the total expansion at the country level ($\sum_i CLE_{i,t}$). We use FAOSTAT's country scale 'crops and livestock products' statistics ($CL_{i,t}$) to estimate these expansions[13], maintaining the methodology and lag used previously (Supplementary equation (10)). The only exception is Brazil, where we use municipality-level (i.e., second-level administrative boundary) data from the Brazilian Institute of Geography and Statistics (IBGE)[22]. Notably, IBGE also estimates harvested areas for certain crops – specifically maize, groundnuts, potatoes, and beans – that are planted multiple times annually. To prevent double or triple counting of the deforestation attributable to these crops, we only use their first harvested area estimates rather than the total cumulative harvested area over the year. We note that currently, our focus is limited to Brazil due to the lack of available sub-national statistics in other countries. However, we anticipate incorporating these statistics in the future, as higher-quality data becomes available.

If FAOSTAT or IBGE's total crop expansion ($\sum_i CLE_{i,t}$) exceeds the forest loss attributed to cropland ($FL_{CL,t}$; Supplementary equation (1)), we use the lower value between the two (Supplementary equation (9)). Additionally, any surplus ($FL_{CL,surplus,t}$) is apportioned among commodities based on their annual harvested areas, preserving proportionality and reflecting possible land-use changes (Supplementary equation (11)-(12)).

$$FL_{CL,statistical,i,t} = \left(\left(\max\left\{ \min\left\{ FL_{CL,t},\ \sum_i CLE_{i,t} \right\} - \sum_i FL_{CL,spatial,i,t}, 0 \right\} \right) \times \frac{CLE_{i,t}}{\left(\sum_i CLE_{i,t} - \sum_j CLE_{j,t} \right)} \right) + FL_{CL,surplus,i,t} \qquad (9)$$

$$CLE_{i,t} = \max\left\{ \frac{CL_{i,t+lag} - CL_{i,t}}{lag}, 0 \right\} \qquad (10)$$

$$FL_{CL,surplus,t} = FL_{CL,t} - \left(\max\left\{ \min\left\{ FL_{CL,t},\ \sum_i CLE_{i,t} \right\} - \sum_j FL_{CL,spatial,i,t}, 0 \right\} \right) - \sum_j FL_{CL,spatial,i,t} \qquad if\ \ FL_{CL,t} > \sum_i CLE_{i,t} \qquad (11)$$

$$FL_{CL,surplus,i,t} = FL_{CL,surplus,t} \times \frac{CL_{i,t}}{\sum_i CL_{i,t}} \tag{12}$$

Here, $\sum FL_{CL,spatial,i,t}$ is the sum of all spatially attributed forest loss commodities. Since we prioritise deforestation estimated through remote sensing data over agricultural statistics, spatially attributed commodities with a score greater than 0.85 are excluded from statistical attribution. This threshold indicates a high confidence in the data reflecting the true extent of deforestation by that commodity, such as soybeans in South America and oil palm in Indonesia (scores for all datasets are mentioned in Supplementary Table 6, with the scoring methodology outlined in the 'Quality assessment' section). To compensate for this exclusion, we adjust the total crop commodity expansion by deducting $\sum_j CLE_{j,t}$ (i.e., the sum of harvested areas of commodities scoring above 0.85 or $FL_{CL,spatial,i,t} > CLE_{i,t}$) from $\sum_i CLE_{i,t}$ (Supplementary equation (10)). Additionally, as FAOSTAT provides harvest area data up to 2021, enabling commodity-driven expansions calculation up to 2020, we apply a similar methodology as before gap-fill for the year 2021 and 2022 (Supplementary equation (4)-(6)).

4.2 Deforestation attributed to pasture commodities

In the case of deforestation attributed to pastures ($FL_{PP,t}$), we attribute these losses to just two commodities: cattle meat and leather at 95% and 5% of the total deforested area, respectively, based on an economic allocation logic[23]. Although some studies have utilised weighted cattle density[24] data to minimise the inclusion of pastures used for other grazing livestock (e.g., sheep, camels, goats and horses)[25] and associated products (e.g., dairy), significant uncertainties remain[26,27]. For instance, in some regions, the impact on pastoral communities could be considerable[28,29], however, the traditional land use and grazing patterns of these communities may diverge from what is detectable through satellite imagery or fit within formal land-use classifications. Moreover, the variability in cattle density over time poses a challenge, and therefore, is difficult to capture with datasets aggregated temporally, which might lead to under- or over-estimation of cattle meat-driven deforestation. As a result, we adopted an approach grounded in economic-allocation logic to attribute commodities to pastures[23].

4.3 Deforestation attributed to forestry commodities

Forest loss attributed to forest plantations ($FL_{FP,t}$) is categorised as 'Forest plantation (Unclassified)', unless the specific species of the plantations can be spatially attributed using the global plantation dataset[5]. In these cases, where the species information is available, the forest plantation is referred to as 'Forest plantation (*species name*)'.

5. Peatland drainage emissions

Peatland emissions can continue for many years, even decades, after initial land-use change due to the ongoing oxidation of organic carbon in the peat[30]. Assessing emissions from peatland drainage is difficult due to uncertainties in peat subsidence, which can vary with local conditions and management practices[31]. This variability, alongside the inherent challenges in measuring peatland emissions due to the dynamic nature of peat decomposition and water table fluctuations, complicates the accuracy of such estimates[30].

Unlike other deforestation emissions (AGB, BGB, etc.), which are considered locked-in or committed, the continuous emission profile of peatland emissions necessitates annual emission accounting to accurately reflect their ongoing impact. Furthermore, international frameworks such as the IPCC guidelines[32] require countries to report their peatland emissions annually, which aligns with our approach to reporting peatland emissions.

Of the literature used for estimating peatland drainage emission factors[31–34], the factors from ref.[34] are based on the IPCC Wetland supplement[32]. For forest plantations, we prioritize the values from ref.[33], resorting to the IPCC values[32] only when ref.[33] does not provide the necessary emission factors. The ref.[33] indicates that the IPCC values for peatlands in tropical and boreal forestry regions are significantly lower in magnitude. They suggest that emission factors for forestry on drained organic soils provided by the IPCC are based on a limited number of measurements, often using trenching or the eddy covariance technique. These techniques might not fully capture the ongoing carbon emissions, especially for below-ground litter input, which can be significant in peatlands.

6. Intention of amortised and unamortised estimates

When a forested land is cleared, the majority of carbon is released during the initial clearing, while emissions from subsequent decay of biomass continues over the next few years. Thus, in environmental impact assessments, particularly regarding the impact of deforestation, it's crucial to consider not just the immediate impact of forest loss, but also the extended effects of this transformation[23,35]. Consequently, the deforestation emissions presented here are 'committed emissions', reflecting the long-term change in biomass carbon stocks due to the land-use change from forest to agricultural or forest plantation land-use, including adjustments in soil carbon contents and carbon sequestration in tree crops for instance.

When attributing these emissions to commodities produced on cleared forest land—calculating a 'deforestation carbon footprint'—these committed emissions from the land-use change event must be distributed over the production period. This is done using an 'amortisation' period, which conceptually distributes the consequences of deforestation (i.e., committed emissions) across multiple years to account for the enduring productivity of the land. This is a common practice in land-use change-related impact assessments (e.g., IPCC[32], GHG Protocol[36]) and here this approach is adopted for calculating the estimates of deforestation emissions embodied in international trade, displayed in Extended Data Fig. 2.

Interestingly, several studies have criticised the use of an amortisation period for its arbitrary nature and weak scientific justification[37]. Since its introduction for GHG accounting (IPCC, 1996[38]), a 20-year amortisation period has been commonly used, albeit non-mandatory. The IPCC guidelines[38] explicitly state that "*the choice of a 20-year period represents a compromise*", and that amortized carbon emissions may not adequately capture the underlying biophysical processes related to carbon balance[37]. Following ref.[23], we adopt a shorter, 5-year amortisation period to better capture the immediate effects of deforestation while also allowing for the analysis of the dynamic nature of current food systems, such as the influence of recent consumption patterns on deforestation (exemplified in Extended Data Fig. 2). However, our choice of a 5-year amortisation period does not impact the core DeDuCE model estimates, i.e., the annual emissions from deforestation attributed to commodities. Stakeholders have the flexibility to use this unamortized data to calculate emission for any amortisation period that aligns with their reporting standards and requirements.

Furthermore, understanding these annualised/unamortised and amortised estimates helps balance immediate actions with long-term planning in climate change mitigation efforts. For example, commodities associated with peatland emissions require continuous (or annualised) monitoring and long-term regulatory measures. This approach enables policymakers to respond swiftly to sudden spikes in emissions, which is essential for implementing urgent regulatory actions. To identify and prioritize the most critical cases for intervention—particularly commodities causing significant near-term deforestation, such as palm oil and cattle meat—unamortized emission estimates are more effective. Amortization, by its nature, tends to smooth out the temporal dynamics of land-use change, potentially obscuring the urgency of recent impacts. For this reason, unamortised emissions highlight annual fluctuations, which are crucial for detecting trends and anomalies in specific commodities or regions. Understanding this annual variability is essential for grasping the dynamic nature of deforestation and its impact, thus facilitating more responsive and effective policy measures.

In contrast, amortised emissions (e.g., AGB, BGB, etc.) linked to deforestation might benefit from development of intervention strategies, informing more targeted climate-change mitigation efforts and encouraging the adoption of sustainable practices[37]. Amortisation account for these annualised variabilities in deforestation emissions and assists in evaluating the effectiveness of intervention strategies. Furthermore, it also provides a clearer picture to investors and stakeholders about the long-term carbon liabilities associated with different commodities, aiding in more informed investment and operational decisions[39].

Both methods complement each other and provide a comprehensive understanding of the deforestation and carbon emissions landscape, helping to prioritise commodities and regions for targeted climate change mitigation efforts.

7. Quality Index assessment

7.1 Scoring metric justification

Since the datasets used in deforestation attribution vary in spatio-temporal granularity (or resolutions) and explicitness (e.g., some datasets provide only land-use information while others capture the spatial extent of commodities), they differ in their ability to actually capture deforestation due to commodity production. The scoring metric normalises the scope of all datasets, making them comparable and allowing for a consistent assessment of the reliability of deforestation estimates.

For instance, a spatial dataset for cropland and oil palm may both exhibit 90% overall accuracy (OA), but their precision in pinpointing oil palm-induced deforestation differs significantly. This difference arises because spatial data on oil palm is explicitly designed to identify areas where oil palm is grown, making it more suitable for linking deforestation specifically to oil palm plantations (dLUC). In contrast, cropland spatial data only indicates that a crop commodity is leading to deforestation without explicitly identifying the commodity-specific driver. In the latter case, assessing the commodity's impact will require using agricultural statistics (Extended Data Fig. 1) to help associate the deforestation likely driven by oil palm (sLUC) from overall deforestation estimates resulting from cropland expansion. Therefore, a higher accuracy spatial dataset does not necessarily equate to a more reliable deforestation estimate.

Similarly, two oil palm datasets with the same temporal resolution and overall accuracy but varying spatial resolution will differ in their capacity to attribute deforestation accurately at a 30-meter pixel scale. The scoring metric adjusts the overall accuracy (OA_j; equation (2)) to account for differences in spatial, temporal, and explicitness aspects, thereby providing a nuanced understanding of the reliability of deforestation estimates produced by the DeDuCE model.

7.2 Calculation of Quality Index

Examples of when deforestation estimates are calculated using only the spatial commodity datasets

Soya beans – Bolivia (2015)
Deforestation: 20840.45 ha

Only one dataset contributed to deforestation estimates:

1. Song et al.[40]-Soya beans: 20840.45 ha
   (QA = 0.95; Score = 0.93)

$$\textbf{Quality Index} = \frac{(20840.45 \times 0.95 \times 0.93)}{20840.45} = \textbf{0.88}$$

Oil palm fruit – Indonesia (2016)
Deforestation: 261034.13 ha

More than one dataset contributed to deforestation estimates (note that the spatial attributions from the datasets below are non-overlapping):

1. MapBiomas[3]-Oil palm fruit: 5904.05 ha
   (QA = 0.85; Score = 0.83)
2. Descals et al.[41]-Oil palm fruit: 2883.93 ha
   (QA = 0.9852; Score = 0.72)
3. Gaveau et al.[4]-Oil palm fruit: 252246.15 ha
   (QA = 0.956; Score = 1)

$$\textbf{Quality Index} = \frac{\begin{array}{l}(5904.05 \times 0.85 \times 0.83) + \\ (2883.93 \times 0.9852 \times 0.72) + \\ (252246.15 \times 0.956 \times 1)\end{array}}{261034.13} = \textbf{0.95}$$

Example of when deforestation estimates are calculated using spatial land-use data and agricultural statistics

Sugar cane – Belize (2014)
Deforestation: 3031.61 ha

Agriculture statistics (see Supplementary Table 12):

1. $Flag_{Land\ use}$ = E
2. $Flag_{Production}$ = A

Multiple land-use datasets that contributed to the aggregation of deforestation estimates:

1. Potapov et al.[42]-Cropland (post-statistical attribution): 2876.96 ha
   (QA = 0.9735; Score = 0.65)
2. Curtis et al.[20]-Dominant driver (post-statistical attribution): 154.65 ha
   (QA = 0.89; Score = 0.40)

Modified QA with agricultural flags (see equation (2) and Supplementary Table 6):

$$QA = QA_j \times \left(\frac{0.80 + 1}{2} - \frac{0.5}{3} \right) = 0.73$$

$$\textbf{Quality Index} = \frac{(2876.96 \times 0.9735 \times 0.65) + (154.65 \times 0.89 \times 0.40)}{3031.61} \times 0.73 = \textbf{0.45}$$

Example of when deforestation estimates are primarily calculated using good-quality agricultural statistics

Wheat – Kazakhstan (2006)
Deforestation: 717.05 ha

Agriculture statistics (see Supplementary Table 12):

1. $Flag_{Land\ use}$ = A
2. $Flag_{Production}$ = A

Multiple land-use datasets that contributed to the aggregation of deforestation estimates:

1. Potapov et al.[42]-Cropland (post-statistical attribution): 17.76 ha
   (QA = 0.9735; Score = 0.65)
2. Curtis et al.[20]-Dominant driver (post-statistical attribution): 0.08 ha
   (QA = 0.89; Score = 0.40)
3. Hansen et al.[2]-Tree cover loss (post-statistical attribution): 699.21 ha
   (QA = 0.996; Score = 0.53)

Modified QA with agricultural flags (see equation (2) and Supplementary Table 6):

$$QA = QA_j \times \left(\frac{1+1}{2} - \frac{0.5}{3} \right) = 0.83$$

$$\textbf{Quality Index} = \frac{(17.76 \times 0.9735 \times 0.65) + (0.08 \times 0.89 \times 0.40) + (699.21 \times 0.996 \times 0.53)}{717.05} \times 0.83 = \mathbf{0.44}$$

Example of when deforestation estimates are primarily calculated using poor-quality agricultural statistics

Rubber – Cambodia (2017)
Deforestation: 27419.11 ha

Agriculture statistics (see Supplementary Table 12):

1. $Flag_{Land\ use}$ = E
2. $Flag_{Production}$ = T

Multiple land-use datasets that contributed to the aggregation of deforestation estimates:

1. Potapov et al.[42]-Cropland (post-statistical attribution): 4297.33 ha
   (QA = 0.9735; Score = 0.65)
2. Curtis et al.[20]-Dominant driver (post-statistical attribution): 23121.03 ha
   (QA = 0.89; Score = 0.40)
3. Du et al.[5]-Global Forest Plantation (directly classifies Rubber): 0.75 ha
   (QA = 0.7825; Score = 0.70)

Modified QA with agricultural flags (see equation (2) and Supplementary Table 6):

$$QA = QA_j \times \left(\frac{0.8+0.6}{2} - \frac{0.5}{3} \right) = 0.53$$

$$\textbf{Quality Index} = \frac{(4297.33 \times 0.9735 \times 0.65) + (23121.03 \times 0.89 \times 0.40)}{27419.11} \times 0.53 + \frac{(0.75 \times 0.7825 \times 0.70)}{27419.11} = \mathbf{0.21}$$

B. Supplementary Figures

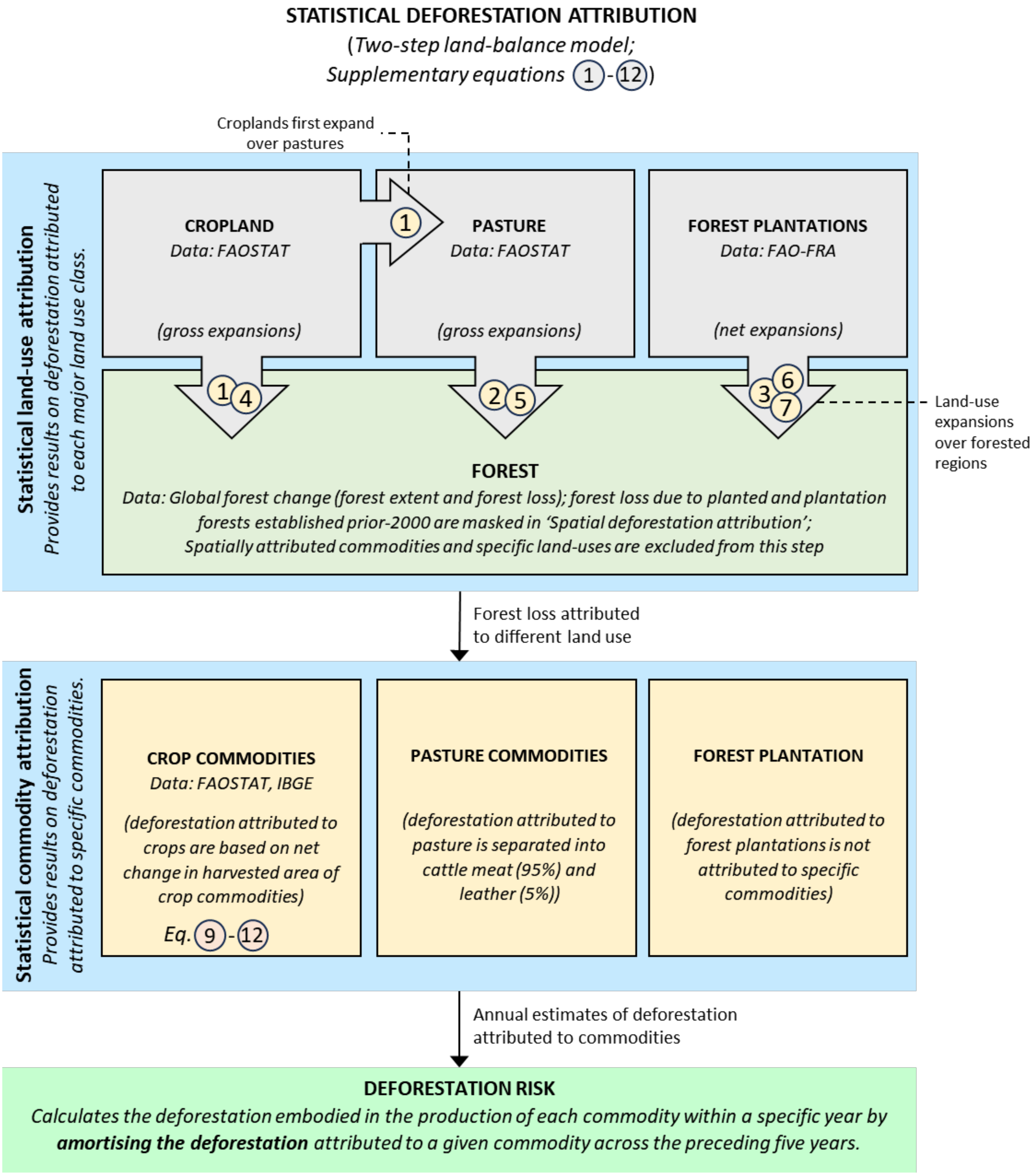

Supplementary Fig. 1 | Visual representation of the statistical deforestation attribution (i.e., two-step land balance model). The figure is adapted from ref.[17].

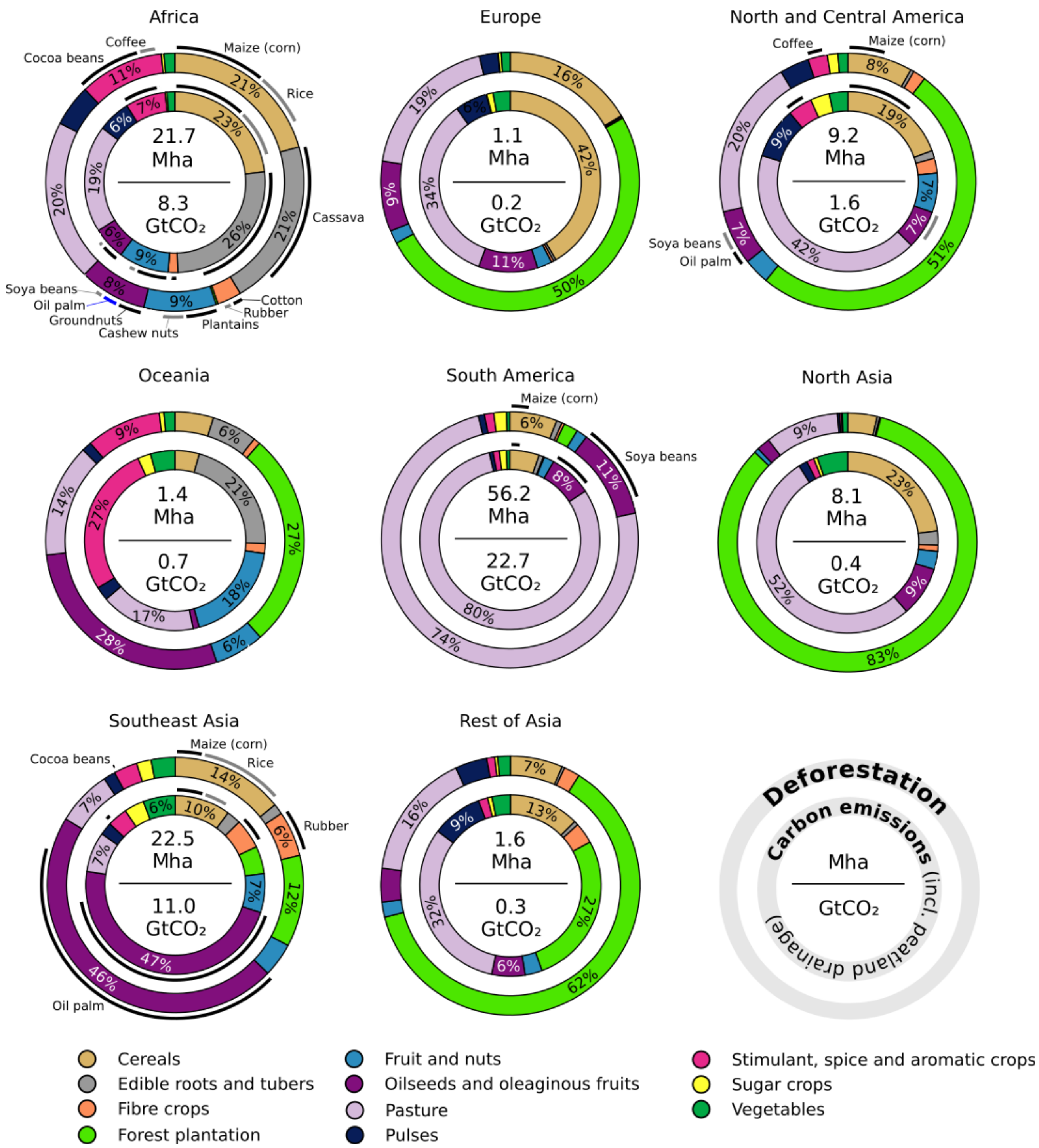

Supplementary Fig. 2 | Geographical overview of commodity-driven deforestation (2001-2022). Similar to Fig. 3b in the main text, this figure shows agriculture and forestry-driven deforestation and corresponding carbon emissions across but here broken down by different geographical regions. In the concentric rings, the outer ring depicts the proportion of deforestation by area, while the inner ring shows carbon emissions, including peatland emissions, with selected major deforestation commodities accentuated along the periphery of the concentric circles. Negative carbon emission values are excluded from the visualisation.

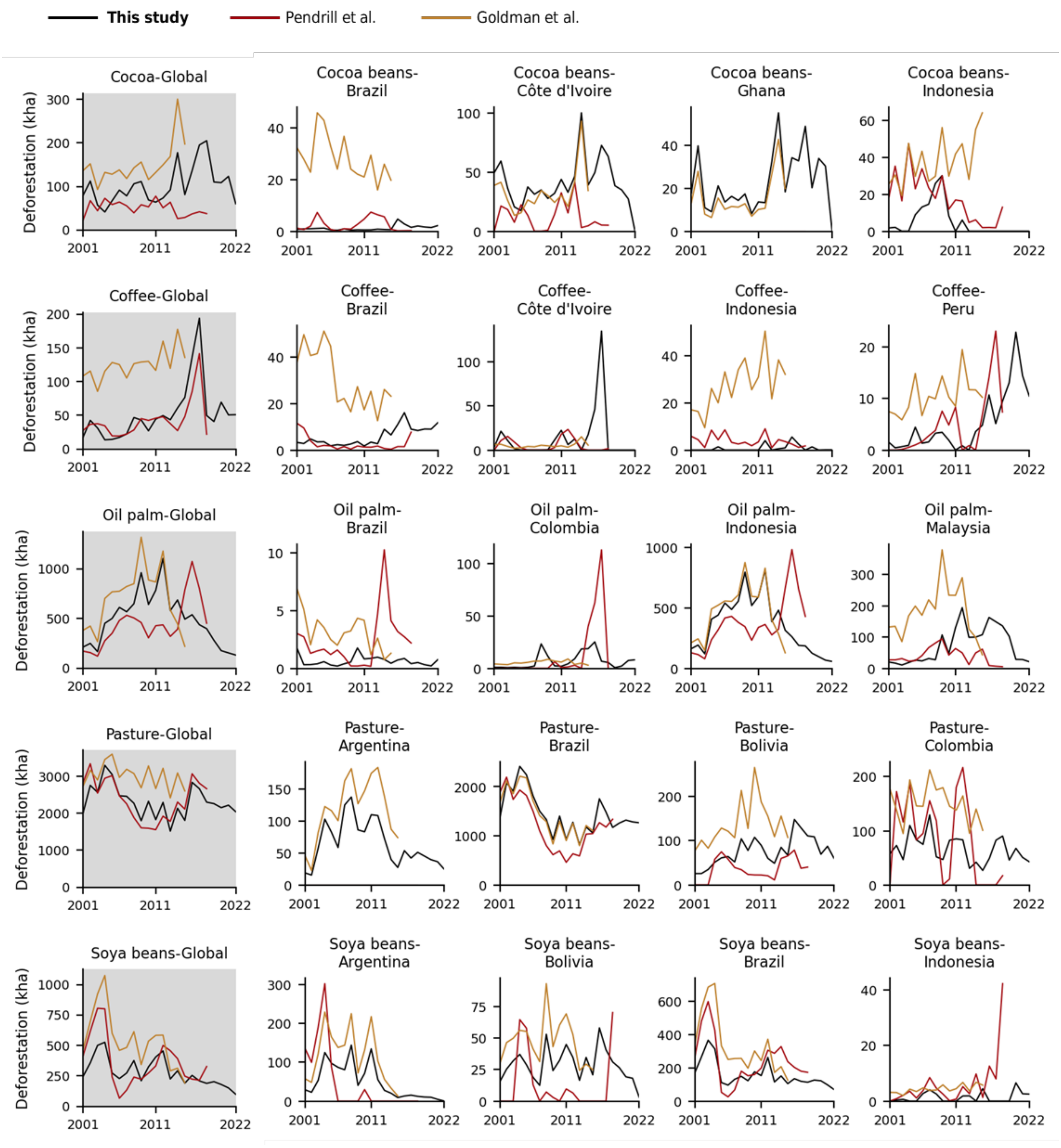

Supplementary Fig. 3 | Comparison of deforestation estimates of major deforestation-risk commodities and countries with other studies. Studies include estimates from Pendrill et al.[23] and Goldman et al.[25].

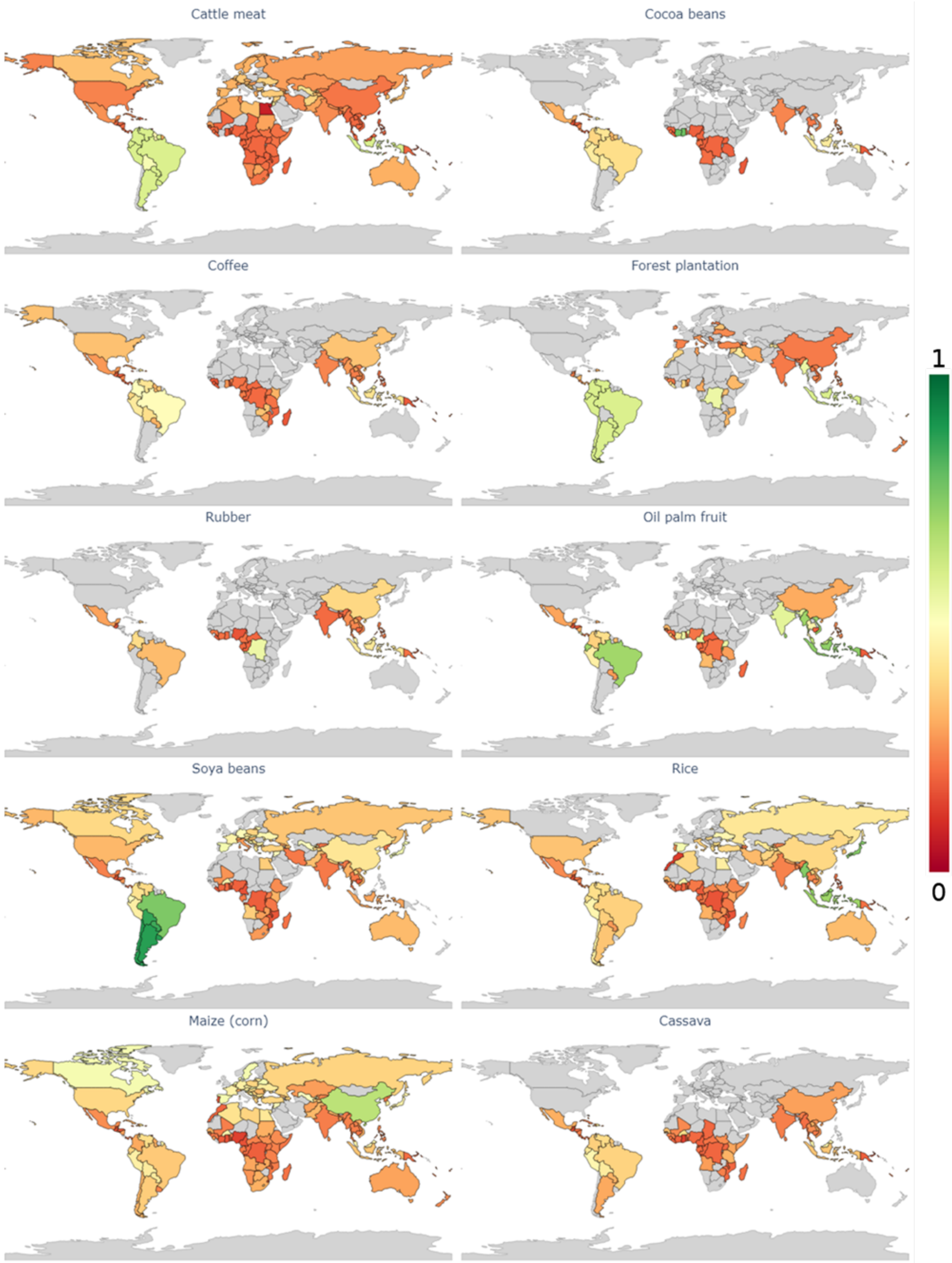

Supplementary Fig. 4 | Quality index of major deforestation-risk commodities as shown in Fig. 4. The quality index above is weighted for estimates from 2018 to 2022. Here, higher values of the quality index indicate better quality of deforestation attribution.

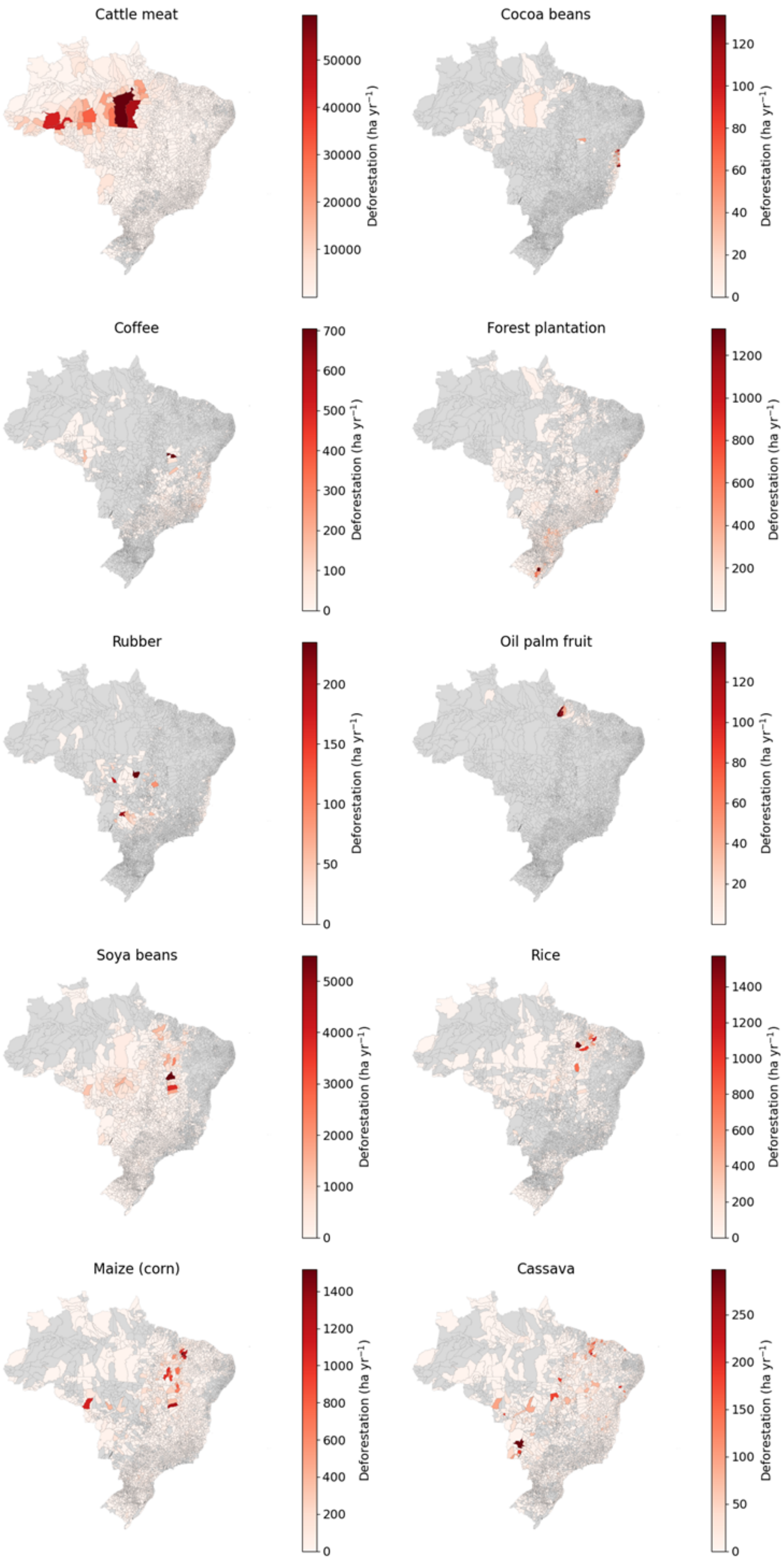

Supplementary Fig. 5 | Hotspots of major deforestation-risk commodities for Brazil (aggregated for 2018-2022).

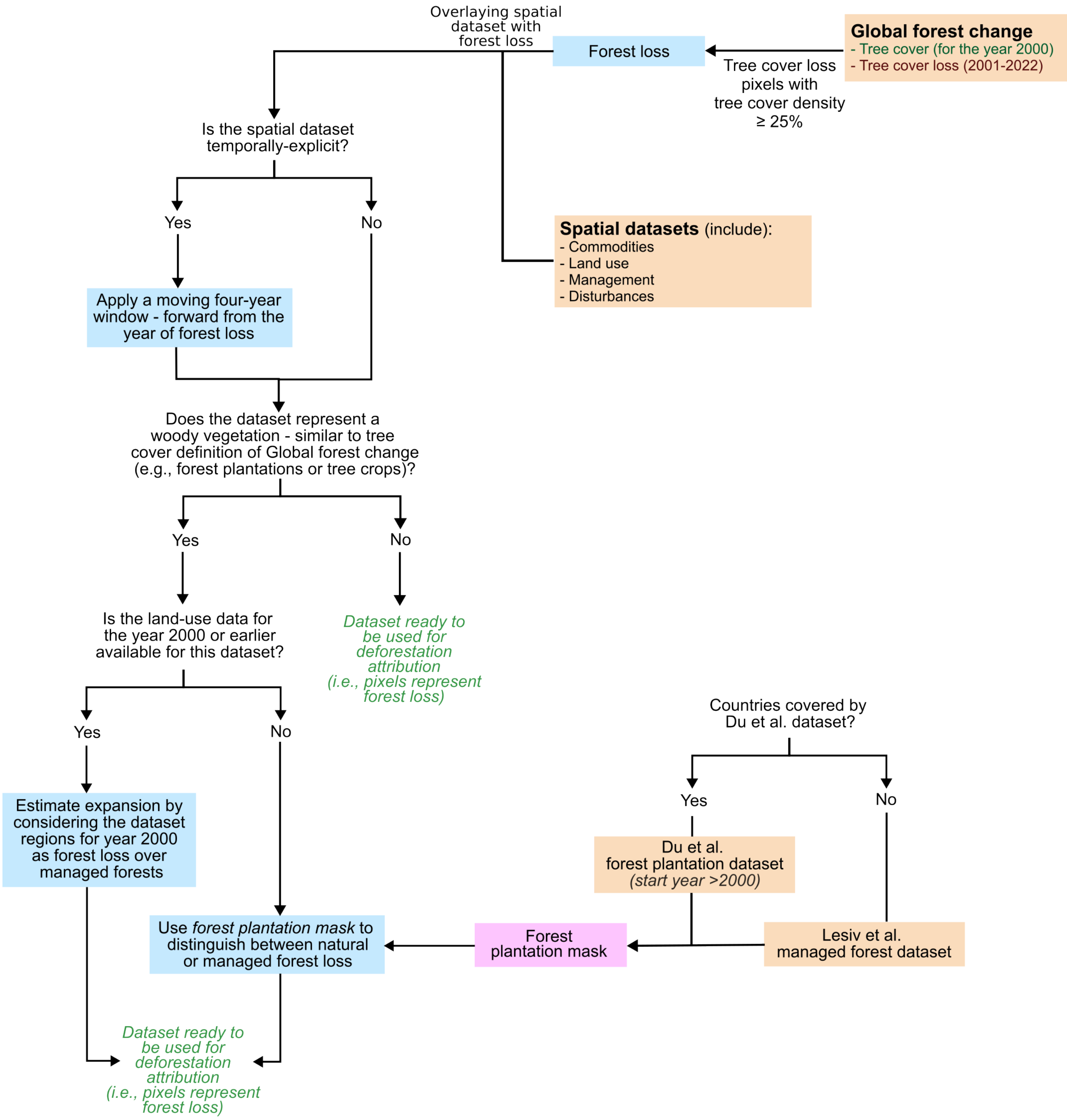

Supplementary Fig. 6 | Framework for distinguishing natural forest loss and loss over managed forests. Global forest plantation mask based on Du et al.[5] and Lesiv et al.[6].

C. Supplementary Tables

Supplementary Table 1 | Countries and their respective deforestation-carbon emission estimates and quality index (2001-2022). Note that the table below excludes countries that either experienced no deforestation or lacked FAOSTAT agricultural statistics for the period from 2001 to 2021. Absolute values are archived on Zenodo (see data availability).

Sr.No.	Producer country	Deforestation attribution, unamortized (ha)	Deforestation emissions excl. peat drainage, unamortized ($MtCO_2$)	Peatland drainage emissions ($MtCO_2$)	Quality Index
1	Afghanistan	442	0.12	<0.01	0.44
2	Albania	11,040	1.00	<0.01	0.26
3	Algeria	7,477	1.85	0.03	0.44
4	Angola	1,229,575	320.31	2.20	0.29
5	Antigua and Barbuda	403	0.10	<0.01	0.34
6	Argentina	3,910,144	633.00	0.80	0.62
7	Armenia	1,011	0.35	<0.01	0.42
8	Australia	397,501	29.68	3.01	0.28
9	Austria	1,515	0.53	<0.01	0.45
10	Azerbaijan	4,061	1.04	0.03	0.42
11	Bahamas	4,028	0.57	0.20	0.28
12	Bangladesh	9,569	3.47	0.86	0.32
13	Barbados	114	0.03	<0.01	0.33
14	Belarus	16,391	1.85	0.49	0.42
15	Belgium	11,138	1.47	<0.01	0.3
16	Belize	48,093	19.52	1.07	0.36
17	Benin	29,837	7.24	<0.01	0.34
18	Bhutan	6,549	3.34	0.02	0.3
19	Bolivia	3,765,912	1,472.31	8.85	0.56
20	Bosnia and Herzegovina	6,092	2.45	<0.01	0.4
21	Botswana	953	0.11	0.03	0.34
22	Brazil *(results also available at municipality level)*	38,329,215	16,955.99	40.51	0.61
23	Brunei	6,834	4.69	0.45	0.23
24	Bulgaria	10,161	2.88	0.01	0.44
25	Burkina Faso	325	0.06	<0.01	0.36
26	Burundi	10,690	2.73	0.01	0.32
27	Cabo Verde	87	-0.01	0	0.31
28	Cambodia	1,431,351	618.80	14.06	0.28
29	Cameroon	661,389	304.11	4.15	0.24
30	Canada	420,166	68.23	60.52	0.43
31	Central African Republic	174,117	63.01	0.69	0.26
32	Chad	88,550	18.92	<0.01	0.34
33	Chile	409,016	-2.71	0.72	0.56
34	China	7,221,282	-97.61	2.58	0.27
35	Colombia	2,381,122	1,203.89	17.57	0.53
36	Comoros	448	0.17	<0.01	0.27
37	Costa Rica	192,229	70.59	3.43	0.26
38	Croatia	5,984	2.02	0	0.42
39	Cuba	75,325	26.40	0.83	0.33
40	Cyprus	231	0.05	0	0.42
41	Czechia	10,912	3.86	<0.01	0.36

42	Côte d'Ivoire	3,012,391	693.27	6.52	0.39
43	Democratic Republic of the Congo	7,307,966	3,807.59	117.35	0.24
44	Denmark	19,547	-2.11	0.05	0.29
45	Dominica	93	0.04	<0.01	0.27
46	Dominican Republic	28,600	4.86	0.13	0.34
47	Ecuador	312,273	191.06	1.83	0.53
48	Egypt	2,061	0.38	0.28	0.5
49	El Salvador	13,421	4.00	0.12	0.29
50	Equatorial Guinea	22,689	13.33	0.28	0.22
51	Eritrea	1	<0.01	0	0.38
52	Estonia	11,407	2.45	0.22	0.34
53	Ethiopia	184,646	63.53	0.13	0.39
54	Fiji	15,117	3.31	0	0.31
55	Finland	49,138	6.21	3.39	0.42
56	France	62,045	24.10	0.21	0.41
57	Gabon	239,489	129.40	4.65	0.22
58	Gambia	697	0.12	<0.01	0.41
59	Georgia	6,183	1.90	0	0.37
60	Germany	28,041	11.18	0.28	0.43
61	Ghana	1,496,210	414.30	1.32	0.42
62	Greece	16,470	0.62	0.06	0.35
63	Grenada	400	0.19	<0.01	0.28
64	Guatemala	575,289	167.99	2.06	0.25
65	Guinea	286,794	79.62	0.62	0.24
66	Guinea-Bissau	18,432	4.19	0.25	0.24
67	Guyana	12,422	4.73	0.67	0.49
68	Haiti	8,262	1.94	0.08	0.29
69	Honduras	653,215	240.69	3.57	0.22
70	Hungary	41,102	-1.11	0.07	0.28
71	India	1,325,328	263.24	14.80	0.27
72	Indonesia	10,920,308	3,889.18	2,057.52	0.82
73	Iran	2,935	0.56	0.02	0.4
74	Iraq	119	0.03	<0.01	0.4
75	Ireland	63,993	-1.49	0.97	0.27
76	Israel	646	0.12	<0.01	0.41
77	Italy	36,905	7.48	0.02	0.4
78	Jamaica	5,659	1.96	0.10	0.26
79	Japan	28,612	11.52	0.18	0.45
80	Jordan	3	<0.01	0	0.44
81	Kazakhstan	20,761	5.92	0.04	0.42
82	Kenya	354,793	134.35	0.20	0.31
83	Kyrgyzstan	1,088	0.28	0	0.44
84	Laos	354,108	159.66	3.75	0.3
85	Latvia	24,474	-3.80	0.62	0.28
86	Lebanon	581	0.13	<0.01	0.36
87	Lesotho	166	0.04	0	0.34
88	Liberia	567,701	204.30	10.15	0.25
89	Libya	119	0.02	0	0.33
90	Lithuania	1,700	0.35	0.06	0.47
91	Luxembourg	530	0.26	<0.01	0.32
92	Madagascar	651,826	247.64	1.98	0.25
93	Malawi	227,698	76.22	0.18	0.24
94	Malaysia	3,029,870	1,409.66	277.49	0.44
95	Maldives	49	-0.00	0.01	0.33
96	Mali	5,095	1.39	<0.01	0.38
97	Malta	11	<0.01	<0.01	0.23
98	Mauritania	34	<0.01	0	0.42

99	Mauritius	933	0.28	0	0.33
100	Micronesia	2	<0.01	<0.01	0.29
101	Moldova	2,971	0.72	<0.01	0.38
102	Mongolia	8,439	1.43	0.63	0.37
103	Montenegro *(2006-2022)*	725	0.28	<0.01	0.41
104	Morocco	6,569	1.08	<0.01	0.43
105	Mozambique	864,875	243.82	0.55	0.32
106	Myanmar	2,050,186	915.69	25.96	0.3
107	México	1,238,121	369.63	3.55	0.28
108	Namibia	2,162	0.27	0.02	0.31
109	Nepal	32,545	12.52	0.07	0.31
110	Netherlands	4,219	1.48	0.11	0.42
111	New Caledonia	7,040	2.66	0.13	0.26
112	New Zealand	158,143	12.21	0.09	0.3
113	Nicaragua	395,093	173.63	10.06	0.26
114	Niger	3	<0.01	0	0.44
115	Nigeria	1,508,779	395.87	14.86	0.24
116	North Korea	36,425	10.40	0.13	0.27
117	North Macedonia	1,452	0.45	0	0.4
118	Norway	151,189	3.29	2.22	0.28
119	Oman	<1	<0.01	0	0.41
120	Pakistan	3,046	1.22	<0.01	0.36
121	Palestine	17	<0.01	0	0.42
122	Panama	128,445	57.32	2.89	0.25
123	Papua New Guinea	780,327	481.72	37.64	0.22
124	Paraguay	4,779,935	741.34	1.34	0.6
125	Peru	1,757,432	1,031.77	13.26	0.53
126	Philippines	880,043	410.17	8.14	0.27
127	Poland	25,544	5.41	0.36	0.41
128	Portugal	64,197	-6.08	0.14	0.25
129	Puerto Rico	2,635	0.70	0.04	0.32
130	Republic of the Congo	240,491	125.38	8.22	0.22
131	Romania	10,631	3.01	<0.01	0.39
132	Russia	653,874	167.14	15.02	0.38
133	Rwanda	31,136	10.84	0.10	0.29
134	Saint Kitts and Nevis	274	0.10	<0.01	0.36
135	Saint Lucia	155	0.07	<0.01	0.26
136	Saint Vincent and the Grenadines	174	0.05	<0.01	0.34
137	Senegal	1,661	0.42	0.01	0.34
138	Serbia *(2006-2022)*	23,006	2.34	0	0.32
139	Serbia and Montenegro *(2001-2005)*	7,635	0.04	<0.01	0.25
140	Seychelles	3	<0.01	<0.01	0.28
141	Sierra Leone	38,386	10.79	1.08	0.24
142	Singapore	178	0.05	<0.01	0.36
143	Slovakia	11,716	2.01	0.01	0.31
144	Slovenia	977	0.39	<0.01	0.44
145	Solomon Islands	39,855	21.27	3.19	0.23
146	Somalia	3,849	0.50	<0.01	0.28
147	South Africa	210,940	67.59	0.17	0.27
148	South Korea	90,047	-12.32	0.01	0.27
149	South Sudan *(2012-2022)*	26,522	5.69	0.10	0.27
150	Spain	107,469	4.64	0.34	0.3
151	Sri Lanka	122,109	21.89	0.63	0.32
152	Sudan *(2012-2022)*	544	0.11	<0.01	0.29
153	Sudan and South Sudan *(2001-2011)*	55,400	11.20	0.06	0.35

154	Suriname	16,895	8.21	1.15	0.54
155	Swaziland	6,105	1.32	<0.01	0.28
156	Sweden	93,175	-2.99	8.88	0.29
157	Switzerland	6,016	3.05	0.02	0.31
158	Syria	1,828	0.34	0.01	0.47
159	São Tomé and Príncipe	33	0.02	0	0.41
160	Taiwan	8,758	1.73	<0.01	0.3
161	Tajikistan	274	0.05	<0.01	0.45
162	Tanzania	999,896	245.03	0.48	0.36
163	Thailand	1,670,507	518.20	13.64	0.28
164	Timor-Leste	4,763	2.12	0.03	0.33
165	Togo	16,633	4.16	<0.01	0.32
166	Trinidad and Tobago	2,458	0.97	0.06	0.27
167	Tunisia	2,243	0.48	<0.01	0.42
168	Turkey	69,685	6.80	0.04	0.38
169	Turkmenistan	207	0.04	0.01	0.3
170	Uganda	269,413	71.51	0.98	0.35
171	Ukraine	102,998	13.23	0.88	0.38
172	United Kingdom	24,753	9.70	0.40	0.46
173	United States	5,446,756	-137.03	18.87	0.27
174	Uruguay	66,314	4.68	0.04	0.65
175	Uzbekistan	871	-0.03	<0.01	0.39
176	Vanuatu	4,490	1.67	0.16	0.28
177	Venezuela	500,925	190.20	1.51	0.54
178	Vietnam	2,156,294	697.81	10.73	0.28
179	Yemen	<1	<0.01	0	0.37
180	Zambia	719,074	234.95	0.49	0.34
181	Zimbabwe	93,327	20.71	0.03	0.36

Supplementary Table 2 | Commodities and their respective deforestation-carbon emission estimates and quality index (2001-2022). Note that while FAOSTAT tracks 171 agricultural commodities, those not contributing to deforestation are omitted from the table below. Absolute values are archived on Zenodo (see data availability).

Sr.No.	Commodity	Deforestation attribution, unamortized (ha)	Deforestation emissions excl. peat drainage, unamortized ($MtCO_2$)	Peatland drainage emissions ($MtCO_2$)	Quality Index
1	Abaca, manila hemp, raw	8,743	6.39	0.18	0.29
2	Agave fibres, raw, n.e.c.	1,619	0.95	0.02	0.33
3	Almonds, in shell	17,063	2.73	0.07	0.45
4	Anise, badian, coriander, cumin, caraway, fennel and juniper berries, raw	28,800	11.36	0.20	0.27
5	Apples	15,051	4.83	0.07	0.38
6	Apricots	1,158	0.29	<0.01	0.42
7	Areca nuts	31,410	19.44	2.35	0.35
8	Artichokes	5,071	3.89	0.05	0.44
9	Asparagus	12,922	7.15	0.12	0.38
10	Avocados	167,592	85.63	2.58	0.37
11	Bambara beans, dry	34,834	14.32	0.38	0.32
12	Bananas	690,579	496.20	20.00	0.31
13	Barley	316,417	94.88	3.39	0.42
14	Beans, dry	1,455,196	648.85	12.65	0.34
15	Blueberries	31,909	19.10	0.24	0.4
16	Broad beans and horse beans, dry	29,020	14.20	0.33	0.41
17	Broad beans and horse beans, green	17,964	10.13	0.12	0.37
18	Buckwheat	13,228	4.52	0.21	0.42
19	Cabbages	83,213	49.54	4.25	0.31
20	Canary seed	10,930	5.22	0.63	0.33
21	Cantaloupes and other melons	25,964	13.99	0.62	0.34
22	Carrots and turnips	22,348	13.70	1.14	0.4
23	Cashew nuts, in shell	681,524	156.24	3.42	0.25
24	Cashewapple	292	0.09	<0.01	0.24
25	Cassava leaves	2,183	1.28	0.13	0.24
26	Cassava, fresh	4,153,056	2,113.98	53.38	0.26
27	Castor oil seeds	35,382	8.65	0.19	0.4
28	Cattle meat	48,505,298	20,513.01	189.49	0.53
29	Cauliflowers and broccoli	20,289	12.97	0.72	0.38
30	Cereals n.e.c.	52,828	22.58	0.53	0.38
31	Cherries	10,479	2.90	0.07	0.42
32	Chestnuts, in shell	21,468	7.19	0.11	0.38
33	Chick peas, dry	108,625	51.78	1.97	0.35
34	Chicory roots	158	0.07	<0.01	0.33
35	Chillies and peppers, dry (Capsicum spp., Pimenta spp.), raw	32,490	19.44	1.11	0.29
36	Chillies and peppers, green (Capsicum spp. and Pimenta spp.)	83,529	62.77	7.02	0.4
37	Cinnamon and cinnamon-tree flowers, raw	74,096	38.59	1.60	0.26
38	Cloves (whole stems), raw	91,515	-6.51	0.37	0.42
39	Cocoa beans	2,240,279	913.53	46.26	0.61
40	Coconuts, in shell	655,944	-6.41	12.25	0.34
41	Coffee, green	1,142,700	235.15	11.10	0.32
42	Cow peas, dry	269,557	122.55	3.26	0.29

43	Cranberries	99	0.02	0.02	0.44
44	Cucumbers and gherkins	43,048	32.76	2.71	0.3
45	Currants	465	0.11	<0.01	0.38
46	Dates	1,551	0.38	<0.01	0.37
47	Edible roots and tubers with high starch or inulin content, n.e.c., fresh	113,357	86.46	4.41	0.3
48	Eggplants (aubergines)	18,851	12.17	0.78	0.33
49	Figs	1,262	0.35	<0.01	0.41
50	Flax, processed but not spun	1,059	0.45	<0.01	0.44
51	Flax, raw or retted	290	0.09	<0.01	0.44
52	Fonio	19,645	6.15	0.07	0.26
53	Forest plantation *(Aggregates all forestry commodities)*	16,989,601	-683.41	435.31	0.3
54	Ginger, raw	15,154	11.74	1.18	0.35
55	Gooseberries	71	0.02	<0.01	0.37
56	Grapes	46,780	20.98	0.26	0.43
57	Green corn (maize)	53,285	38.91	2.51	0.33
58	Green garlic	22,531	14.39	0.65	0.41
59	Groundnuts, excluding shelled	942,915	446.55	9.75	0.31
60	Guavas	2,090	0.54	<0.01	0.47
61	Hazelnuts, in shell	7,887	1.88	0.04	0.43
62	Hempseed	230	0.07	<0.01	0.37
63	Hop cones	1,100	0.23	<0.01	0.43
64	Jojoba seeds	1	<0.01	<0.01	0.31
65	Jute, raw or retted	1,453	0.79	0.07	0.32
66	Kapok fruit	6,055	4.95	1.31	0.4
67	Karite nuts (sheanuts)	6,795	1.79	0.05	0.27
68	Kenaf, and other textile bast fibres, raw or retted	5,869	4.67	0.42	0.25
69	Kiwi fruit	3,789	1.15	0.01	0.36
70	Kola nuts	12,225	3.59	0.10	0.26
71	Leather	2,552,910	1,079.63	9.97	0.53
72	Leeks and other alliaceous vegetables	5,526	4.51	0.84	0.41
73	Lemons and limes	78,060	33.36	1.06	0.35
74	Lentils, dry	59,803	16.93	6.31	0.42
75	Lettuce and chicory	29,681	24.04	2.01	0.32
76	Linseed	35,578	6.50	1.66	0.4
77	Locust beans (carobs)	76	0.02	<0.01	0.39
78	Lupins	10,062	4.61	0.09	0.44
79	Maize (corn)	5,210,465	2,181.13	86.99	0.35
80	Mangoes	5,121	-0.17	<0.01	0.47
81	Mangoes, guavas and mangosteens	385,321	196.85	16.53	0.29
82	Maté leaves	10,549	1.29	<0.01	0.4
83	Melonseed	45,941	19.83	1.19	0.25
84	Millet	253,863	107.48	1.85	0.3
85	Mixed grain	3,717	1.14	0.19	0.46
86	Mustard seed	10,603	4.37	0.87	0.38
87	Natural rubber in primary forms	1,564,009	471.30	76.40	0.29
88	Nutmeg, mace, cardamoms, raw	72,935	50.10	9.48	0.42
89	Oats	115,116	39.20	2.23	0.41
90	Oil palm fruit	10,764,220	3,081.66	1,514.22	0.81
91	Okra	49,991	23.74	1.63	0.27
92	Olives	57,789	27.43	0.21	0.41
93	Onions and shallots, dry (excluding dehydrated)	136,291	87.37	5.40	0.35
94	Onions and shallots, green	10,133	3.65	0.03	0.43
95	Oranges	144,226	79.52	2.89	0.34
96	Other beans, green	17,895	12.44	0.48	0.38
97	Other berries and fruits of the genus vaccinium	7,283	8.62	0.63	0.27

	n.e.c.				
98	Other citrus fruit, n.e.c.	45,797	16.51	1.68	0.33
99	Other fibre crops, raw, n.e.c.	14,612	5.96	0.09	0.33
100	Other fruits, n.e.c.	238,616	170.32	11.68	0.28
101	Other nuts (excluding wild edible nuts and groundnuts), in shell, n.e.c.	19,695	11.42	1.27	0.33
102	Other oil seeds, n.e.c.	206,233	150.69	21.95	0.24
103	Other pome fruits	66	0.01	<0.01	0.46
104	Other pulses n.e.c.	207,425	112.28	3.16	0.28
105	Other stimulant, spice and aromatic crops, n.e.c.	26,729	12.95	0.59	0.36
106	Other stone fruits	357	0.25	<0.01	0.33
107	Other sugar crops n.e.c.	4,710	4.43	0.85	0.34
108	Other tropical and subtropical fruits, n.e.c.	9,788	2.64	0.03	0.45
109	Other tropical fruits, n.e.c.	74,400	40.74	2.73	0.31
110	Other vegetables, fresh n.e.c.	432,775	300.59	14.77	0.29
111	Palm nuts and kernels	2,371	0.92	<0.01	0.5
112	Papayas	35,314	17.54	1.00	0.35
113	Peaches and nectarines	19,473	6.30	0.08	0.36
114	Pears	4,967	1.24	0.02	0.39
115	Peas, dry	86,499	30.69	2.56	0.39
116	Peas, green	23,677	12.80	0.22	0.39
117	Pepper (Piper spp.), raw	93,880	52.91	4.58	0.32
118	Peppermint, spearmint	25	<0.01	<0.01	0.35
119	Persimmons	3,259	0.86	0.02	0.36
120	Pigeon peas, dry	93,939	48.67	0.86	0.32
121	Pineapples	134,490	71.31	6.81	0.32
122	Pistachios, in shell	13,930	3.25	0.05	0.35
123	Plantains and cooking bananas	1,041,585	549.22	11.29	0.26
124	Plums and sloes	9,580	2.37	0.05	0.37
125	Pomelos and grapefruits	58,658	26.24	1.07	0.28
126	Poppy seed	553	0.14	<0.01	0.44
127	Potatoes	272,835	139.32	2.83	0.38
128	Pulses, n.e.c.	4,163	1.26	<0.01	0.46
129	Pumpkins, squash and gourds	46,664	30.42	1.74	0.33
130	Pyrethrum, dried flowers	2,450	1.70	0.08	0.31
131	Quinces	431	0.15	<0.01	0.41
132	Quinoa	107,696	51.55	0.56	0.42
133	Ramie, raw or retted	166	0.10	<0.01	0.36
134	Rape or colza seed	245,163	8.70	8.09	0.46
135	Raspberries	2,219	0.61	0.01	0.34
136	Rice	4,336,380	1,323.94	96.10	0.34
137	Rye	31,463	9.47	1.05	0.45
138	Safflower seed	42,984	8.89	0.18	0.34
139	Seed cotton, unginned	556,810	177.42	2.57	0.33
140	Sesame seed	331,689	111.91	2.38	0.37
141	Sisal, raw	10,458	3.30	<0.01	0.4
142	Sorghum	1,179,575	446.05	3.52	0.37
143	Sour cherries	472	0.13	<0.01	0.41
144	Soya beans	6,161,078	1,857.26	17.38	0.81
145	Spinach	24,348	23.18	3.02	0.33
146	Stimulant, spice and aromatic crops, n.e.c.	10,532	2.51	0.02	0.47
147	Strawberries	6,646	2.95	0.06	0.42
148	String beans	3,705	2.18	0.05	0.34
149	Sugar beet	12,511	4.46	0.26	0.44
150	Sugar cane	1,517,216	757.86	18.70	0.52
151	Sunflower seed	534,056	207.35	2.83	0.4
152	Sweet potatoes	293,997	191.62	8.99	0.28

153	Tallowtree seeds	360	0.10	<0.01	0.34
154	Tangerines and mandarins	6,946	2.06	<0.01	0.47
155	Tangerines, mandarins, clementines	58,701	23.94	0.40	0.4
156	Taro	66,204	38.74	1.34	0.25
157	Tea leaves	164,011	76.56	2.06	0.44
158	Tomatoes	100,681	50.54	2.30	0.34
159	Triticale	21,921	7.96	0.53	0.45
160	True hemp, raw or retted	469	0.20	<0.01	0.4
161	Tung nuts	998	0.23	<0.01	0.36
162	Unmanufactured tobacco	168,139	87.43	8.90	0.39
163	Vanilla, raw	11,317	6.46	0.84	0.29
164	Vetches	4,110	1.48	0.02	0.41
165	Walnuts, in shell	30,858	7.96	0.12	0.37
166	Watermelons	138,008	102.52	10.47	0.32
167	Wheat	731,718	253.86	10.54	0.41
168	Yams	490,377	182.10	4.13	0.24
169	Yautia	2,741	1.47	0.04	0.33

Supplementary Table 3 | Datasets used in this study and their description.

Datasets	Spatial extent	Spatial resolution	Temporal resolution	References
Datasets used for spatial deforestation attribution				
Global forest change-v1.10: Tree cover (2000) and tree cover loss (2001-2022)	Global	30 m	2001-2022	2
Global plantation dataset* *(*Based on the spatial database of planted trees[7])*	Argentina, Australia, Brazil, Cambodia, Cameroon, Chile, China, Colombia, Costa Rica, Democratic Republic of the Congo, Ecuador, European countries, Gabon, Ghana, Guatemala, Honduras, India, Indonesia, Côte d'Ivoire, Japan, Kenya, Liberia, Malawi, Malaysia, Mexico, Myanmar, Nepal, New Zealand, Nicaragua, Nigeria, Pakistan, Panama, Papua New Guinea, Peru, Philippines, Rwanda, Solomon Islands, South Africa, South Korea, Sri Lanka, Thailand, Uruguay, United States, Venezuela, Vietnam	30 m	1982-2020	5
MapBiomas Collection	Argentina, Bolivia, Brazil, Chile, Colombia, Ecuador, French Guiana, Guyana, Paraguay, Peru, Suriname, Uruguay, Venezuela, Indonesia	30 m	2001-2022 (for all countries, except Bolivia); 2001-2021 (for Bolivia)	3
Croplands	Global	30 m	Aggregated temporally at every 4-year intervals between 2000-2019	42
Sugarcane	Brazil	30 m	Aggregated temporally using data for year 2016-2019	43
Soya beans	South America	30 m	2001-2022	40
Rice	Northeast and Southeast Asia	10 m	Aggregated temporally using the data for year 2017-2019	44
Rapeseed	Argentina, Europe, United States and Canada	10 m	Aggregated temporally using data for year 2017-2019	45
Maize (corn)	China	30 m	2001-2020	46
Cocoa	Côte d'Ivoire and Ghana	10 m	Aggregated temporally using data for year 2018-2021	10
Coconut	Pan-tropical	20 m	2020	47
Oil palm fruit	Indonesia	Vector	2000-2019	4
	Malaysia and Indonesia[#] ([#]not considered for Indonesia)	100 m	2001-2018	48
	Pan-tropical	10 m	2019	41
Forest loss due to fire	Global	30 m	2001-2022	49
Forest management	Global	100 m	Aggregated temporally using data for year 2014-2016	6
Dominant drivers of forest loss	Global	10 km	Aggregated temporally using data for year 2001-2022	20
Datasets used for statistical deforestation attribution				
FAOSTAT-Land use (values extracted for 'Cropland' and 'Permanent meadows and pastures')	Global	Aggregated at national level	1961-2021	13
FAOSTAT-Production	Global	Aggregated at national	1961-2021	13

		level		
Forest Resource Assessment (FAO-FRA) (for forest plantation)	Global	Aggregated at national level	1990, 2000, 2010, 2015, 2016, 2017, 2018, 2019, 2020	[1]
Forestry statistics	Taiwan	Aggregated at national level	2000, 2005, 2010, 2015, 2020	[50]
Brazilian Institute of Geography and Statistics (IBGE)	Brazil	Aggregated at municipality level	1974-2022	[22]
Crop and grass loss	Global	300 m	1992-2020	[14,15,51]
Datasets used for estimating carbon emissions				
Aboveground biomass$ *($Used to estimate belowground biomass[52], deadwood and litter carbon stocks[53])*	Global	30 m	2000	[53]
Root-to-shoot biomass ratio	Global	1 km	Aggregated temporally using datasets from several years	[54]
Soil organic carbon stocks	Global	250 m	Aggregated temporally using datasets from several years	[55]
Peatland extent$^{\varphi}$ *($^{\varphi}$Globally aggregated peatland extent is based on refs.[56–60])*	Global	30 m	Aggregated temporally using datasets from several years	[61]
Ecoregions	Global	Vector		[62]
Precipitation	Global	5 km	1981-2022	[63]
Elevation	Global	90 m		[64]
Other datasets				
Database of Global Administrative Areas-v4.1 (GADM)	Global	Vector		[65]

Supplementary Table 4 | Summary of the datasets and models used for deforestation and carbon emission comparisons in Fig. 2. A comparison of deforestation estimates for major food commodities between this study, Pendrill et al., and Goldman et al. is presented in Supplementary Fig. 3.

Study or dataset	Brief methodology	Scope and comprehensiveness of the output	Accessibility, replicability and updates
DeDuCE model ***(present study)***	*Input*: Several remote sensing datasets and agricultural statistics (see Supplementary Table 3) *Deforestation attribution model*: Hybrid (Spatial and statistical) *Carbon emission accounting*: Hybrid (includes emission due to loss of AGB, BGB, deadwood, litter, SOC, and carbon stocks of replacing commodity)	*Spatial and temporal coverage:* Global (2001-2022) *Spatial aggregation:* Deforestation and carbon emission estimates aggregated at national level (sub-national for Brazil) *Comprehensiveness of estimates:* Commodity-level estimates	*Data availability:* Openly available (✓) *Code for replicability:* Openly available (✓) *Updated post-publication:* N.A.
Pendrill et al.[66]	*Input*: Spatial tree cover loss, agricultural statistics and AGB stocks *Deforestation attribution model*: Statistical *Carbon emission accounting*: Statistical (includes AGB, BGB, SOC and carbon stocks of replacing commodity)	*Spatial and temporal coverage:* Tropical countries (2001-2018) *Spatial aggregation:* Deforestation and carbon emission estimates aggregated at national level (sub-national for Brazil and Indonesia) *Comprehensiveness of estimates:* Commodity-level estimates	*Data availability:* ✓ *Code for replicability:* Not openly available (✗) *Updated post-publication:* Yes (✓; now covers 2001-2018)
Goldman et al.[25]	*Input*: Spatial tree cover loss, commodity maps and dominant driver of forest loss *Deforestation attribution model*: Spatial *Carbon emission accounting*: Not estimated	*Spatial and temporal coverage:* Global, though spatial coverage limited to coverage of spatial datasets (2001-2015) *Spatial aggregation:* Deforestation estimates aggregated at national level *Comprehensiveness of estimates:* Commodity-level estimates for EUDR commodities (Oil palm, Soybeans, Cattle meat, Wood fibre, Cocoa beans, Coffee and Rubber)	*Data availability:* Can be requested from corresponding authors (✓) *Code for replicability:* ✗ *Updated post-publication:* No (✗)
Hoang et al.[67] (uses Curtis et al. [20])	*Input*: Spatial tree cover loss, forest plantation mask and dominant drivers of forest loss *Deforestation attribution model*: Spatial *Carbon emission accounting*: Not estimated	*Spatial and temporal coverage:* Global (2001-2015); however, results only included G7 member counties, China, India, Brazil, Indonesia, Mexico, and remaining G20 countries *Spatial aggregation:* Deforestation estimates aggregated at national level. Although it's theoretically possible to extract pixel-level emissions at 10-km resolution	*Data availability:* ✓ *Code for replicability:* ✓ *Updated post-publication:* ✗

		Comprehensiveness of estimates: Not quantified at commodity level	
Crippa et al.[68]	*Input*: FAOSTAT statistics *Deforestation attribution model*: Not estimated. However, all land use and land-use changes from FAOSTAT are considered. *Carbon emission accounting*: Statistical (includes all greenhouse gas emissions from the food supply chain)	*Spatial and temporal coverage:* Global (1990-2018) *Spatial aggregation:* Carbon emission estimates aggregated at national level *Comprehensiveness of estimates:* Not quantified at commodity level	*Data availability:* ✓ *Code for replicability:* ✗ *Updated post-publication:* ✓ (now covers 1990-2018)
Feng et al.[69] (uses Curtis et al. [20])	*Input*: Spatial tree cover loss and dominant drivers of forest loss *Deforestation attribution model*: Spatial *Carbon emission accounting*: Spatial (includes emission due to loss of AGB, BGB, SOC)	*Spatial and temporal coverage:* Tropical countries (2001-2019) *Spatial aggregation:* Carbon emission estimates aggregated at national level. Although it's theoretically possible to extract pixel-level emissions at 10-km resolution *Comprehensiveness of estimates:* Categorised into agriculture, forestry and other drivers	*Data availability:* ✓ *Code for replicability:* ✓ *Updated post-publication:* ✗
Curtis et al.[20] dominant driver (on which Global Forest Watch[61] estimates are based)	*Input*: Spatial tree cover loss and field training samples *Deforestation attribution model*: Spatial *Carbon emission accounting*: Not estimates	*Spatial and temporal coverage:* Global (Aggregated for whole time series, 2001-2022) *Spatial aggregation:* Dominant deforestation driver estimates at 10-km resolution *Comprehensiveness of estimates:* Dominant drivers of deforestation are broadly classified as Commodity-driven deforestation, Shifting agriculture, Forestry, Wildfire and Urbanisation.	*Data availability:* ✓ *Code for replicability:* ✓ (only initial code is available) *Updated post-publication:* ✓ (now covers 2001-2022)

Supplementary Table 5 | Absolute values of deforestation and carbon emission estimates used for sensitivity analysis. The IDs will facilitate the association of results from various sensitivity analyses archived on Zenodo (see data availability).

<table>
<tr><th rowspan="2">ID</th><th rowspan="2">Broad category</th><th rowspan="2" colspan="2">Sensitivity control</th><th colspan="2">Sensitivity analysis (2001-2022)</th><th colspan="2">Reference analysis (2001-2022)</th><th rowspan="2">Remarks</th></tr>
<tr><th>Deforestation (Total; ha)</th><th>Carbon Emissions incl. peatland drainage (Total; $MtCO_2$)</th><th>Deforestation (Total; ha)</th><th>Carbon Emissions incl. peatland drainage (Total; $MtCO_2$)</th></tr>
<tr><td colspan="9">Forests are composed of trees established though natural regeneration. Conversion of these natural forests to other land uses is referred to deforestation. Forest plantations, i.e., forests that are intensively managed for wood, fibre and energy, are excluded from this definition of forest.
This study: We define forest using tree cover threshold (≥25%; expressing canopy density for all vegetation taller than 5m in height within a pixel), with complete removal of tree cover canopy in a pixel representing tree cover loss. Using spatio-temporal extent of forest plantation data, we exclude tree cover loss over forest plantations established prior to year 2000 (i.e., rotational clearing; Supplementary Fig. 6), thus, reflecting deforestation (i.e., loss of natural forests).
Sensitivity analysis: We modify tree cover thresholds, forest cover and deforestation data.</td></tr>
<tr><td>S1</td><td rowspan="4">Forest and deforestation</td><td colspan="2">Tree cover ≥ 10%</td><td>129,821,626</td><td>44,742</td><td rowspan="2">121,794,096</td><td rowspan="2">44,118</td><td rowspan="2">Lower tree cover threshold allows for inclusion of more forest loss pixels and vice versa</td></tr>
<tr><td>S2</td><td colspan="2">Tree cover ≥ 75%</td><td>85,276,875</td><td>39,280</td></tr>
<tr><td>S3</td><td colspan="2">JRC Global Forest Cover 2020
(compared only to estimates from 2020-2022)</td><td>12,088,808</td><td>3,362</td><td>13,605,957</td><td>5,577</td><td>Lower estimates are likely due to differing methodologies in delineating forests between JRC and Global Forest Change. Since JRC forest cover already excludes agricultural plantations (e.g., cocoa and oil palm plantations) from its forest coverage, this could be the possible reason for lower estimates.</td></tr>
<tr><td>S4</td><td colspan="2">JRC TMF Deforestation
(compared only for countries where TMF has spatial coverage)</td><td>72,163,858</td><td>34,757</td><td>100,460,663</td><td>42,825</td><td>JRC TMF deforestation accounts for disturbances over multiple years (excluding regions of regrowth to be classified as deforestation)[70], and excludes loss over dry forests (unlike GFC), thus being more conservative.</td></tr>
<tr><td rowspan="2">S5</td><td rowspan="2">Forest plantation</td><td rowspan="2">All plantations from SDPT established before the year 2000</td><td>(All commodity estimates)</td><td>121,756,874</td><td>44,116</td><td>121,794,096</td><td>44,118</td><td rowspan="2">Excluding all known forest plantation reduces deforestation attributed to forestry activities</td></tr>
<tr><td>(Forest plantation estimates only)</td><td>16,961,350</td><td>-247</td><td>16,989,601</td><td>-248</td></tr>
<tr><td colspan="9">The lag between the clearing of forest and the establishment of a productive agricultural or forestry land can vary widely depending on several factors, including the method of clearing, the intended use of the land, environmental conditions, and local agricultural practices.</td></tr>
</table>

This study: With spatio-temporal data, we attribute forest loss to land-use with a higher rotation period within a 4-year moving window (i.e., maximum lag of 3-years from the year of forest loss). The attribution is in the order of forest plantations, followed by woody perennial crops, pastures, herbaceous perennial and temporary crops. In statistical attribution, we use a lag period of 3 years. *Sensitivity analysis*: We modify spatial and statistical lag, and the combined effect of both.								
S6	**Lag period**	Spatial lag period = 1 year *(compared only for MapBiomas countries)*		60,479,552	25,915	67,161,919	28,469	Longer lag period captures more delayed land-use changes and vice versa
S7		Spatial lag period = 5 year *(compared only for MapBiomas countries)*		70,013,040	29,557			
S8		Statistical lag period = 1 year		120,912,241	43,749	121,794,096	44,118	
S9		Statistical lag period = 5 year		121,909,645	44,354			
S10		Both spatial and statistical lag = 1 year *(compared only for MapBiomas countries)*		60,454,479	25,954	67,161,919	28,469	
S11		Both spatial and statistical lag = 5 year *(compared only for MapBiomas countries)*		70,017,034	29,538			
This study: We overlay several **spatial datasets** providing extent of specific commodities, land use and dominant drivers to attribute forest loss. *Sensitivity analysis*: We analyse deforestation attribution using only Dominant Driver of tree cover loss and only tree cover loss dataset.								
S12	**Inclusion of spatial datasets**	Partial statistical attribution (Global Forest Change + Dominant driver + agricultural statistics)	Global	171,153,029	61,534	121,794,096	44,118	Poor quality data that overlooks spatio-temporal heterogeneity. Furthermore, deforestation from non-agriculture and forestry sectors (e.g., mining) might contribute to inflating these estimates, if not removed from attribution.
			Oil palm-Indonesia	9,326,754	5,900	7,790,477	4,250	
			Cocoa-Côte d'Ivoire	634,953	137	896,994	238	
			Soya beans-Brazil	11,589,175	4,835	3,461,413	1,021	
S13		Full statistical attribution (Global Forest Change + agricultural statistics)	Global	226,530,991	76,377	121,794,096	44,118	
			Oil palm-Indonesia	9,369,761	5,788	7,790,477	4,250	
			Cocoa-Côte d'Ivoire	637,999	138	896,994	238	
			Soya beans-Brazil	8,716,920	3,533	3,461,413	1,021	
This study: We use sub-national **agricultural statistics** to improve granularity of forest loss attribution in Brazil. *Sensitivity analysis*: We directly assess deforestation in Brazil using FAOSTAT national agricultural statistics.								
S14	**Agriculture statistics**	National agricultural statistics *(analysed only for Brazil)*		38,375,103	17,013	38,329,216	16,997	Different datasets
Net land-use change shows the difference in total area between different time steps, while gross land-use change accounts for area gains and losses. In absence of spatio-temporal remote sensing dataset, it is difficult to discern gross losses over agricultural land systems. *This study*: We use crop and grass loss data and an assumption that cropland expands over pastures as a proxy to statistically assess gross land-use expansion for agricultural land systems. *Sensitivity analysis*: We analyse deforestation attribution assuming cropland directly led to deforestation (and do not expand over pastures first), and using net expansion estimates derived from agricultural statistics, not accounting for gross land-use change. Furthermore, we restrict (using only the right part for Supplementary equations (4)-(6) and don't restrict (left part for Supplementary equations (4)-(6) all land-use attributions.								
S15	**Land-use expansion**	Croplands do not expand over pastures, directly forests		122,067,977	44,249	121,794,096	44,118	More crop-commodity driven deforestation

		Net expansion for agricultural land systems		112,500,734	40,060			Net land-use change doesn't account for losses in pasture and crops (such as those resulting from crop failure), which in turn reduces the contribution of these commodities to deforestation estimates.
S16		All statistical land-use attribution restricted by FAOSTAT		120,295,888	43,389			Influences land-use expansion driven deforestation for certain and uncertain mosaics (see Supplementary equations (4)-(6))
S17		Statistical land-use attribution not restricted by FAOSTAT		147,103,233	56,508			
Multi-cropping: When two or more crops are grown on the same plot of land under different growing season.								
S18	**Multiple cropping**	Not accounting for harvested area from multiple cropping *(analysed only for Brazil)*	Maize	724,624	207	535,248	153	Not accounting for multi-cropping increases deforestation estimates for commodities with higher harvested areas (potentially due to proportional commodity attribution in Supplementary equation (9)-(12)), and vice versa.
			Beans	239,455	67	200,274	52	
			Potatoes	8,534	3.17	5,781	2.27	
			Groundnuts	7,730	2.48	8,323	2.73	
Amortisation period conceptually spreads the consequences of deforestation across multiple years to account for the enduring productivity of the land. *This study:* We use a 5-year amortisation period.								
S19	**Amortisation period**	10 years *(compared with amortised estimates of year 2020)*		5,611,693	2,089			There is no universal global pattern, but selecting an appropriate amortization period can help reflect recent or historical trends for specific countries or commodities, such as changes in commodity demand, production trends, domestic consumption, and trade dynamics.
S20		15 years *(compared with amortised estimates of year 2020)*		5,739,464	2,160	5,644,532	2,113	
S21		20 years *(compared with amortised estimates of year 2020)*		5,625,950	2,134			

Supplementary Table 6 | Scoring individual datasets for attribution and quality assessment. The criteria for the scoring methodology are detailed in Supplementary Table 11. Commodities are attributed in descending order of their scores, starting with the highest-scored commodity and proceeding to the lowest.

Dataset	Space	Time	Explicitness	Score	Special remarks
Oil palm fruit (Indonesia)	1.00	1.00	1.00	**1.00**	Reduce the score by 0.05 for every year after 2019
Maize (China)	0.90	1.00	1.00	**0.97**	
Soya beans (South America)	0.80	1.00	1.00	**0.93**	
Sugarcane (Brazil)	0.90	0.70	1.00	**0.87**	
Oil palm fruit (Malaysia)	0.65	0.90	1.00	**0.85**	Reduce the score by 0.05 for every year after 2018
Cocoa (Côte d'Ivoire and Ghana)	0.95	0.60	1.00	**0.85**	
MapBiomas collection (Commodities)	0.80	1.00	0.70	**0.83**	Includes only explicitly defined commodities
Rice (Asia)	0.90	0.60	1.00	**0.83**	
Rapeseed (North America, Canada, Europe and Chile)	0.85	0.60	1.00	**0.82**	
Oil palm fruit (Pan-tropical)	0.75	0.40	1.00	**0.72**	
Coconut (Pan-tropical)	0.70	0.40	1.00	**0.70**	
Global plantation dataset	0.65	0.80	0.65	**0.70**	
MapBiomas collection (Land use)	0.80	1.00	0.30	**0.70**	Includes all land-use classifications excluding commodities
Croplands	0.65	0.80	0.50	**0.65**	
Forest loss due to fire	0.65	1.00	0.10	**0.58**	Dataset not used for attribution, but for screening forest loss due to fire
Global forest change (Forest loss)	0.65	0.85	0.10	**0.53**	
Dominant forest loss drivers	0.10	0.70	0.40	**0.40**	
Subnational stats	1.00	1.00	1.00	**-**	We do not penalise this dataset when flagging (equation (2))
FAOSTAT national stats	0.50	1.00	1.00	**-**	Besides penalising the dataset based on flags (equation (2); Supplementary Table 12), we further reduce the FAOSTAT dataset score by '-0.50/3' for both land use and production statistics individually.

Supplementary Table 7 | Pre-processing and attribution assumptions for the spatial datasets.

Datasets	Pre-processing and attribution assumptions
Global forest change	- Forest loss is only considered for pixels with tree cover ≥ 25%
Global plantation dataset	- Only considered as forest plantation-driven deforestation if the start year of the dataset > 2000. 'Start year' defines the year when the first plantation was established based on the temporal extent of remote sensing datasets - Forest loss pixels classified with start year ≤ 2000 are considered under rotational clearing and excluded from deforestation attribution - *Attribution*: For this dataset, deforestation attribution is not temporally restricted
MapBiomas Collection	- Forest loss is attributed to MapBiomas when a commodity-driven land use occurs within a four-year window from the year of forest loss - In case of multiple land use changes occurring within this four-year window, forest plantations will be prioritised over perennial crops, and perennial crops prioritised over pastures, followed by temporary crops - If MapBiomas(t) land use is the same as MapBiomas(2000), we consider forest loss as 'historical/rotational clearing' - *Attribution*: For this dataset, deforestation attribution is temporally restricted to 2021 only for Bolivia; not restricted for other MapBiomas countries
Croplands	- Forest loss recorded from 2001 to 2003 is attributed to cropland only if cropland extent is defined for the period of 2000-2003 - Forest loss recorded from 2001 to 2007 is attributed to cropland defined for the period of 2004-2007. The delay between forest loss and cropland extent is given to accommodate for forest loss and establishment of cropland - Forest loss recorded from 2005 to 2011 is attributed to cropland defined for the period of 2008-2011 - Forest loss recorded from 2008 to 2015 is attributed to cropland defined for the period of 2012-2015 - Forest loss recorded from 2012 to 2019 is attributed to cropland defined for the period of 2016-2019 - *Attribution*: For this dataset, deforestation attribution (following above) is temporally restricted to 2019
Sugarcane	- *Attribution*: For this dataset, deforestation attribution is temporally restricted to 2019
Soya beans	- Forest loss is attributed to Soya beans when a Soya bean land use occurs within a four-year window from the year of forest loss - *Attribution*: For this dataset, deforestation attribution is temporally restricted to 2022
Rice	- Resolution of the dataset is downscaled to 30 m (same resolution as Global forest change), determined by the majority of pixels within the designated reducer window - *Attribution*: For this dataset, deforestation attribution takes place to 2019
Rapeseed	- Resolution of the dataset is downscaled to 30 m (same resolution as Global forest change), determined by the majority of pixels within the designated reducer window - *Attribution*: For this dataset, deforestation attribution is temporally restricted to 2019
Maize (corn)	- Forest loss is attributed to Maize when a Maize land use occurs within a four-year window from the year of forest loss - *Attribution*: For this dataset, deforestation attribution is temporally restricted to 2020
Cocoa	- Resolution of the dataset is downscaled to 30 m (same resolution as Global forest change), determined by the majority of pixels within the designated reducer window - Pixels of forest loss classified as Cocoa and overlapping with plantation mask are considered under 'rotational clearing' - *Attribution*: For this dataset, deforestation attribution is temporally restricted to 2021
Coconut	- Resolution of the dataset is downscaled to 30 m (same resolution as Global forest change), determined by the majority of pixels within the designated reducer window - Pixels of forest loss classified as Coconut and overlapping with plantation mask are considered under 'rotational clearing' - *Attribution*: For this dataset, deforestation attribution is temporally restricted to 2020
Oil palm fruit (Indonesia)	- Forest loss occurring in the regions (i.e., delineated within a boundary) of Oil palm plantations for the year 2000 are classified as 'rotational clearing', and these pixels are

	excluded from commodity-driven deforestation - *Attribution*: This dataset is not temporally restricted, thus assuming that if a forest loss occurs in a pixel post-2019 (data's temporal extent), we consider it as forest loss due to Oil palm for that year
Oil palm fruit (Malaysia)	- Forest loss is attributed to Oil palm when an Oil palm land use occurs within a four-year window from the year of forest loss - Pixels of forest loss classified as Oil palm and overlapping with plantation mask are considered under 'rotational clearing' - *Attribution*: This dataset is not temporally restricted, thus assuming that if a forest loss occurs in a pixel post-2018 (data's temporal extent), we consider it as forest loss due to Oil palm for that year
Oil palm fruit (Global)	- Resolution of the dataset is downscaled to 30 m (same resolution as Global forest change), determined by the majority of pixels within the designated reducer window - Pixels of forest loss classified as Oil palm and overlapping with plantation mask are considered under 'rotational clearing' - *Attribution*: For this dataset, deforestation attribution is temporally restricted to 2019
Forest loss due to fire	- Forest loss pixels classified under '1. Forest loss due to other (non-fire) drivers' are open for attribution by other datasets - Forest loss pixels classified under '2. Low certainty of forest loss due to fire' are open for attribution by other datasets - Forest loss pixels classified under '3. Medium' and '4. High' certainty are excluded from commodity-driven deforestation - Forest loss pixels classified under '5. Forest loss due to fire in Africa' are excluded from commodity-driven deforestation
Forest management	- Forest loss is considered 'rotational clearing' if the pixel falls under '20. Naturally regenerating forest with signs of management, e.g., logging, clear cuts etc', '31: Planted forests (rotation >15 years)', '32: Plantation forests (rotation ≤15 years)', '40: Oil palm plantations' and '53: Agroforestry' - The above only applies to the spatial extent of countries covered in Supplementary Table 3 for 'Forest management'
Dominant drivers of forest loss	- Forest loss pixels classified under 'Commodity-driven deforestation' and 'Shifting agriculture' are considered under agricultural-driven deforestation - Forest loss pixels classified under 'Forestry' are considered under forestry-induced deforestation - Forest loss pixels classified under 'Wildfire' and 'Urbanisation' are excluded from commodity-driven deforestation - Pixels of forest loss classified by this dataset and overlapping with plantation mask are considered under 'rotational clearing'

Supplementary Table 8 | Loss of soil organic carbon (SOC) across different land use and biomes. The values represent the % loss of actual SOC. Note that for depths 30-100 cm, the data is scarce. Thus, we use the 0-100 cm data to estimate SOC loss for 30-100 cm depth. We do this by assuming that SOC $loss_{0\text{-}100\ cm}$ = SOC $loss_{0\text{-}30\ cm}$ + SOC $loss_{30\text{-}100\ cm}$.

		Land use replacing forest (values in %)			
Depth	**Ecoregion group**	**Cropland**	**Pasture**	**Forest plantation**	**References**
0-30 cm	Global	26.6	18	13	71,72
0-30 cm	Tropical	29	4	22	73–75
0-30 cm	Temperate	31.4	4.15	15	72,76,77
0-30 cm	Boreal	21	18†	13†	78
30-100 cm	Global	13.8#	9.7#	23#	71,79
30-100 cm	Tropical	15	2	7	75
30-100 cm	Temperate	25	6.925*	19*	76
30-100 cm	Boreal	17.4*	13.85*	18*	

†Imputed using global average estimates

#Values available for depths of 0-100 cm

*Calculated using the average of global and respective ecoregions 0-30m estimates; consider these values for 0-100 cm

Supplementary Table 9 | Plant carbon stocks of replacing commodities and commodity groups across different biomes.

	(Values in MgC ha^{-1})			
Crop or Commodity group	**Tropical**	**Temperate**	**Boreal**	**References**
Cereals	4.44	3.15		80,81
Maize (corn)		6.3		80
Rice		4.5		80
Wheat		2.3		80
Barley		5.5		82
Sorghum		4.12		80
Millet		3.13		83
Edible roots and tubers with high starch or inulin content		3		81
Cassava		4.5		84
Potatoes		0.5		85
Fibre crops		3.71		80
Natural rubber in primary forms		79.05		86
Jute, raw or retted		3.9		80
Seed cotton, unginned		4.3		80
Forest plantation	120.23	130.99	96.07	52,87
Fruit and nuts	31.96	39.53		88,89
Apples		26.48		90
Bananas		6.2		91
Cashew nuts, in shell		37.6		92
Grapes		12.3		93
Mangoes		84.75		94
Oranges		7.69		95
Other citrus fruit, n.e.c.	20.65	23.73		91
Plantains and cooking bananas		6.2		91

Oilseeds and oleaginous fruits	31.96	39.53	88,89
Oil palm fruit	52.28		86
Soya beans	3		80
Sunflower seed	1.1		80
Groundnuts, excluding shelled	1.1		80
Olives	5.3		96
Coconuts, in shell	57.38	65.93	91
Pasture	6.8		80
Pulses (dried leguminous vegetables)	1.56		80
Beans, dry	2.39		83
Chick peas, dry	1.28		83
Cow peas, dry	1.82		83
Pigeon peas, dry	3		83
Lentils, dry	1.25		83
Peas, dry	0.9		80
Stimulant, spice and aromatic crops	31.96	39.53	88,89
Coffee, green	77.12		97
Cocoa beans	34.55		98
Tea leaves	21.06		99
Sugar crops	10.17		*Average of commodities in the group*
Sugar beet	8.32		85
Sugar cane	12.02		100
Vegetables	0.43		101
Cabbages	1.65		80
Lettuce and chicory	1.15		102
Tomatoes	3.48		102
Cauliflowers and broccoli	4.05		102

Supplementary Table 10 | Emission factor used to estimate carbon emissions from deforestation on peatlands. Emission factors from ref.[34] are based on IPCC Wetland Supplement[32].

	(values in $MgCO_2\ ha^{-1}\ yr^{-1}$)			
Land use replacing forest	**Tropical**	**Temperate**	**Boreal**	**References**
Cropland	45	28.6	27.9	34
Pasture	37.4	17.95	20.2	34
Forest plantation	40.34	2.5	6.42	32,33
Oil palm fruit	54.41			31

Supplementary Table 11 | Criteria's for scoring different aspects of spatial datasets.

Aspect	Criteria	Penalisation
Space (representing both resolution and area of focus)	Perfect score is given when the pixel size is ≤ 10m and is explicitly mapped for a country	0
	Resolution of 20 m	-0.05
	Resolution of 30 m	-0.1
	Resolution of 100 m	-0.3
	Resolution of 1 km	-0.5
	Resolution of 10 km	-0.75
	Mapped for two countries	-0.05
	Mapped for more than two countries or a continent	-0.1
	Multiple continents	-0.15
	Mapped globally	-0.25
Time (representing temporal resolution and standalone ability of the data to differentiate pre- and post-2000's deforestation)	Perfect score is given when the dataset is available from 2001-2022 for herbaceous crops, and at least the year 2000- or prior-onwards for woody vegetation crops (i.e., tree crops) and forest plantations (allowing for differentiation between post-2000's deforestation from the rotational clearing of managed plantations)	0
	For tree crops and forest plantations, deforestation is not differentiable from rotational clearing (need to be complimented with plantation mask to extract this information)	Using Du et al: -0.1 Using Lesiv et al: -0.2
	After the latest detection year (in cases allowed)	-0.05 each year
	Temporal aggregation based on a single year of remote sensing dataset	-0.3
	Temporal aggregation based on 2-3 years of remote sensing dataset	-0.2
	Temporal aggregation based on 4-6 years of remote sensing dataset	-0.1
	Temporal aggregation based on >6 years of remote sensing dataset	0
	Temporally-explicit estimates every 2-3 years between 2001-2022	-0.1
	Temporally-explicit estimates every 4-6 years between 2001-2022	-0.2
	Temporally-explicit estimates >6 years between 2001-2022	-0.3
	Starting year of detection is 1-5 years away from 2001 (i.e., the first year of analysed deforestation)	-0.05
	Starting year of detection is 6-10 years away from 2001	-0.1
	Starting year of detection is 11-15 years away from 2001	-0.15
	Starting year of detection is >15 years away from 2001	-0.2
Explicitness (representation of the deforestation driver and consideration given to training algorithm of the data)	Perfect score is given to datasets that maps a single commodity, where model training is performed using field samples	0
	When training is primarily based on remote sensing trends, without using field samples (including visual interpretations)	-0.5
	When multiple commodities or land uses are predicted by the same model using the same field samples	-0.1
	Dataset maps two or more than two commodities (differentiable)	-0.2
	Dataset maps a single land use	-0.3
	Dataset maps two or more than two different land uses (differentiable)	-0.4
	Dataset maps two or more than two different land uses (indifferentiable, i.e., mosaics)	-0.6
	Information about forest loss drivers is unavailable	-0.9

Supplementary Table 12 | The FAO flags, their description and associated penalisation. A detailed description of FAO flags is documented in ref.[103]. Since our statistical attribution relies on the expansion of land-use and commodities, we obtain flags for two years (*t+lag* and *t*; see Supplementary equations (1) and (9)). In the quality assessment, we use the flag with the lower penalization between the two.

Flag	Description	Penalisation
A	**Official figure**: Value provided as official when the source agency assigns sufficient confidence that it is not expected to be dramatically revised	0
B	**Time series break**: Observations are characterised as such when different content exists or a different methodology has been applied to this observation as compared with the preceding one	-0.10
E	**Estimated value**: Observation obtained through an estimation methodology or based on the use of a limited amount of data	-0.20
I	**Imputed value**: Observation imputed by a receiving agency to replace or fill gaps in reported data series	-0.30
P	**Provisional value**: An observation is characterised as "provisional" when the source agency – while it bases its calculations on its standard production methodology – considers that the data, almost certainly, are expected to be revised	-0.40
T	**Unofficial figure**: Observations are "temporary" or "tentative", indicating that the figure should be used with caution and may be subject to revision or replacement with official statistics once they become available.	-0.40
X	**Figure from international organisations**: Observation from an international or a supranational organisation that does not use any flagging system in data sharing	-0.50
M	**Missing value**: Used to denote empty cells resulting from the impossibility to collect a statistical value	-0.70
Z	**Authors gap filling**: Gap filled by authors of this study (*not part of FAOSTAT flags*)	-0.70

References

1. FAO-FRA. Global Forest Resource Assessment 2020. https://fra-data.fao.org/assessments/fra/2020 (2023).
2. Hansen, M. C. *et al.* High-Resolution Global Maps of 21st-Century Forest Cover Change. *Science* **342**, 850–853 (2013).
3. MapBiomas. *MapBiomas General "Handbook": Algorithm Theoretical Basis Document (ATBD)*. https://mapbiomas-br-site.s3.amazonaws.com/ATBD_Collection_7_v2.pdf (2022).
4. Gaveau, D. L. A. *et al.* Slowing deforestation in Indonesia follows declining oil palm expansion and lower oil prices. *PLOS ONE* **17**, e0266178 (2022).
5. Du, Z. *et al.* A global map of planting years of plantations. *Sci Data* **9**, 141 (2022).
6. Lesiv, M. *et al.* Global forest management data for 2015 at a 100 m resolution. *Sci Data* **9**, 199 (2022).
7. Harris, N., Goldman, E. D. & Gibbes, S. *Spatial Database of Planted Trees (SDPT Version 1.0)*. https://www.wri.org/research/spatial-database-planted-trees-sdpt-version-10 (2019).
8. Maraseni, T. N., Son, H. L., Cockfield, G., Duy, H. V. & Nghia, T. D. Comparing the financial returns from acacia plantations with different plantation densities and rotation ages in Vietnam. *Forest Policy and Economics* **83**, 80–87 (2017).
9. Steinfeld, H. *Livestock's Long Shadow: Environmental Issues and Options*. (Food and Agriculture Organization of the United Nations, Rome, 2006).
10. Kalischek, N. *et al.* Cocoa plantations are associated with deforestation in Côte d'Ivoire and Ghana. *Nat Food* **4**, 384–393 (2023).
11. Gibbs, H. K. *et al.* Brazil's Soy Moratorium. *Science* **347**, 377–378 (2015).
12. Gaveau, D. L. A. *et al.* Rapid conversions and avoided deforestation: Examining four decades of industrial plantation expansion in Borneo. *Sci. Rep.* **6**, (2016).
13. FAOSTAT. https://www.fao.org/faostat/en/#data.
14. Li, W. *et al.* Gross and net land cover changes in the main plant functional types derived from the annual ESA CCI land cover maps (1992–2015). *Earth System Science Data* **10**, 219–234 (2018).
15. Harper, K. L. *et al.* A 29-year time series of annual 300m resolution plant-functional-type maps for climate models. *Earth System Science Data* **15**, 1465–1499 (2023).
16. Graesser, J., Aide, T. M., Grau, H. R. & Ramankutty, N. Cropland/pastureland dynamics and the slowdown of deforestation in Latin America. *Environ. Res. Lett.* **10**, 034017 (2015).
17. Pendrill, F., Persson, U. M., Godar, J. & Kastner, T. Deforestation displaced: trade in forest-risk commodities and the prospects for a global forest transition. *Environ. Res. Lett.* **14**, 055003 (2019).
18. Opio, C. *et al. Greenhouse Gas Emissions from Ruminant Supply Chains – a Global Life Cycle Assessment*. (Food and Agriculture Organization of the United Nations, Rome, 2013).
19. Pendrill, F. *et al.* Disentangling the numbers behind agriculture-driven tropical deforestation. *Science* **377**, eabm9267 (2022).
20. Curtis, P. G., Slay, C. M., Harris, N. L., Tyukavina, A. & Hansen, M. C. Classifying drivers of global forest loss. *Science* **361**, 1108–1111 (2018).
21. Ahlström, A., Canadell, J. G. & Metcalfe, D. B. Widespread Unquantified Conversion of Old Boreal Forests to Plantations. *Earth's Future* **10**, e2022EF003221 (2022).
22. Instituto Brasileiro de Geografia e Estatística (IBGE). IBGE Produção Agrícola Municipal. https://sidra.ibge.gov.br/pesquisa/pam/tabelas (2022).
23. Pendrill, F. *et al.* Agricultural and forestry trade drives large share of tropical deforestation emissions. *Global Environmental Change* **56**, 1–10 (2019).
24. Gilbert, M. *et al.* Global distribution data for cattle, buffaloes, horses, sheep, goats, pigs, chickens and ducks in 2010. *Sci Data* **5**, 180227 (2018).
25. Goldman, E., Weisse, M., Harris, N. & Schneider, M. Estimating the Role of Seven Commodities in Agriculture-Linked Deforestation: Oil Palm, Soy, Cattle, Wood Fiber, Cocoa, Coffee, and Rubber. *WRIPUB* (2020) doi:10.46830/writn.na.00001.
26. Godde, C. M., Mason-D'Croz, D., Mayberry, D. E., Thornton, P. K. & Herrero, M. Impacts of climate change on the livestock food supply chain; a review of the evidence. *Global Food Security* **28**, 100488 (2021).
27. Rahimi, J. *et al.* A shift from cattle to camel and goat farming can sustain milk production with lower inputs and emissions in north sub-Saharan Africa's drylands. *Nat Food* **3**, 523–531 (2022).
28. Fernández, P. D. *et al.* Understanding the distribution of cattle production systems in the South American Chaco. *Journal of Land Use Science* **15**, 52–68 (2020).
29. Yoshikawa, S. Agro-Pastoral Expansion and Land Use/Land Cover Change Dynamics in Mato Grosso, Brazil. *Earth* **4**, 823–844 (2023).

30. John Couwenberg. *Emission Factors for Managed Peat Soils - An Analysis of IPCC Default Values*. https://www.wetlands.org/publications/emission-factors-for-managed-peat-soils-an-analysis-of-ipcc-default-values/ (2009).
31. Cooper, H. V. *et al.* Greenhouse gas emissions resulting from conversion of peat swamp forest to oil palm plantation. *Nat Commun* **11**, 407 (2020).
32. *2006 IPCC Guidelines for National Greenhouse Gas Inventories - Volume 4*. https://www.ipcc.ch/report/2006-ipcc-guidelines-for-national-greenhouse-gas-inventories/ (2006).
33. John Couwenberg. Greenhouse gas emissions from managed peat soils: is the IPCC reporting guidance realistic? *Mires and Peat 8* **Art. 2**, (2011).
34. Günther, A. *et al.* Prompt rewetting of drained peatlands reduces climate warming despite methane emissions. *Nat Commun* **11**, 1644 (2020).
35. Persson, U. M., Henders, S. & Cederberg, C. A method for calculating a land-use change carbon footprint (LUC-CFP) for agricultural commodities - applications to Brazilian beef and soy, Indonesian palm oil. *Glob Change Biol* **20**, 3482–3491 (2014).
36. WRI & WBCSD. Greenhouse Gas Protocol Land Sector and Removals Guidance.
37. Maciel, V. G. *et al.* Towards a non-ambiguous view of the amortization period for quantifying direct land-use change in LCA. *Int J Life Cycle Assess* **27**, 1299–1315 (2022).
38. IPCC. *Revised 1996 IPCC Guidelines for National Greenhouse Gas Inventories (Volume 3)*. https://www.ipcc-nggip.iges.or.jp/public/gl/guidelin/ch5ref1.pdf (1996).
39. zu Ermgassen, E. K. H. J. *et al.* The origin, supply chain, and deforestation risk of Brazil's beef exports. *Proceedings of the National Academy of Sciences* **117**, 31770–31779 (2020).
40. Song, X.-P. *et al.* Massive soybean expansion in South America since 2000 and implications for conservation. *Nat Sustain* 1–9 (2021) doi:10.1038/s41893-021-00729-z.
41. Descals, A. *et al.* High-resolution global map of smallholder and industrial closed-canopy oil palm plantations. *Earth System Science Data* **13**, 1211–1231 (2021).
42. Potapov, P. *et al.* Global maps of cropland extent and change show accelerated cropland expansion in the twenty-first century. *Nat Food* **3**, 19–28 (2022).
43. Zheng, Y., dos Santos Luciano, A. C., Dong, J. & Yuan, W. High-resolution map of sugarcane cultivation in Brazil using a phenology-based method. *Earth System Science Data* **14**, 2065–2080 (2022).
44. Han, J. *et al.* NESEA-Rice10: high-resolution annual paddy rice maps for Northeast and Southeast Asia from 2017 to 2019. *Earth System Science Data* **13**, 5969–5986 (2021).
45. Han, J. *et al.* The RapeseedMap10 database: annual maps of rapeseed at a spatial resolution of 10m based on multi-source data. *Earth System Science Data* **13**, 2857–2874 (2021).
46. Peng, Q. *et al.* A twenty-year dataset of high-resolution maize distribution in China. *Sci Data* **10**, 658 (2023).
47. Descals, A. *et al.* High-resolution global map of closed-canopy coconut palm. *Earth System Science Data* **15**, 3991–4010 (2023).
48. Xu, Y. *et al.* Annual oil palm plantation maps in Malaysia and Indonesia from 2001 to 2016. *Earth System Science Data* **12**, 847–867 (2020).
49. Tyukavina, A. *et al.* Global Trends of Forest Loss Due to Fire From 2001 to 2019. *Frontiers in Remote Sensing* **3**, (2022).
50. Agriculture, Forestry, Fishery and Animal Husbandry Census. *National Statistics, Republic of China (Taiwan)* https://eng.stat.gov.tw/cl.aspx?n=2405.
51. Copernicus Climate Change Service. Land cover classification gridded maps from 1992 to present derived from satellite observations. ECMWF https://doi.org/10.24381/CDS.006F2C9A (2019).
52. Mokany, K., Raison, R. J. & Prokushkin, A. S. Critical analysis of root : shoot ratios in terrestrial biomes. *Global Change Biology* **12**, 84–96 (2006).
53. Harris, N. L. *et al.* Global maps of twenty-first century forest carbon fluxes. *Nat. Clim. Chang.* **11**, 234–240 (2021).
54. Huang, Y. *et al.* A global map of root biomass across the world's forests. *Earth System Science Data* **13**, 4263–4274 (2021).
55. Poggio, L. *et al.* SoilGrids 2.0: producing soil information for the globe with quantified spatial uncertainty. *SOIL* **7**, 217–240 (2021).
56. Crezee, B. *et al.* Mapping peat thickness and carbon stocks of the central Congo Basin using field data. *Nat. Geosci.* **15**, 639–644 (2022).
57. Gumbricht, T. *et al.* An expert system model for mapping tropical wetlands and peatlands reveals South America as the largest contributor. *Global Change Biology* **23**, 3581–3599 (2017).
58. Hastie, A. *et al.* Risks to carbon storage from land-use change revealed by peat thickness maps of Peru. *Nat. Geosci.* **15**, 369–374 (2022).

59. Xu, J., Morris, P. J., Liu, J. & Holden, J. PEATMAP: Refining estimates of global peatland distribution based on a meta-analysis. *CATENA* **160**, 134–140 (2018).
60. Miettinen, J., Shi, C. & Liew, S. C. Land cover distribution in the peatlands of Peninsular Malaysia, Sumatra and Borneo in 2015 with changes since 1990. *Global Ecology and Conservation* **6**, 67–78 (2016).
61. Global Forest Watch (GFW). Global Peatlands. https://data.globalforestwatch.org/datasets/gfw::global-peatlands/about.
62. Dinerstein, E. *et al.* An Ecoregion-Based Approach to Protecting Half the Terrestrial Realm. *BioScience* **67**, 534–545 (2017).
63. Funk, C. *et al.* The climate hazards infrared precipitation with stations—a new environmental record for monitoring extremes. *Scientific Data* **2**, 150066 (2015).
64. Jarvis, A., Guevara, E., Reuter, H. I. & Nelson, A. D. Hole-filled SRTM for the globe : version 4 : data grid. (2008).
65. GADM. Database of Global Administrative Areas (Version v4.1). https://gadm.org/.
66. Pendrill, F. *et al.* Disentangling the numbers behind agriculture-driven tropical deforestation. *Science* **377**, eabm9267 (2022).
67. Hoang, N. T. & Kanemoto, K. Mapping the deforestation footprint of nations reveals growing threat to tropical forests. *Nat Ecol Evol* **5**, 845–853 (2021).
68. Crippa, M. *et al.* Food systems are responsible for a third of global anthropogenic GHG emissions. *Nat Food* **2**, 198–209 (2021).
69. Feng, Y. *et al.* Doubling of annual forest carbon loss over the tropics during the early twenty-first century. *Nat Sustain* **5**, 444–451 (2022).
70. Sims, M. *et al.* Differences Between Global Forest Watch's Tree Cover Loss Data and JRC's Tropical Moist Forest Data Explained. *Global Forest Watch Content* https://www.globalforestwatch.org/blog/data-and-tools/tree-cover-loss-and-tropical-moist-forest-data-compared (2024).
71. Sanderman, J., Hengl, T. & Fiske, G. J. Soil carbon debt of 12,000 years of human land use. *Proceedings of the National Academy of Sciences* **114**, 9575–9580 (2017).
72. Guo, L. B. & Gifford, R. M. Soil carbon stocks and land use change: a meta analysis. *Global Change Biology* **8**, 345–360 (2002).
73. Don, A., Schumacher, J. & Freibauer, A. Impact of tropical land-use change on soil organic carbon stocks – a meta-analysis. *Global Change Biology* **17**, 1658–1670 (2011).
74. Powers, J. S., Corre, M. D., Twine, T. E. & Veldkamp, E. Geographic bias of field observations of soil carbon stocks with tropical land-use changes precludes spatial extrapolation. *Proceedings of the National Academy of Sciences* **108**, 6318–6322 (2011).
75. Veldkamp, E., Schmidt, M., Powers, J. S. & Corre, M. D. Deforestation and reforestation impacts on soils in the tropics. *Nat Rev Earth Environ* **1**, 590–605 (2020).
76. Poeplau, C. *et al.* Temporal dynamics of soil organic carbon after land-use change in the temperate zone – carbon response functions as a model approach. *Global Change Biology* **17**, 2415–2427 (2011).
77. Dlamini, P., Chivenge, P. & Chaplot, V. Overgrazing decreases soil organic carbon stocks the most under dry climates and low soil pH: A meta-analysis shows. *Agriculture, Ecosystems & Environment* **221**, 258–269 (2016).
78. Wei, X., Shao, M., Gale, W. & Li, L. Global pattern of soil carbon losses due to the conversion of forests to agricultural land. *Sci Rep* **4**, 4062 (2014).
79. Beillouin, D. *et al.* A global meta-analysis of soil organic carbon in the Anthropocene. *Nat Commun* **14**, 3700 (2023).
80. Mathew, I., Shimelis, H., Mutema, M. & Chaplot, V. What crop type for atmospheric carbon sequestration: Results from a global data analysis. *Agriculture, Ecosystems & Environment* **243**, 34–46 (2017).
81. Wiesmeier, M. *et al.* Estimation of past and recent carbon input by crops into agricultural soils of southeast Germany. *European Journal of Agronomy* **61**, 10–23 (2014).
82. Durán Zuazo, V. H., Francia Martínez, J. R., Pleguezuelo, C. R. R. & Tavira, S. C. Biomass carbon stock in relation to different land uses in a semiarid environment. *Journal of Land Use Science* **9**, 474–486 (2014).
83. Kuyah, S. *et al.* Grain legumes and dryland cereals contribute to carbon sequestration in the drylands of Africa and South Asia. *Agriculture, Ecosystems & Environment* **355**, 108583 (2023).
84. K, R. & B, B. Potential of wastelands for carbon sequestration- A review. *Int. J. Chem. Stud.* **8**, 2873–2881 (2020).
85. Koga, N. *et al.* Estimating net primary production and annual plant carbon inputs, and modelling future changes in soil carbon stocks in arable farmlands of northern Japan. *Agriculture, Ecosystems & Environment* **144**, 51–60 (2011).
86. Guillaume, T. *et al.* Carbon costs and benefits of Indonesian rainforest conversion to plantations. *Nat Commun* **9**, 2388 (2018).
87. Bukoski, J. J. *et al.* Rates and drivers of aboveground carbon accumulation in global monoculture plantation forests. *Nat Commun* **13**, 4206 (2022).

88. Brakas, S. G. & Aune, J. B. Biomass and Carbon Accumulation in Land Use Systems of Claveria, the Philippines. in *Carbon Sequestration Potential of Agroforestry Systems: Opportunities and Challenges* (eds. Kumar, B. M. & Nair, P. K. R.) 163–175 (Springer Netherlands, Dordrecht, 2011). doi:10.1007/978-94-007-1630-8_9.
89. Schafer, L. J., Lysák, M. & Henriksen, C. B. Tree layer carbon stock quantification in a temperate food forest: A peri-urban polyculture case study. *Urban Forestry & Urban Greening* **45**, 126466 (2019).
90. Zahoor, S. *et al.* Apple-based agroforestry systems for biomass production and carbon sequestration: implication for food security and climate change contemplates in temperate region of Northern Himalaya, India. *Agroforest Syst* **95**, 367–382 (2021).
91. Toensmeier, E. & Herren, H. *The Carbon Farming Solution: A Global Toolkit of Perennial Crops and Regenerative Agriculture Practices for Climate Change Mitigation and Food Security*. (Chelsea Green Publishing, White River Junction, Vermont, UNITED STATES, 2016).
92. Victor, A. D., Valery, N. N., Boris, N., Aimé, V. B. T. & Louis, Z. Carbon storage in cashew plantations in Central Africa: case of Cameroon. *Carbon Management* **12**, 25–35 (2021).
93. Morandé, J. A. *et al.* From berries to blocks: carbon stock quantification of a California vineyard. *Carbon Balance and Management* **12**, 5 (2017).
94. Sharma, S., Rana, V. S., Prasad, H., Lakra, J. & Sharma, U. Appraisal of Carbon Capture, Storage, and Utilization Through Fruit Crops. *Frontiers in Environmental Science* **9**, (2021).
95. Sahoo, U. K., Nath, A. J. & Lalnunpuii, K. Biomass estimation models, biomass storage and ecosystem carbon stock in sweet orange orchards: Implications for land use management. *Acta Ecologica Sinica* **41**, 57–63 (2021).
96. Lopez-Bellido, P. J., Lopez-Bellido, L., Fernandez-Garcia, P., Muñoz-Romero, V. & Lopez-Bellido, F. J. Assessment of carbon sequestration and the carbon footprint in olive groves in Southern Spain. *Carbon Management* **7**, 161–170 (2016).
97. Singh, K. P. *et al.* Biomass, carbon stock, CO2 mitigation and carbon credits of coffee-based multitier cropping model in Central India. *Environ Monit Assess* **195**, 1250 (2023).
98. Asigbaase, M., Dawoe, E., Lomax, B. H. & Sjogersten, S. Biomass and carbon stocks of organic and conventional cocoa agroforests, Ghana. *Agriculture, Ecosystems & Environment* **306**, 107192 (2021).
99. Das, M. *et al.* Biomass models for estimating carbon storage in *Areca* palm plantations. *Environmental and Sustainability Indicators* **10**, 100115 (2021).
100. Liang, X. *et al.* Quantifying shoot and root biomass production and soil carbon under perennial bioenergy grasses in a subtropical environment. *Biomass and Bioenergy* **128**, 105323 (2019).
101. Toensmeier, E., Ferguson, R. & Mehra, M. Perennial vegetables: A neglected resource for biodiversity, carbon sequestration, and nutrition. *PLOS ONE* **15**, e0234611 (2020).
102. Farina, R. *et al.* Potential carbon sequestration in a Mediterranean organic vegetable cropping system. A model approach for evaluating the effects of compost and Agro-ecological Service Crops (ASCs). *Agricultural Systems* **162**, 239–248 (2018).
103. FAO. *Statistical Standard Series: Observation Status Code List (Version 3).* https://www.fao.org/3/cc6208en/cc6208en.pdf (2023).